

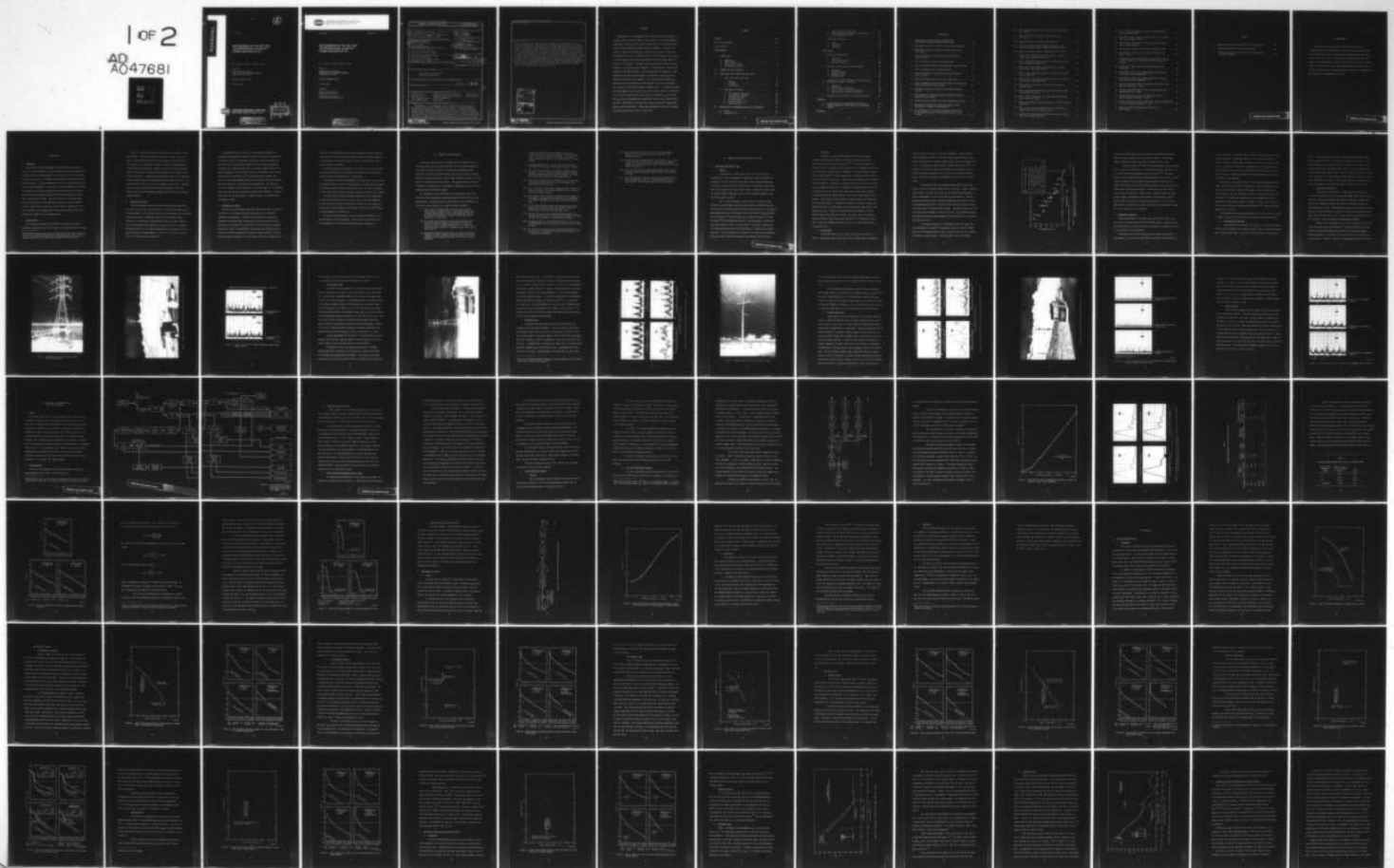
AD-A047 681

STANFORD RESEARCH INST MENLO PARK CALIF
MEASUREMENT OF THE APD AND THE DEGRADATION CAUSED BY POWER LINE--ETC(U)
APR 76 R A SHEPHERD, J C GADDIE

F/6 9/5
N00039-74-C-0077
NL

UNCLASSIFIED

1 OF 2
AD
A047681



AD A047681

2

Final Report

**MEASUREMENTS OF THE APD AND
THE DEGRADATION CAUSED BY
POWER LINE NOISE AT HF**

By: RICHARD A. SHEPHERD and JAMES C. GADDIE

Prepared for:

DEPARTMENT OF THE NAVY
NAVAL ELECTRONIC SYSTEMS COMMAND
WASHINGTON, D.C. 20360

CONTRACT N00039-74-C-0077

SRI Project 2997



STANFORD RESEARCH INSTITUTE
Menlo Park, California 94025 • U.S.A.

DISTRIBUTION STATEMENT A
Approved for public release;
Distribution Unlimited

DDC
RECEIVED
DEC 15 1977
B



STANFORD RESEARCH INSTITUTE
Menlo Park, California 94025 · U.S.A.

Final Report

April 1976

MEASUREMENTS OF THE APD AND THE DEGRADATION CAUSED BY POWER LINE NOISE AT HF

By: RICHARD A. SHEPHERD and JAMES C. GADDIE

Prepared for:

DEPARTMENT OF THE NAVY
NAVAL ELECTRONIC SYSTEMS COMMAND
WASHINGTON, D.C. 20360

CONTRACT N00039-74-C-0077

SRI Project 2997

Approved by:

DONALD L. NIELSON, *Director*
Telecommunications Sciences Center

BONNAR COX, *Executive Director*
Information Science and Engineering Division

DISTRIBUTION STATEMENT A

Approved for public release;
Distribution Unlimited

SECURITY CLASSIFICATION OF THIS PAGE (When Data Entered)

REPORT DOCUMENTATION PAGE		READ INSTRUCTIONS BEFORE COMPLETING FORM
1. REPORT NUMBER	2. GOVT ACCESSION NO.	3. RECIPIENT'S CATALOG NUMBER
4. TITLE (and Subtitle)		5. TYPE OF REPORT & PERIOD COVERED
(6) MEASUREMENT OF THE <u>APD</u> AND THE <u>DEGRADATION</u> CAUSED BY POWER LINE NOISE AT HF.		(9) Final Report
7. AUTHOR(s)		6. PERFORMING ORG. REPORT NUMBER
(10) Richard A./Shepherd James C./Gaddie		SRI-Project 2997
9. PERFORMING ORGANIZATION NAME AND ADDRESS		8. CONTRACT OR GRANT NUMBER(s)
Stanford Research Institute ✓ Menlo Park, California 94025		(15) N00039-74-C-0077
11. CONTROLLING OFFICE NAME AND ADDRESS		10. PROGRAM ELEMENT, PROJECT, TASK AREA & WORK UNIT NUMBERS
Department of the Navy Naval Electronic Systems Command Washington, D.C. 20360		12. REPORT DATE
14. MONITORING AGENCY NAME & ADDRESS (if diff. from Controlling Office)		13. NO. OF PAGES
		Apr 1976 158
		15. SECURITY CLASS. (of this report)
		Unclassified (12) 147P.
		15a. DECLASSIFICATION/DOWNGRADING SCHEDULE
16. DISTRIBUTION STATEMENT (of this report)		
Approved for public release; distribution unlimited.		
17. DISTRIBUTION STATEMENT (of the abstract entered in Block 20, if different from report)		
332 500		
18. SUPPLEMENTARY NOTES		
19. KEY WORDS (Continue on reverse side if necessary and identify by block number)		
Man-made noise Communication system degradation NAVELEX man-made Power-line noise Amplitude probability distribution noise program Electromagnetic noise Gap and corona noise Noise measurements Radio noise		
20. ABSTRACT (Continue on reverse side if necessary and identify by block number)		
Measurements of electromagnetic noise from power lines were made by Stanford Research Institute (SRI) in direct support of the Electromagnetic Compatibility Analysis Center (ECAC) in their work in the Naval Electronic Systems Command (NAVELEX) man-made radio noise program. Tests were conducted at 3 MHz in the late spring of 1975 in the vicinity of three power transmission lines (two at 230-kV and one at 115-kV) expected to be sources of corona noise and three low-voltage power distribution lines expected to be sources of gap		

DD FORM 1 JAN 73 1473

EDITION OF 1 NOV 65 IS OBSOLETE

SECURITY CLASSIFICATION OF THIS PAGE (When Data Entered)

19. KEY WORDS (Continued)

20. ABSTRACT (Continued)

noise. The power-line noise was used to degrade the performance of a binary FSK modem (AN/URA-17). Simultaneously, the amplitude probability distribution (APD) of the noise envelope was measured in three bandwidths, and in the unused channel of the URA-17, using specially developed instrumentation and software. This instrumentation samples and digitizes the noise envelope from each receiver at a rate of 200 samples per second and records these samples on magnetic tape. A computer processes the noise samples to calculate the rms noise voltage, (which is convertible to the effective antenna noise factor F_a), the parameter V_d , and the APD. The V_{rms} and V_d measurements were compared with those from a Singer NM-26T receiver. Photographs of both gap and corona noise envelope voltage were made in several bandwidths. Corona noise measurements were made in weather conditions ranging from no-rain to heavy rain.

ACCESSION for	
NTIS	White Section <input checked="" type="checkbox"/>
DDC	Buff Section <input type="checkbox"/>
UNANNOUNCED	<input type="checkbox"/>
JUSTIFICATION	
BY	
DISTRIBUTION/AVAILABILITY CODES	
Dist.	AVAIL or SPECIAL
A	

ABSTRACT

Measurements of electromagnetic noise from power lines were made by Stanford Research Institute (SRI) in direct support of the Electromagnetic Compatibility Analysis Center (ECAC) in their work in the Naval Electronic Systems Command (NAVELEX) man-made radio noise program. Tests were conducted at 3 MHz in the late spring of 1975 in the vicinity of three power transmission lines (two at 230-kV and one at 115-kV) expected to be sources of corona noise and three low-voltage power distribution lines expected to be sources of gap noise. The power-line noise was used to degrade the performance of a binary FSK modem (AN/URA-17). Simultaneously, the amplitude probability distribution (APD) of the noise envelope was measured in three bandwidths, and in the unused channel of the URA-17, using specially developed instrumentation and software. This instrumentation samples and digitizes the noise envelope from each receiver at a rate of 200 samples per second and records these samples on magnetic tape. A computer processes the noise samples to calculate the rms noise voltage, (which is convertible to the effective antenna noise factor F_a), the parameter V_d , and the APD. The V_{rms} and V_d measurements were compared with those from a Singer NM-26T receiver. Photographs of both gap and corona noise envelope voltage were made in several bandwidths. Corona noise measurements were made in weather conditions ranging from no-rain to heavy rain.

CONTENTS

ABSTRACT	111
LIST OF ILLUSTRATIONS	vii
LIST OF TABLES	x
ACKNOWLEDGMENTS	xi
 I INTRODUCTION	 1
A. Background	1
B. Report Format	1
C. Objectives and Scope	2
D. Description of Tests	3
 II SUMMARY AND MAJOR FINDINGS	 5
 III POWER LINE NOISE SOURCES AND TEST SITES	 9
A. Radio Noise from Power Lines	9
1. General	9
2. Gap Noise	10
3. Corona Noise	10
B. Measurement Locations	13
1. The Dumbarton Substation	14
2. The Cupertino Hillside	15
3. The Sunnyvale Dump	19
4. Bernardo Avenue	21
5. Ed Levin County Park	24
6. Agnews Hospital	28
 IV DESCRIPTION OF INSTRUMENTATION AND TEST PROCEDURES	 31
A. General	31
B. Instrumentation	31

1.	Signal Distribution System	35
2.	Modem Performance-Degradation Test System	35
3.	Noise Measurement System	37
C.	Measurement Procedure	50
1.	Setup	50
2.	Calibration	53
3.	Operation	55
V	TEST RESULTS	57
A.	Error-Rate Measurements	57
1.	Background	57
2.	Corona Noise Sources	60
3.	Gap Noise Sources	68
B.	Decrease in Power-Line Noise with Distance	78
1.	Background	78
2.	General Procedure	81
3.	Bernardo Avenue	81
4.	Sunnyvale Dump	84
C.	Comparison of NM-26T Readings with Computed Results	86
D.	The Effects of Rain on the APDs	90
1.	Background	90
2.	230-kV Lines at Cupertino	93
3.	115-kV Lines at the Sunnyvale Dump	97
4.	230-kV Lines at Dumbarton Substation	99
E.	Comparison of Two Samples at Ed Levin County Park	101
APPENDICES		
A.	CALIBRATION OF NOISE MEASUREMENTS TO OBTAIN F_a	105
B.	COMPUTER PROGRAM LISTINGS FOR SRI NOISE MEASURING SYSTEM	115
REFERENCES	141

ILLUSTRATIONS

1. Median Values of Noise Power Spectral Density Approximately Underneath Selected Power Lines	12
2. Measurement Location for 230-kV Lines Entering Substation . .	16
3. Measurement Location on Cupertino Hillside under High 230-kV Lines	17
4. Detected Envelope of Corona Noise from 230-kV Power Lines--3.0 MHz	18
5. The 115-kV Power Lines at the Sunnyvale Dump	20
6. Detected Envelope of Noise from 115-kV Power Lines--3.4 MHz .	22
7. Power Distribution Line at Bernardo Avenue	23
8. Detected Envelope of Gap Noise from Power Distribution Lines--3.0 MHz	25
9. Power Distribution Line near Ed Levin County Park	26
10. Special Examples of the Detected Envelope of Gap Noise from a Power Distribution Line--3.0 MHz	27
11. Detected Envelope of the Noise at the Agnews Location-- 3.0 MHz	29
12. Block Diagram of Noise-Measurement and Modem-Performance Degradation Test System	33
13. Simplified Block Diagram of SRI Noise Measurement Receiver .	40
14. Peak Output Voltage versus Impulse Strength at Input, SRI Receiver, 3.0-MHz, 0.5-kHz Bandwidth	42
15. Impulse Response of SRI Noise Measurement Receiver and of the R1051B Receiver at the Envelope Detector Output, 3.0 MHz	43

16.	APDs of Gaussian Noise at 3.0 MHz--Power Spectral Density 36.0 dBkT _o	46
17.	APDs of the Impulse Response of the SRI Receivers at 3.0 MHz	49
18.	Envelope Detector for R1051B Lower-Sideband IF	51
19.	Peak Output Voltage versus Impulse Strength at Input, Detected Envelope of Lower Sideband of R1051B Receiver . . .	52
20.	Binary Error Rates Caused by Gaussian Noise at 3.0 MHz . . .	59
21.	Binary Error Rates Caused by Corona Noise at 3.0-MHz, 230-kV Lines, Dumbarton Substation	61
22.	APDs of Power Line Noise (Corona) at 3.0 MHz, near 230-kV Lines at Dumbarton Substation	62
23.	Binary Error Rates Caused by Corona Noise at 3.0-MHz, 230-kV Lines, Cupertino Hillside	64
24.	APDs of Power Line Noise (Corona) at 3.0 MHz, near 230-kV Lines in Cupertino	65
25.	Binary Error Rates Caused by Power-Line Noise at 3.4 MHz, 115-kV Lines at Sunnyvale Dump	67
26.	APDs of Power Line Noise at 3.4 MHz, 115-kV Lines at Sunnyvale Dump	69
27.	Binary Error Rates Caused by Gap Noise at 3.0 MHz, under Line at Bernardo Avenue	70
28.	APDs of Power Line Noise at 3.0 MHz, under Distribution Line at Bernardo Avenue	71
29.	Binary Error Rates Caused by Gap Noise at 3.0 MHz, Ed Levin County Park	73
30.	APDs of (Gap) Power Line Noise at Ed Levin Park and of Impulse Noise at 62 dB μ V/MHz, 3.0 MHz	74
31.	Binary Error Rates Caused by Power-Line Noise at 3.0 MHz, under Line at Agnews Hospital	76

32. APDs of Power-Line Noise at 3.0 MHz, under Distribution Line at Agnews Hospital	77
33. Binary Error Rates Caused by Power-Line Noise at 3.0 MHz, near Line at Agnews Hospital	79
34. APDs of Power Line Noise at 3.0 MHz, near Distribution Line at Agnews Hospital	80
35. Gap Noise as a Function of Distance from Line, 3.0 MHz	82
36. Noise from 115 kV Line as a Function of Distance from Line, 3.0 MHz	85
37. Comparison of Power Spectral Density Measurements Made on an NM-26T Receiver with Those Made on SRI's Receivers--3.0 MHz	88
38. Comparison of Power Line V_d Measurements--NM-26T and SRI Receiver	89
39. Comparison of Power Line V_d Measurements--SRI Receivers with 6-kHz and 3-kHz Bandwidths	91
40. Comparison of Power Line V_d Measurements--SRI Receivers with 6-kHz and 500-Hz Bandwidths	92
41. APDs of Corona Noise near 230-kV Lines (Cupertino) in Four Weather Conditions, 3.0 MHz	94
42. APDs of Corona Noise near 230-kV Lines (Cupertino) With and Without Rain, 3.0 MHz	96
43. APDs of Noise near 115-kV Lines (Sunnyvale Dump) in Several Weather Conditions, 3.0 MHz	98
44. APDs of Corona Noise under 230-kV Lines (Dumbarton Substation) in Several Weather Conditions, 3.0 MHz	100
45. APDs of Gap Noise Demonstrating Stability over Many Minutes	102

TABLES

1.	Computed Power Spectral Density and V_d --Gaussian Noise	44
2.	Measured Bandwidths of the Various Receivers	45
3.	Comparison of Parameters from a 5.0-Minute Sample and a 1.4-Minute Subsample	103

PRECEDING PAGE BLANK-NOT FILMED

ACKNOWLEDGMENTS

The planning of the measurements reported here was done in collaboration with Kitt Gilliland of ECAC/IITRI and George Hagn of SRI. James Gillespie of Pacific Gas and Electric Company helped locate appropriate power lines. Bruce Churchill of ECAC/IITRI participated in all phases of the measurements to ensure that the procedures would be clear to ECAC so that the data collected would be appropriate to further ECAC's efforts in developing and validating mathematical models of man-made noise and its effect on communications systems.

PRECEDING PAGE BLANK-NOT FILMED

I INTRODUCTION

A. Background

This report describes measurements by Stanford Research Institute (SRI) of the electromagnetic noise from electrical power transmission and distribution lines and measurements of the effect of the noise (in terms of binary error rates) on a commonly used frequency-shift-keyed (FSK) communication system. These measurements were made for the Naval Electronics Systems Command (NAVELEX).^{*} The purpose of the measurements was to further the mathematical modeling of man-made noise and the study of its effects on communications systems being done by the DoD Electromagnetic Compatibility Analysis Center (ECAC). All data collected in this measurement project were provided to ECAC immediately after they had been gathered and have already been the subject of an ECAC report by Churchill.⁶ This report discusses the conditions under which the measurements were made to provide some insight for their interpretation.

B. Report Format

The remaining sections of this introduction discuss the project's objectives, explain the scope of the effort, and briefly describe the tests.

^{*} The NAVELEX man-made noise program was described by Gillilland¹; previous reports in the program (dealing with automobile ignition noise) were by Cohen,² Shepherd et al.,³ Gillilland and Brewer,⁴ and Gillilland.⁵

Chapter II summarizes a few of the more important findings from the measurements. Chapter III discusses the sources of power-line noise in general and then describes the specific measurement sites SRI used and the rationale for choosing them. Chapter IV describes the measurement instrumentation and procedures. Chapter V provides detailed measurement results and includes the error-rate measurements, plots of noise attenuation with distance, a comparison of measurements made on SRI's hardware/software system with others made using the Singer NM-26T noise meter, and a discussion of the effect of rain on the APDs of corona noise. Appendix A shows how SRI's calibration method provides absolute, rather than relative, noise power measurements; Appendix B lists the data-processing computer program.

C. Objectives and Scope

The tests described in this report were conducted to provide ECAC with data on radio noise from power lines, at HF, measured simultaneously with measurements of the effects of the noise (interference) on a receiving system consisting of a R1051B/URR radio receiver (commonly called a R1051B) and a CV-483C/URA-17 FSK demodulator (usually called a URA-17). The noise measurements were expected to be useful to ECAC in developing mathematical models for the amplitude probability distribution (APD) of power-line noise; the measurements of the effect of the noise should be useful in checking error-rate models.^{4,5}

In this program SRI's intent was to be completely responsive in providing the measurements requested by ECAC for use in its modeling work. This report details the measurement conditions, the instrumentation and procedures, the data processing methods, and the problems encountered, and gives other information pertinent to a complete understanding of the data as presented. The raw data, consisting of log sheets, chart records, computer printout and plots, and the computer program, together with copies of the original magnetic tapes, were provided to ECAC while measurements were under way, to facilitate its modeling work. Our analysis of the data is limited to that required for an understanding of the conditions under which the data were collected, processed, and displayed. It was not within the scope of this project to relate the data to the models under development by ECAC.

D. Description of Tests

The major noise measurement desired by ECAC was the APD of the power-line noise. We can measure the APD of this noise in four different bandwidths simultaneously. To make these measurements we developed a combination hardware/software system based on an earlier system⁷ whose software had been modified to provide APDs.³ For this project we further improved the system by constructing a receiver portion featuring three IF sections of different bandwidths, following a single RF section. We also used the system to digitize the noise voltage in the lower sideband of the

R1051B, thus providing APDs from the lower sideband at the same time that we measured the errors--caused by the same noise--in the upper sideband. These APDs were not very satisfactory because of the relatively narrow dynamic range of the R1051B.

We made simultaneous measurements of the URA-17's error rate and the power-line noise APDs at six locations, selected because they were near power lines with either gap noise or corona noise.

We provided oscilloscope photographs of the envelope of noise voltage that demonstrated the effect of the bandwidth on the noise and also showed the difference between gap noise and corona noise. The rate of decrease of noise with distance from both gap and corona noise sources was examined.

To ensure that our power-line noise measurements were contaminated as little as possible by noise from other sources, such as automobiles, we chose isolated sites and a measurement frequency of 3 MHz (power-line noise drops off rather rapidly with frequency above about 1 MHz,⁸ whereas automobile ignition noise does not).

We used a calibrated antenna, and we calibrated the system so as to provide absolute noise measurements. The rms noise voltage value on an APD corresponds to the noise power spectral density parameter F_a .

II SUMMARY AND MAJOR FINDINGS

The project objectives were to provide ECAC with measured data on power-line noise and its effects for ECAC's use in developing models for that noise, to serve as input to their receiver performance models. Therefore the project's principal product was the data already furnished ECAC, most of which (except for chart records, computer printouts, and some APDs) are incorporated into this report. The major benefit of the work consisted of furthering ECAC's development of mathematical models for the NAVELEX man-made radio noise program.

Our experiences in the collection and the analysis of these data resulted in some observations concerning power-line noise, which are summarized below. Supportive data and discussions for these statements can be found in other sections of the report, chiefly in Chapter V.

- (1) Radio noise from power lines consists of gap noise and corona noise. Although there is a generally accepted line voltage threshold (about 70 kV) above which gap noise is not expected, we believe we observed both gap and corona noise from a 115-kV line.
- (2) We observed the attenuation of gap and corona power-line noise power spectral density with distance at the rate of about 20 dB per distance decade ($1/r^2$) at 3 MHz. The power-line noise decreased to background noise level within 100 to 200 ft.
- (3) Both gap and corona noise as seen by a receiver consist of individual impulse responses, which may or may not overlap, depending on the impulse repetition rate and the receiver bandwidth.

- (4) Gap noise may consist of such impulses occurring as infrequently as 60 times per second (for a 60-cycle power line). More rapid occurrence of pulses, with groups of pulses bunching in time near line voltage maxima, is more common.
- (5) When gap impulses do not overlap, the APD of the noise is essentially the APD of the receiver's impulse response.
- (6) The short-term rms value of gap noise is highly variable. Changes of 6 dB from second to second have been observed, as various gaps became active and then ceased. No change would have been observed by using a peak detector.
- (7) The longer-term rms values and APDs of this same gap noise (representing integration over 5-minute periods a half-hour apart) are quite stable.
- (8) The rms value of corona noise changes much more slowly than that of gap noise. We observed changes of 1 or 2 dB over periods of several minutes.
- (9) Such changes (8) can usually be associated with changes in the rainfall, although not necessarily at the measurement site itself, implying that the noise propagates along the line.
- (10) We saw 20-dB increases in the corona noise power spectral density from no-rain to rain; this amount is similar to observations by others using quasi-peak meters.
- (11) As rain falls on the line, isolated strong impulses are observed from the receiver; as the rain increases, the number (or rate of occurrence) of these impulses increases.
- (12) We usually observed a rain-related increase of 1 dB or less in the parameter V_d for corona noise, but this was not always the case.
- (13) We did not note any appreciable difference between the V_d of gap and that of corona noise; for both it was around 1.2 to 5, depending on bandwidth.

- (14) The APD for both gap and corona noise generally showed a lower V_d (by 4 or 5 dB) than that of the noise from automobile traffic.
- (15) We made absolute APD measurements (the 0-dB level on the APD is F_a), but our data base is not large enough to suggest whether the noise is generally greater from gap-noise or from corona-noise sources.
- (16) The noise power spectral density measurements made with the three SRI receivers generally agreed within a few tenths of a decibel.
- (17) Both the noise power spectral density (F_a) measurements and the V_d measurements made with the NM-26T generally agree within about 1 dB with those made with the SRI receivers.

III POWER-LINE NOISE SOURCES AND TEST SITES

A. Radio Noise from Power Lines

1. General

The function of a power line, that is, the transmission or distribution of power, determines its operating voltage and thereby the mechanisms by which it produces noise under normal operating conditions. In general, the lower-voltage distribution and transmission lines (below about 70 kV) produce noise from various types of discharges at gaps, while the higher-voltage transmission lines (110 kV and higher) generate noise by various kinds of corona.⁹

Most of the measurements of power-line noise reported in the literature have been made using quasi-peak detectors, although some data on power-line noise measured with peak and average detectors are available.¹⁰ Measurements made with an rms detector have only recently become available in the literature;¹¹ some have been given by Hagn and Shepherd,¹² Disney and Longly,¹³ and Spaulding and Disney.¹⁴ APD measurements of power-line noise were reported in Ref. 13 and by Lauber,¹⁵ although no simultaneous or accompanying measurements of the degradation to communication systems were made. From the standpoint of potential for causing such interference, power-line noise sources are generally objectionable at HF and below.

2. Gap Noise

Gap noise is the noise resulting from a current discharge between two metal objects (sparks) or between a metal object and an electrically charged surface (microsparks).¹⁶ The sources of gap noise include air gaps at insulators, loose tie wires, loose hardware on the pole, or corroded joints between wires or hardware. It is not necessary that the metal at either side of a gap be connected to the conductor; high voltages can be induced in nearby objects. Most types of gap noise are more prevalent during dry weather. Frequently, a gap noise source will disappear at night when dew bridges the gap and will reappear in the morning after a few hours of warming in the sun. Wooden power poles and crossarms absorb moisture during wet weather and expand slightly; they tend to shrink during dry hot periods. This results in loose hardware during dry periods and tight hardware during wet periods. Following an unusually late and wet spring, the weather was still rainy during most of the time we were searching for these gap noise sources. Therefore the gap noise was not present at some locations where we had observed it before. The same scarcity of gap-noise sources provided us with an excellent opportunity for observing the noise from a single gap breaking down once per cycle (at Ed Levin County Park), as discussed later.

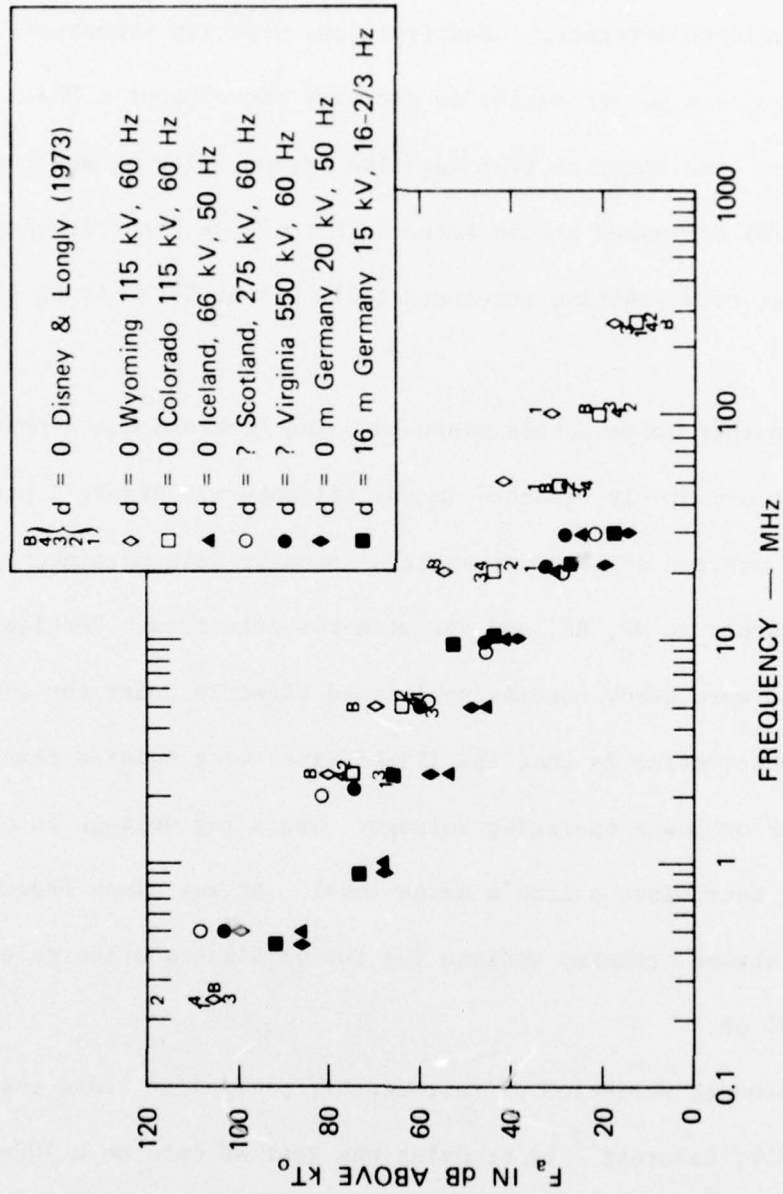
3. Corona Noise

The primary noise source on power lines above about 110 kV is corona. Although gap noise can and does occur on high-voltage transmission

lines, the gaps can usually be found and eliminated. Several types of corona discharge contribute to the radio noise from high-voltage transmission lines (positive streamers, negative glow, negative streamers, and so on). The noise from corona begins to decrease above about 1 MHz. According to Juette,⁸ the spectrum from negative corona (glow as well as negative streamers) decreases at the rate of 20 to 25 dB per frequency decade, while that from positive streamers falls off at 35 to 40 dB per decade.

Fair-weather noise levels measured using peak and quasi-peak detectors have been commonly reported in the literature. Figure 1 presents median values of average noise power spectral density data obtained by several investigators at MF, HF, and VHF with rms detectors. Vertical monopole antennas were used, usually positioned directly under the line. An interesting observation is that the 115-kV lines were noisier than the lines with higher or lower operating voltage. Operating voltage is not the only factor that determines a line's noise level. At any given frequency, the difference between measured medians for the noisiest and the quietest line was about 30 dB.

The seasonal variation of fair-weather power-line radio noise was investigated by LaForest¹⁷ by studying one year of data on a 500-kV line in the northeastern United States. He noted the effects of relative air density, relative humidity, and wind speed, as well as seasonal



SOURCE: HAGN and SHEPHERD (1974).

TA-913522-11R1

FIGURE 1 MEDIAN VALUES OF NOISE POWER SPECTRAL DENSITY APPROXIMATELY UNDERNEATH SELECTED POWER LINES

variations, and he deduced correction terms for fair-weather RI levels (field strengths measured with a quasi-peak detector). He noted that summer readings were higher than winter readings by about 12 dB.

Pakala and Chartier¹⁸ stated that corona noise RI level increases of 17 dB were likely during rain. The IEEE has indicated increases of 15 to 25 dB in quasi-peak readings during foul weather.^{19,20} Data on RI levels taken on a Bonneville Power Administration 345-kV line over a year²¹ showed an average RI level during rain approximately 20 dB above that during clear weather, while during snow the average level was nearly 26 dB higher than the clear-weather level. Forrest pointed out that "defect" noise on lower-voltage (11- to 66-kV) lines, caused by sparks and micro-sparks, tended to determine the fair-weather RI levels above 10 MHz.²² He noted that wet weather could cause RI increases of 5 to 15 dB in the band 100 kHz to 10 MHz, due to corona, and cause RI decreases above 10 MHz, due to the shorting out of arcing gaps.

B. Measurement Locations

We made measurements of the power-line noise and its effect on the error rate of the FSK modem at several different sites, to obtain both gap and corona noise, and in both wet and dry conditions, to observe the effect of foul weather on the corona noise.

Corona-noise sources were relatively easily found (particularly in damp weather), since there are many high-voltage power transmission lines

on the San Francisco Peninsula. However, because of the urbanization that demands this power, transmission lines that are isolated from vehicle traffic, industrial areas, homes, and other contaminating sources of noise, are few. To avoid the problem of contamination of the corona noise with noise of other types, we had to find places where the other noise sources were not present. These were generally rather inaccessible spots--on bay fill land or steep hillsides.

Gap noise is to be expected from the lower-voltage power distribution lines, such as those that serve an urban area. These lines typically run along streets and roads; therefore measurement locations isolated from other sources of noise are difficult to find in a relatively heavily populated area. The problem was complicated by the wet weather which had apparently caused closure of many of the gaps. We found three locations that fit our criterion of having active gap noise but no other known noise sources in the vicinity.

The measurement sites are described below. The first three were chosen to observe corona noise; the last three were chosen as gap-noise sources.

1. The Dumbarton Substation

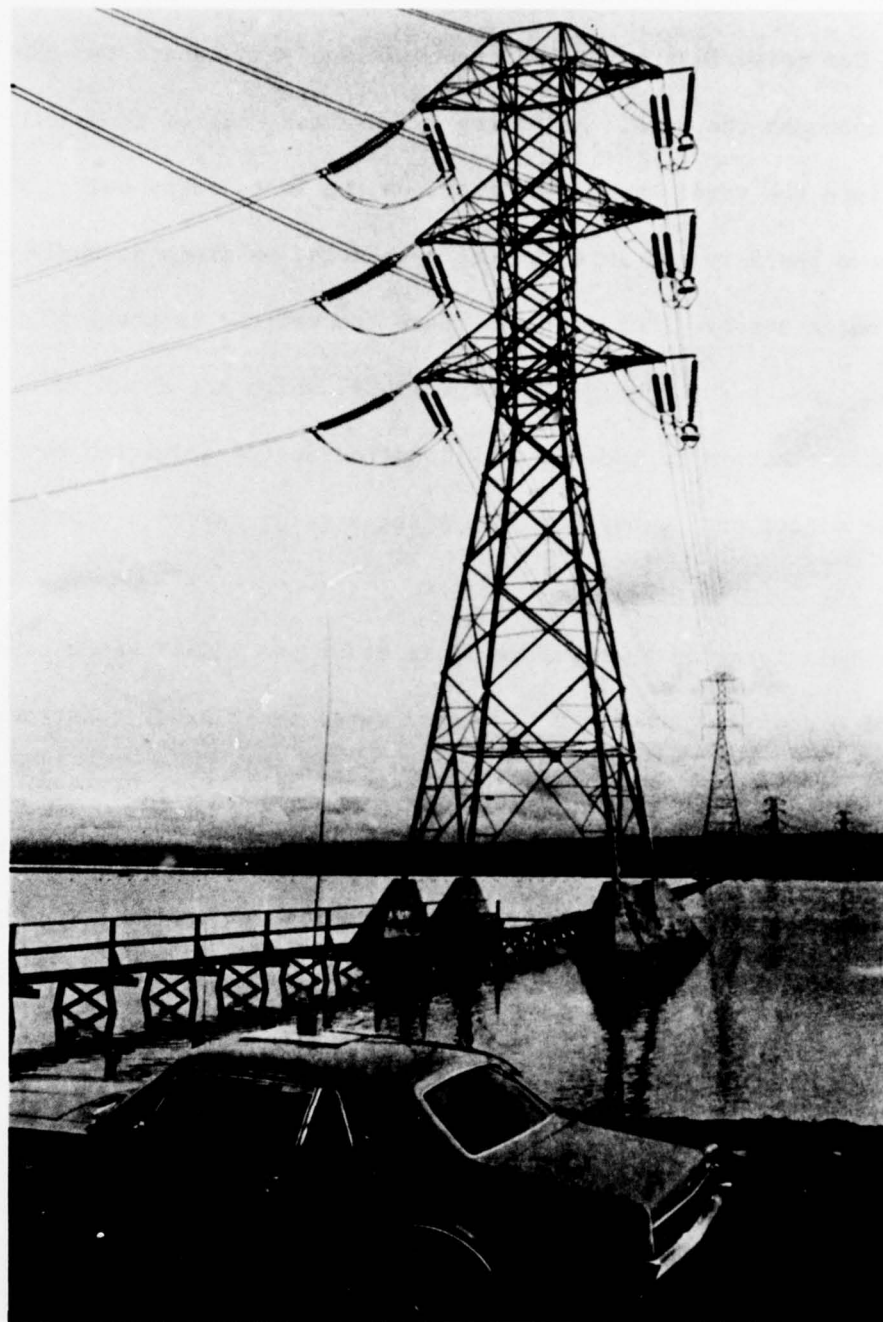
This substation or switching yard covers 3 or 4 acres about 100 m off the western approach to the Dumbarton Bridge, which crosses the southern part of San Francisco Bay. The yard is built on fill just at the edge of

the bay. Our measurements were made outside the yard, where two 230-kV circuits approach the yard. As Figure 2 indicates, one of these circuits descends into the yard, while the other, on the left, turns away. This figure shows the 9-ft rod antenna atop a vehicle, as it is commonly used in radio noise surveys (Ref. 23-29). Here the vehicle is about 50 ft (16 m) from a point under the double-conductor lines, which are about 30 ft (10 m) high. Measurements were made at this location during a driving rain with gale-force winds; on a windy day just after a rain; and on a clear day.

2. The Cupertino Hillside

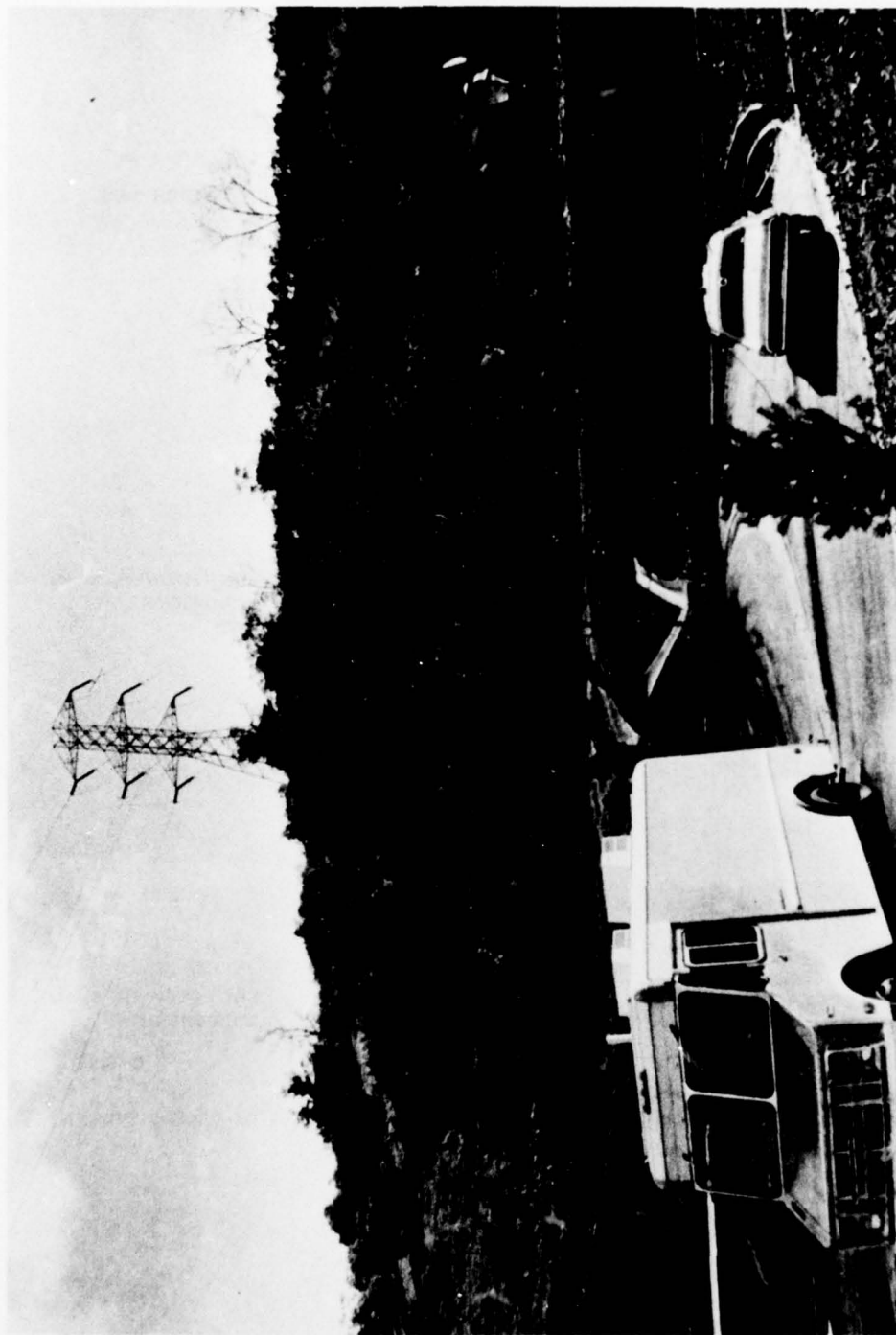
This location (see Figure 3) is under two 230-kV circuits at the end of a dead-end street in a housing development under construction in Cupertino. The double-conductor lines are very high here, probably more than 100 ft, although the height was difficult to estimate because the surroundings are so hilly. Measurements were made at spots 60 ft and 100 ft (about 20 m and 33 m) from the centerline of the two circuits and during light rain, hard rain, and no rain. In the figure, the car is 100 ft from the centerline. The van contained our measurement equipment.

Figure 4 shows photographs of the detected envelope of the corona noise from these lines in two bandwidths. In these bandwidths the noise consists of relatively continuous--and probably overlapping--impulses. Corona discharges are, of course, most likely to occur as the voltage on a line reaches its maximum. There is a voltage maximum every 2.77 ms from



SA-2997-1

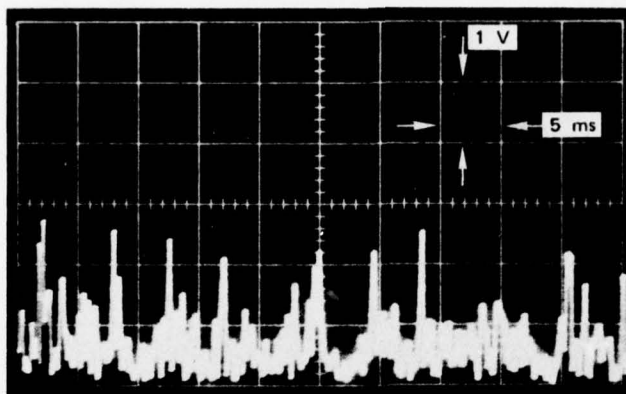
FIGURE 2 MEASUREMENT LOCATION FOR 230-kV LINES
ENTERING SUBSTATION



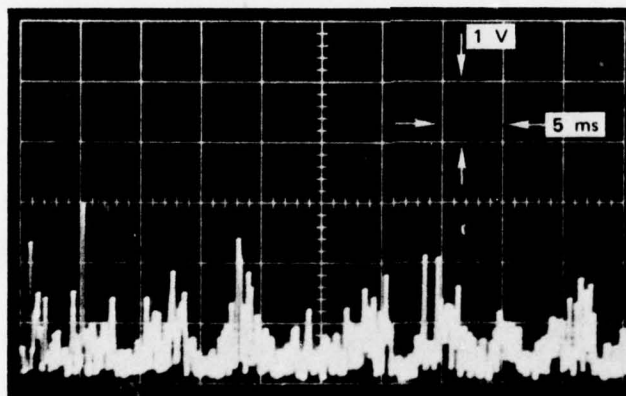
SA-2997-2

FIGURE 3 MEASUREMENT LOCATION ON CUPERTINO HILLSIDE UNDER HIGH 230-KV LINES

MEASURED AT 50 ft FROM LINE CENTERLINE IN CUPERTINO, 19 MARCH 1975



(a) SRI RECEIVER, 3-kHz
BANDWIDTH



(b) SRI RECEIVER, 6-kHz
BANDWIDTH

SA-2997-3

FIGURE 4 DETECTED ENVELOPE OF CORONA NOISE FROM 230-kV POWER
LINES—3.0 MHz

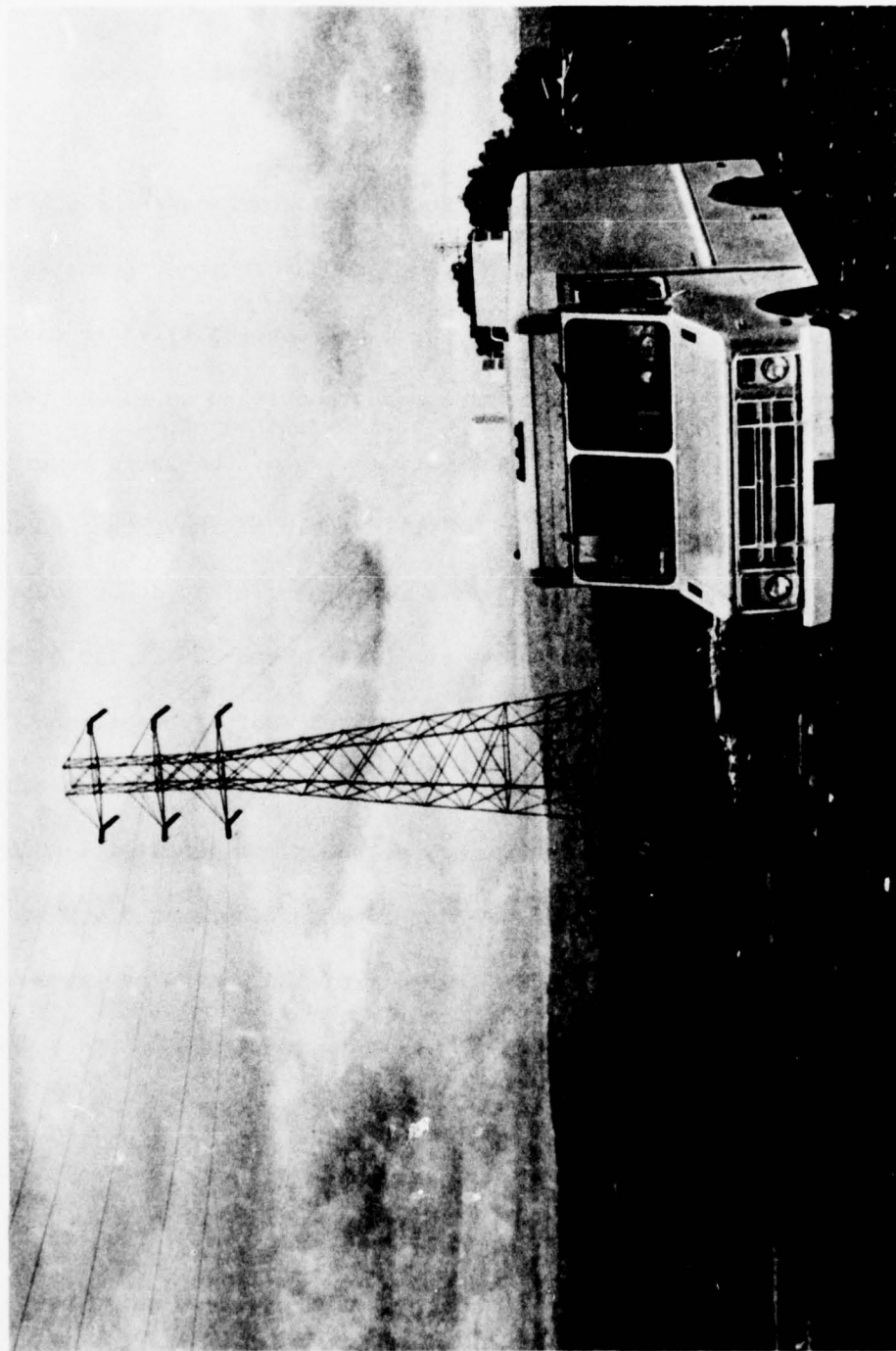
one or another of the lines on the 60-cycle three-phase circuit, but no such relation can be seen in these photographs of the noise.

3. The Sunnyvale Dump

Two 115-kV circuits spaced 17 ft (5.6 m) apart pass through the Sunnyvale Dump area on the edge of San Francisco Bay at its extreme south tip. Here the bare ground was generally wet, and the (salt) water table was about 3 ft below the ground. We made measurements in an unused portion of the sanitary landfill dump at a spot between two of the large towers; the lower conductors were about 25 to 30 ft (8 to 10 m) above the ground. We made more measurements at the Sunnyvale Dump than at any other location. The measurements were made at distances of 50, 100, and 200 ft (16.4, 32.8, and 65.6 m) from the centerline and during various weather conditions. Figure 5 shows the measurement van and the general surroundings. Because on our usual 3.0-MHz measurement frequency we sometimes experienced contamination of the noise by signals, we also took data here at 3.4 MHz.

We made measurements of the fall-off of the rms noise level with distance from this line, using the NM-26T at various points out to a distance of 500 ft (164 m) from the center of the two circuits.

Although the lines at the dump were selected as a probable corona-noise source, analysis of our data lead us to believe that there were probably active gaps during dry weather. The greatest noise power measured here occurred after several days of dry weather and exceeded even



SA-2997-4

FIGURE 5 THE 115-KV POWER LINES AT THE SUNNYVALE DUMP

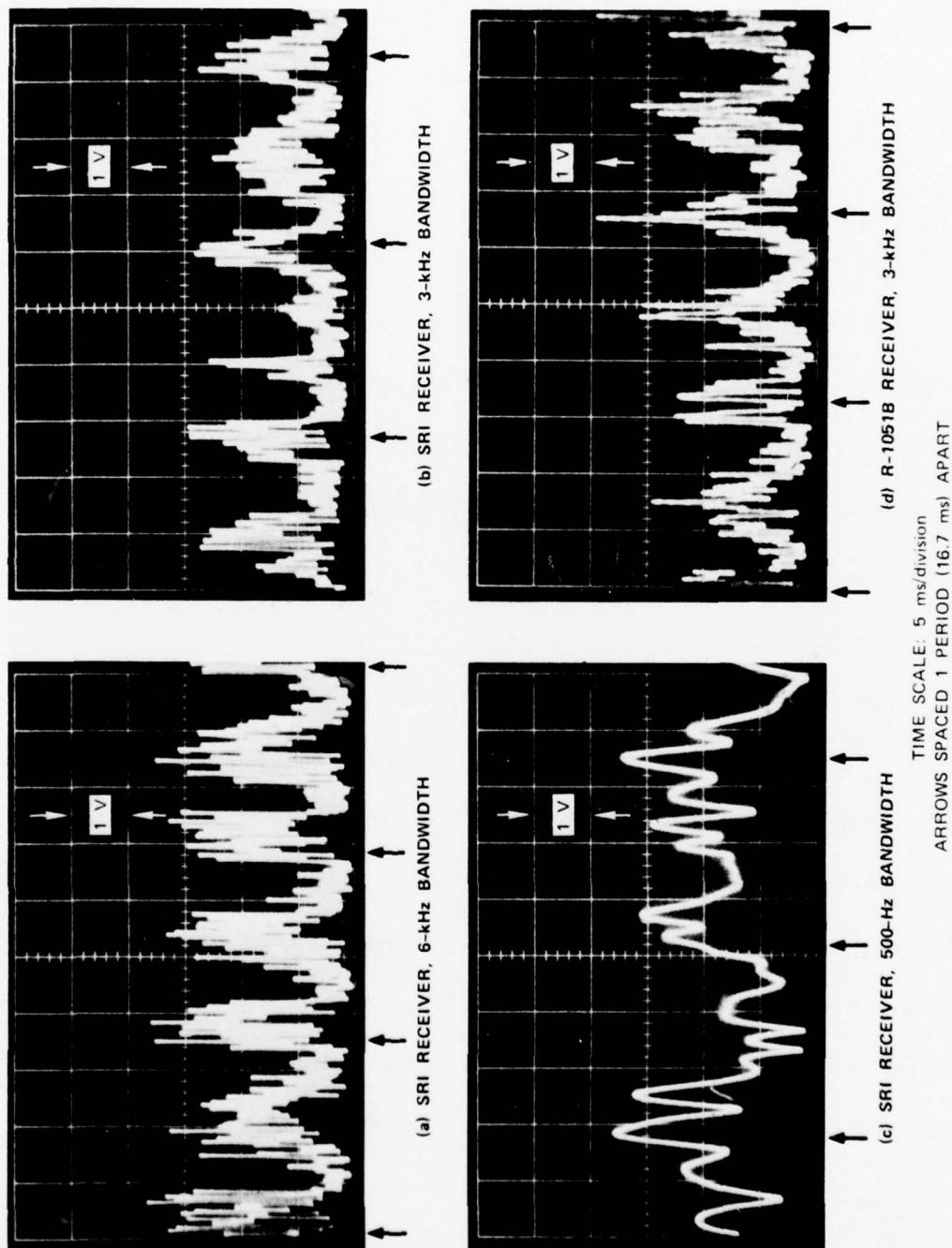
that measured in heavy rain. On damp days, we sometimes noticed periods when the noise abruptly "turned on" and the indicated rms level increased by 8 or 10 dB for periods of from a fraction of a second to several minutes. This behavior suggests gap noise. Figure 6 shows photographs of the time waveforms of this noise in several bandwidths. In the 500-Hz bandwidth the impulse responses overlap. In the wider bandwidths, we see individual impulse responses occurring in two groups per cycle^{*} (i.e., two groups every 16.67 ms). That timing indicates that the source of impulse groups is associated with only one phase of the 3-phase, 115-kV circuit. It is possible that one or more gaps were being fired many times near both the positive and the negative voltage maxima.

4. Bernardo Avenue

We believe that there was a gap noise source(s) within the hardware on the pole shown in Figure 7. The pole carries a distribution line (probably about 12 kV) at the top. Below that is a 220-volt system that supplies three or four homes along the road in this mostly undeveloped section of Sunnyvale. None of the homes was closer than about 100 m from the pole. A telephone line is below the two power lines. The lines change direction slightly here, and the pole is guyed. Measurements here were made only on dry days. APD measurements were made under the line, about

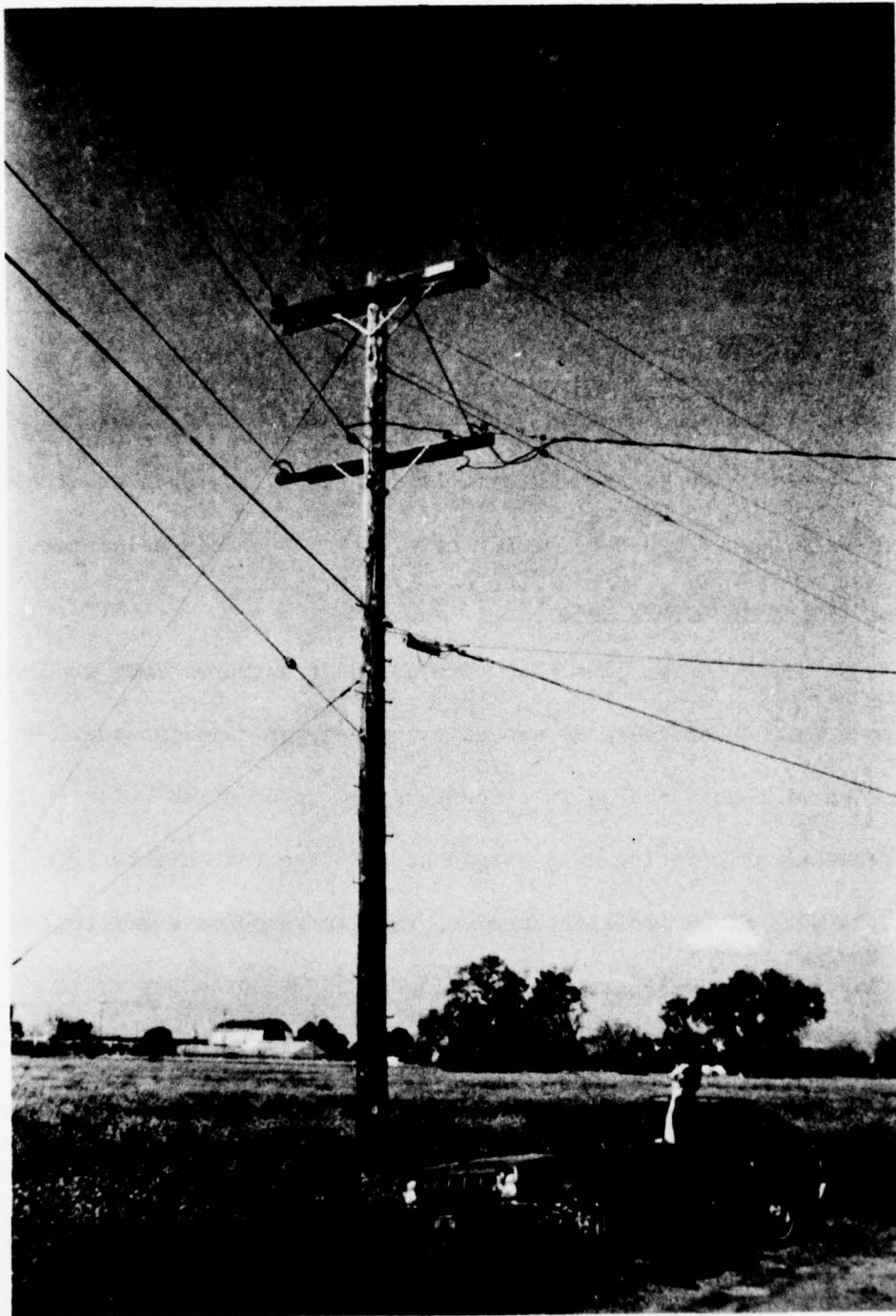
^{*} There is a striking resemblance between these photographs and some reported on a 15-kV, 16.67-Hz line by Hagn.²³

MEASURED 50 ft FROM LINE AT SUNNYVALE DUMP, 19 MARCH 1975



SA-2997-5

FIGURE 6 DETECTED ENVELOPE OF NOISE FROM 115-kV POWER LINES—3.4MHz



SA-2997-6

FIGURE 7 POWER DISTRIBUTION LINE AT BERNARDO AVENUE

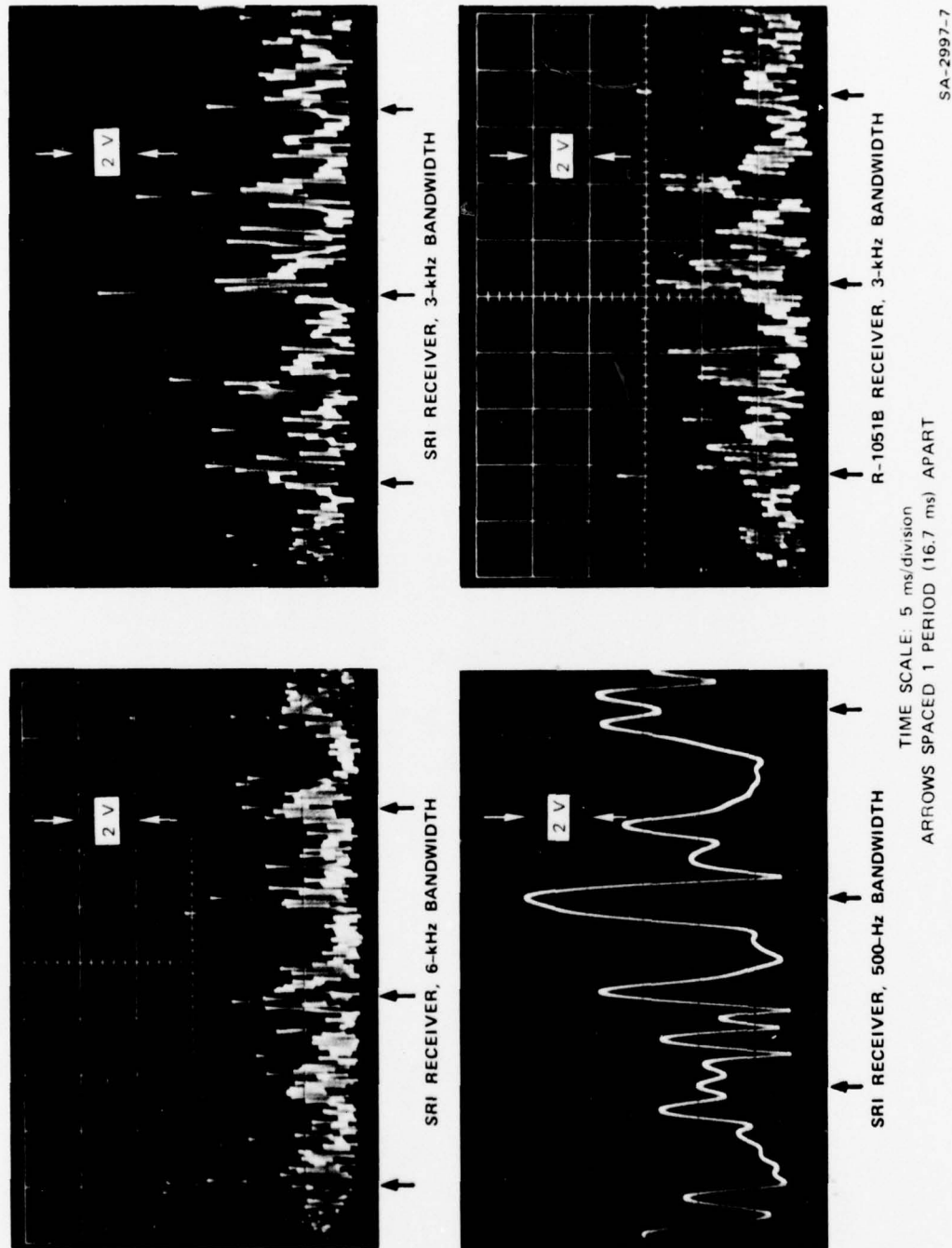
50 ft (16 m) from the pole; rms field strength measurements were made at several points in the field, out to a distance of 300 ft (98 m) from the pole.

Figure 8 shows time waveforms of the gap noise observed here. Many impulses appear, but bunching of the higher impulses is visible twice per cycle, indicating that one of the three phases probably had a gap source (or several such sources) stronger than any on the other two phases. Although the bunching is apparent, it is not as obvious as that at either the Sunnyvale Dump (Figure 6) or Ed Levin Park (to be discussed next).

5. Ed Levin County Park

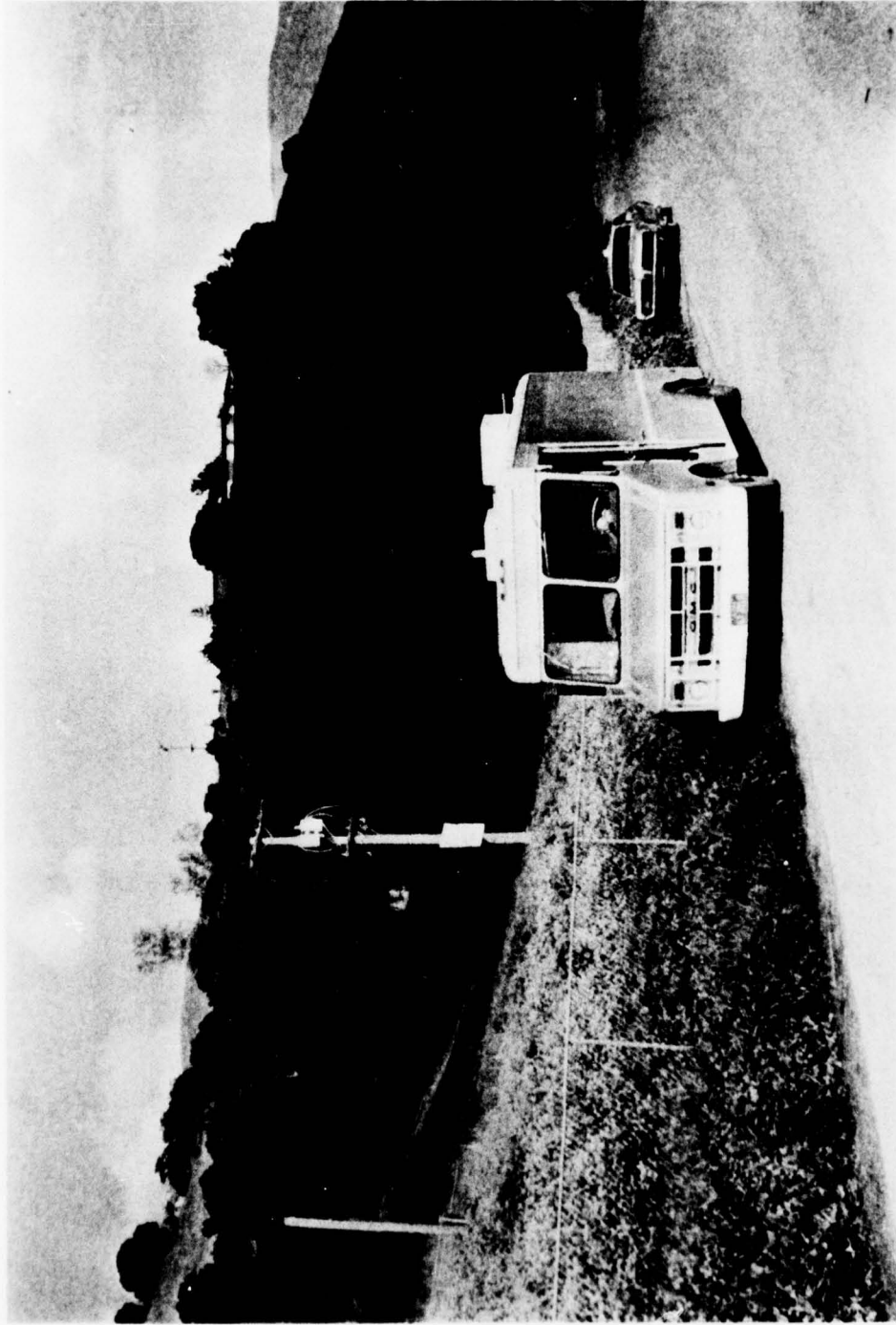
A distribution line that terminated at a transformer supplying power to a pump (see Figure 9) was an excellent gap-noise source. Here, at the edge of a golf course in a county park, we observed noise that we interpreted as originating at a single gap. Often [see Figure 10(a)] this noise consisted of an isolated receiver impulse response every 16.7 ms, indicating that a single gap was breaking down just once per cycle of the 60-cycle voltage waveform. At times, at this location, we observed an impulse response at the same level every 8.3 ms, probably a single gap breaking down at both the positive and the negative peaks of the 60-cycle wave. This can be seen in Figure 10(b), which shows that once the gap failed to fire at one polarity. At still another time [Figure 10(c)] we could observe single impulse responses every 16.7 ms (at or near the maximum of one polarity), interleaved with groups of three closely spaced

MEASUREMENTS MADE APPROXIMATELY UNDER LINE, BERNARDO AVENUE, 18 MARCH 1975



SA-2997-7

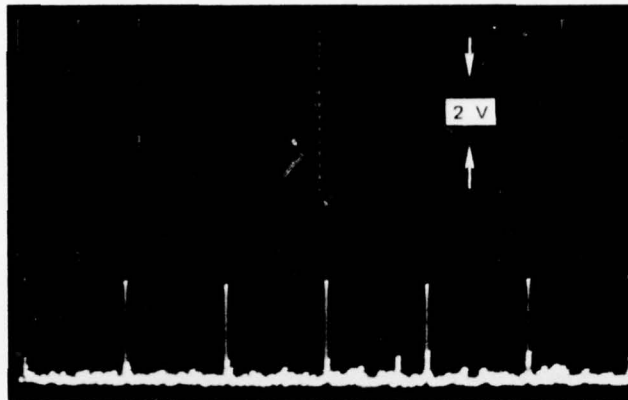
FIGURE 8 DETECTED ENVELOPE OF GAP NOISE FROM POWER DISTRIBUTION LINES—3.0 MHz



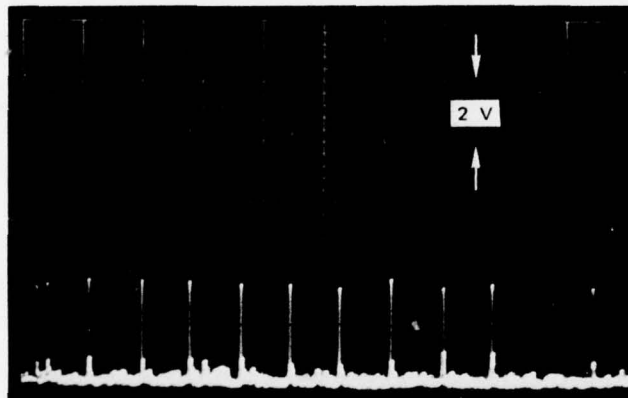
SA-2997-8

FIGURE 9 POWER DISTRIBUTION LINE NEAR ED LEVIN COUNTY PARK

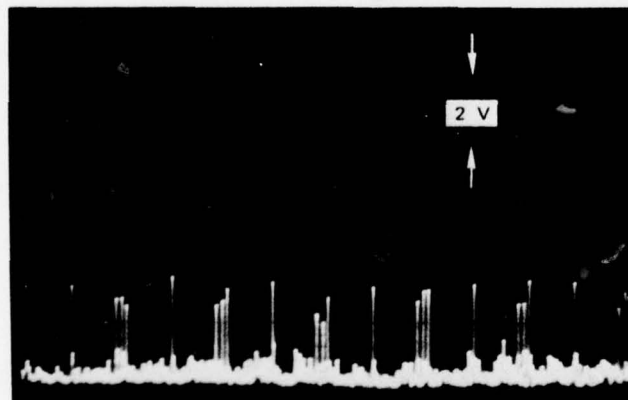
MEASURED AT ED LEVIN COUNTY PARK, 18 MARCH 1975 — WARM, SUNNY WEATHER



(a) A SINGLE GAP FIRING PER CYCLE
(EVERY 16.7 ms)



(b) A GAP FIRING TWICE PER CYCLE
(EVERY 8.3 ms)



(c) A COMPLEX PATTERN OF GAP
FIRINGS

MEASUREMENT BANDWIDTH: 6-kHz
TIME SCALE: 10 ms/division

SA-2997-9

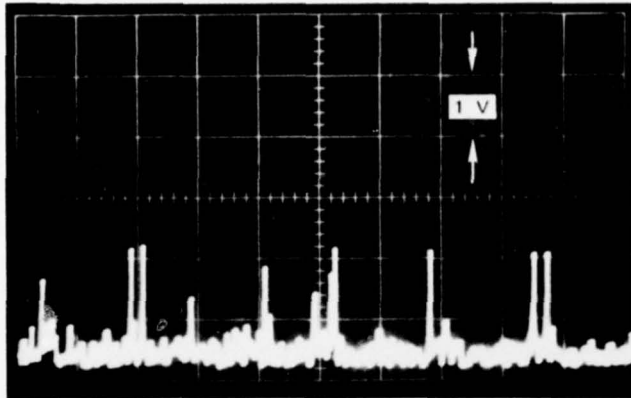
FIGURE 10 SPECIAL EXAMPLES OF THE DETECTED ENVELOPE OF GAP NOISE FROM
A POWER DISTRIBUTION LINE—3.0 MHz

impulses, also occurring every 16.7 ms (near the maximum of the other polarity). The nature of the noise--the number of active gaps--changed abruptly from minute to minute, and the changes could be both heard on the NM-26T and observed by abrupt variation in the indications on the NM-26T's rms and V_d meters. A peak detector, commonly used to measure power-line noise, would have remained stable, because, as Figure 10 shows, the pulse height remained the same.

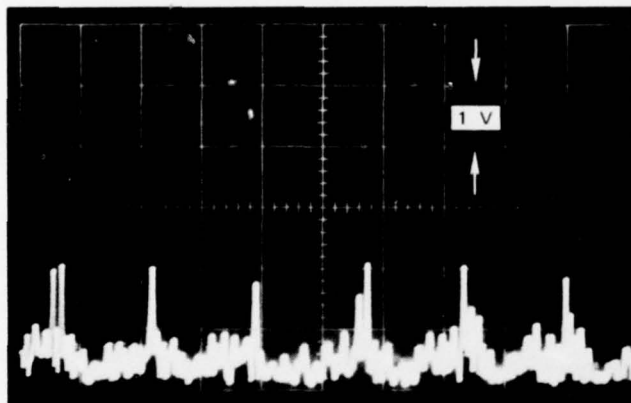
6. Agnews Hospital

This last measurement site was the edge of a road on the grounds of the large mental hospital. The three-phase line (probably 24-kV) ran on wooden poles parallel to the road. No other sources of man-made noise were known to be in the vicinity. The gap noise here was not as clearly defined as at Ed Levin Park. There were apparently a number of active gaps; we could see many receiver impulse responses per cycle of the 60-cycle ac, although there were always prominent pulses occurring every 8.3 ms. These pulses may have been either from major gaps or from closer gaps. Figure 11 shows photographs of the noise time waveforms. At times there may have been some corona noise. The noise was very unstable, changing in rms level by several decibels from one minute to the next.

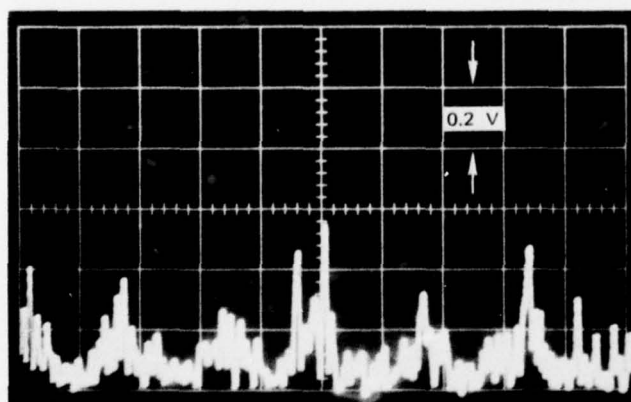
MEASURED DIRECTLY UNDER POWER DISTRIBUTION LINE



(a) SRI RECEIVER, 6-kHz BANDWIDTH
(1204 PDT)



(b) SRI RECEIVER, 3-kHz BANDWIDTH
(1209 PDT)



(c) R-1051B RECEIVER, 3-kHz BANDWIDTH
(1212 PDT)

TIME SCALE: 5 ms/division

SA-2997-10

FIGURE 11 DETECTED ENVELOPE OF THE NOISE AT THE AGNEWS LOCATION—3.0 MHz

IV DESCRIPTION OF INSTRUMENTATION AND TEST PROCEDURES

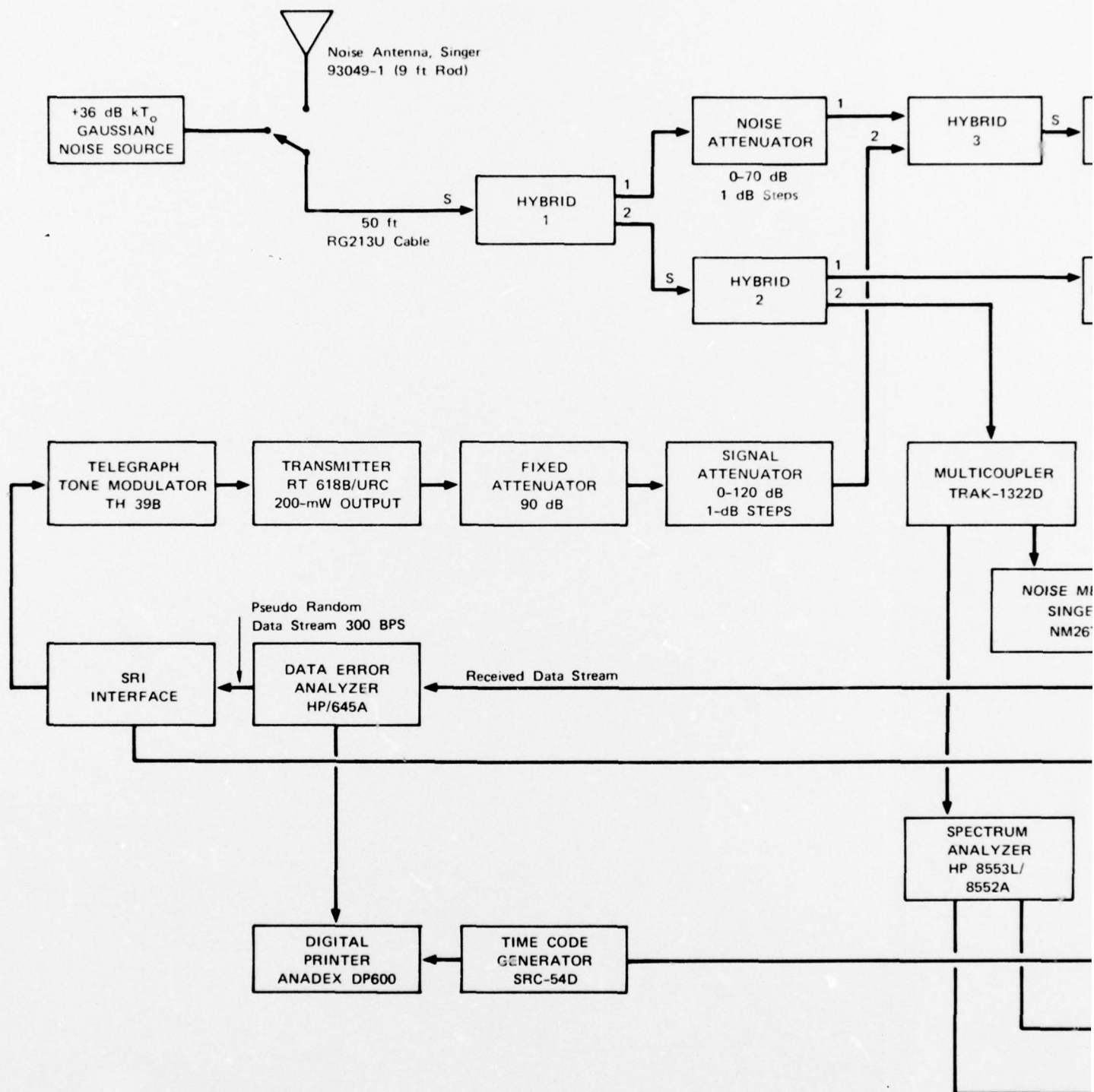
A. General

This chapter discusses the complex instrumentation that we set up to measure the radio noise from the power lines and the effect of that noise upon an HF FSK modem. We measured the APD, the rms value, and the impulsiveness parameter, V_d , of the noise. We measured degradation in performance in terms of the binary error rate caused by the noise. The overall measurement system has two major parts: the hardware and the software. The following sections concentrate on the hardware. The software is almost entirely the same as used in our previous work--on automobile ignition noise.³ It required only minor changes, because we now use envelope detectors instead of the quadrature detectors and because we developed a system to plot the receiver noise on the APD automatically.* Appendix B is a listing of the computer program.

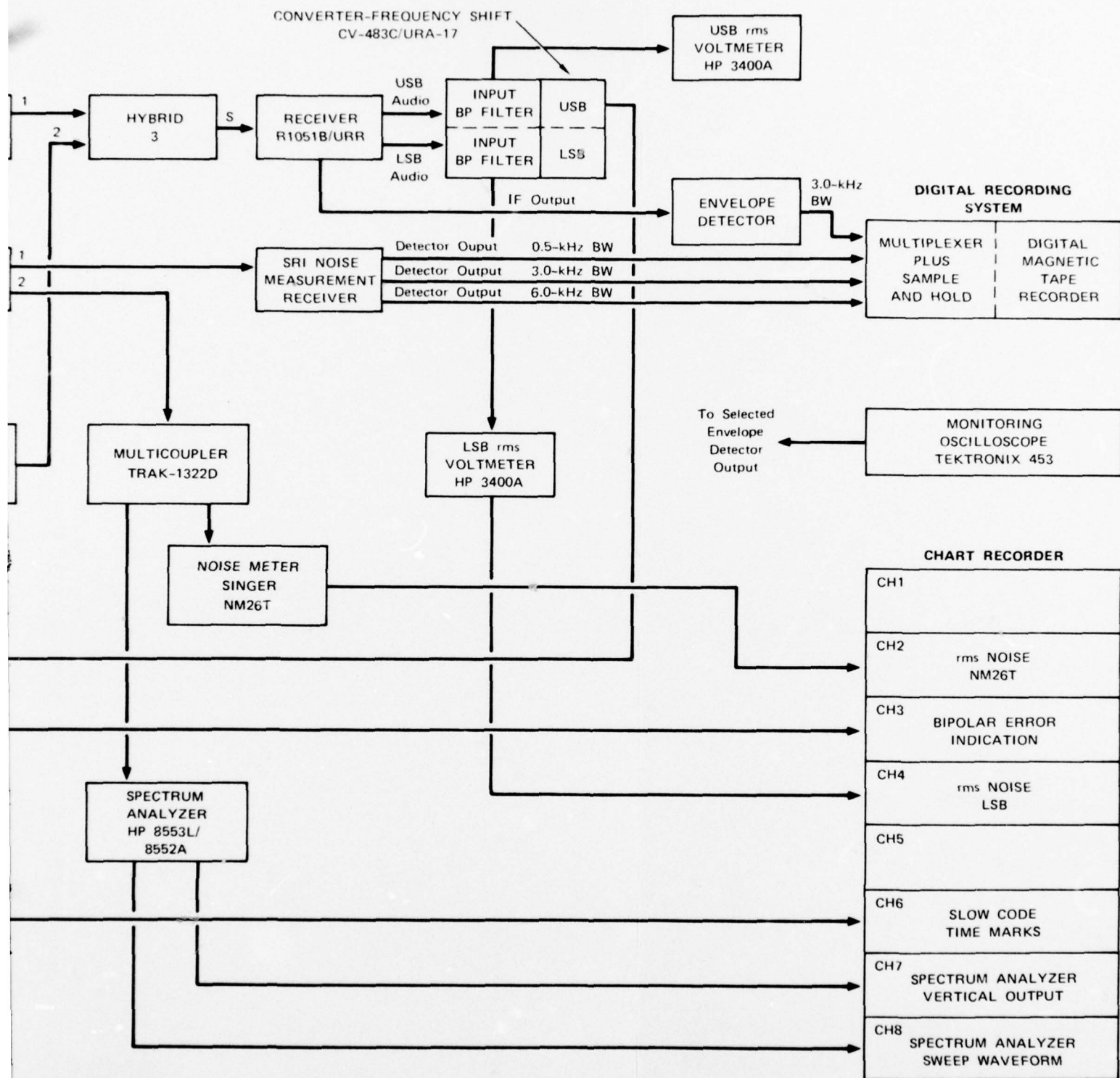
B. Instrumentation

An overall block diagram of the noise measurement system and the modem degradation test system is shown in Figure 12.

* This procedure had a bug that was not discovered until most of the computer runs had been completed. The listing in Appendix B is without that bug.



PRECEDING PAGE BLANK-NOT FILMED



SB-2997-11

FIGURE 12 BLOCK DIAGRAM OF NOISE MEASUREMENT AND MODEM-PERFORMANCE-DEGRADATION TEST SYSTEM

2

1. Signal Distribution System

A Singer 93099-1 9-ft rod antenna was used to receive the noise. This antenna, normally used with the Singer NM-25T and NM-26T noise meters, was placed atop a vehicle that served as a ground plane. The antenna distribution system consists of three hybrids and an active multicoupler.

A Gaussian noise source with power spectral density of 36 dBkT_0 was used as a calibration source at the antenna terminals. Noise from the antenna or the Gaussian noise source entered Hybrid 1, which served as a 3-dB power divider. The two outputs of Hybrid 1 went to Hybrid 2 and to Hybrid 3. Hybrid 3 was used to combine the power-line noise with the signal from the RT618/URC transmitter. The combined signal and noise were provided to the input terminals of the R1051B/URR receiver, which was part of the modem degradation test system, described next. Hybrid 2 functioned as a second 3-dB power divider for the noise; its outputs were provided to the SRI Noise Measurement Receiver and to the Trak Multicoupler. The multicoupler provided outputs for the spectrum analyzer and for the NM-26T noise meter.

2. Modem Performance-Degradation Test System

The modem performance-degradation test system, (see Figure 12) comprises an HP 1645 Data Error Analyzer, a TH39D Telegraph Tone Modulator,

an RT618B/URC Transmitter (the exciter portion of the AN/URC-35B Radio Set), an R1051B receiver, and an AN/URA-17C comparator converter group.

The Data Error Analyzer generated a 300-bps psuedo-random data stream that the Telegraph Tone Modulator used to modulate the RT618B transmitter to produce a radio-frequency FSK signal. The frequency shift (mark-to-space) was 800 Hz. The signal from the transmitter and the noise from the antenna were summed in Hybrid 3 for input to the R1051B receiver. The R1051B was modified to allow manual RF gain control, which was required for these tests. The levels of the signal and noise provided to the receiver were set by the signal and noise attenuators at the inputs to Hybrid 3. The signal-to-noise ratio was measured at the output of the AN/URA-17 predetection filter (FL1 Terminal 3) by using an HP 3400 true rms voltmeter. The filter FL1 has a 3-dB bandwidth of 1800 Hz and a 6-dB bandwidth of 2100 Hz. The signal was tuned so as to be received in the R1051B's upper sideband, and that output was sent to the AN/URA-17 FSK detector. The resulting detected output was returned to the Data Error Analyzer for measurement of the binary error rate and other items, such as the number of data blocks in error, the number of clock slips, and the proportion of errors caused by marks changed to spaces (the bias). All these items of information were printed on a paper tape by the Anadex digital printer--along with the date and the time from the SRC-540 Time Code Generator.

In addition to the error data from the Data Error Analyzer that were printed by the digital printer, an SRI-built interface unit generated a bipolar error signal, which was recorded on the chart recorder. Binary errors were indicated by pen deflections--to the left of a centerline if the error consisted of interpreting a space as mark, and to the right otherwise.

The spectrum analyzer was used to scan slowly the spectrum surrounding the test frequency to detect any interfering signals, whose presence during the test would cause inaccuracy in the various measurements. The vertical output and the sweep waveform from the spectrum analyzer were recorded on adjacent channels of the chart recorder, so that the frequency of any interfering signal could be determined.

The "slow code" output (coded date and time) from the time-code generator was recorded on the chart recorder, providing a real-time indication on the chart every second. This enables matching of the Anadex paper tape with the chart recorder's record.

The chart records were given to ECAC, and SRI did not attempt any analysis of the data they contained.

3. Noise Measurement System

a. General

APDs were measured using the digitally recorded outputs of the envelope detectors in the SRI Noise Measurement Receiver and the detected lower-sideband output of the R1051B receiver.

The amplitude of each of the envelop detector outputs was sampled at a rate of 200 samples per second. The detector output voltage (0-5 V) was digitized at one of 1024 levels^{*} and recorded on the digital magnetic tape recorder. The recorded data were later processed in a digital computer to produce the APD curve and other data. These procedures were described fully in Ref. 3; as noted, Appendix B contains a listing of the computer program.

The signal for the modem performance degradation test was transmitted and received in the upper sideband. Therefore, only noise appeared in the lower sideband (LSB) of the R1051B; because of the broadband characteristic of impulsive noise, the noise in the two sidebands can be assumed to be identical. The noise power in the lower sideband was measured with the LSB rms voltmeter connected to Terminal 3 of FL1, the output of the AN/URA-17C predetection filter.

At times, we manually recorded the rms level and V_d of the noise from the NM-26T; we also recorded its rms level on the chart recorder.

b. SRI Noise Measurement Receiver

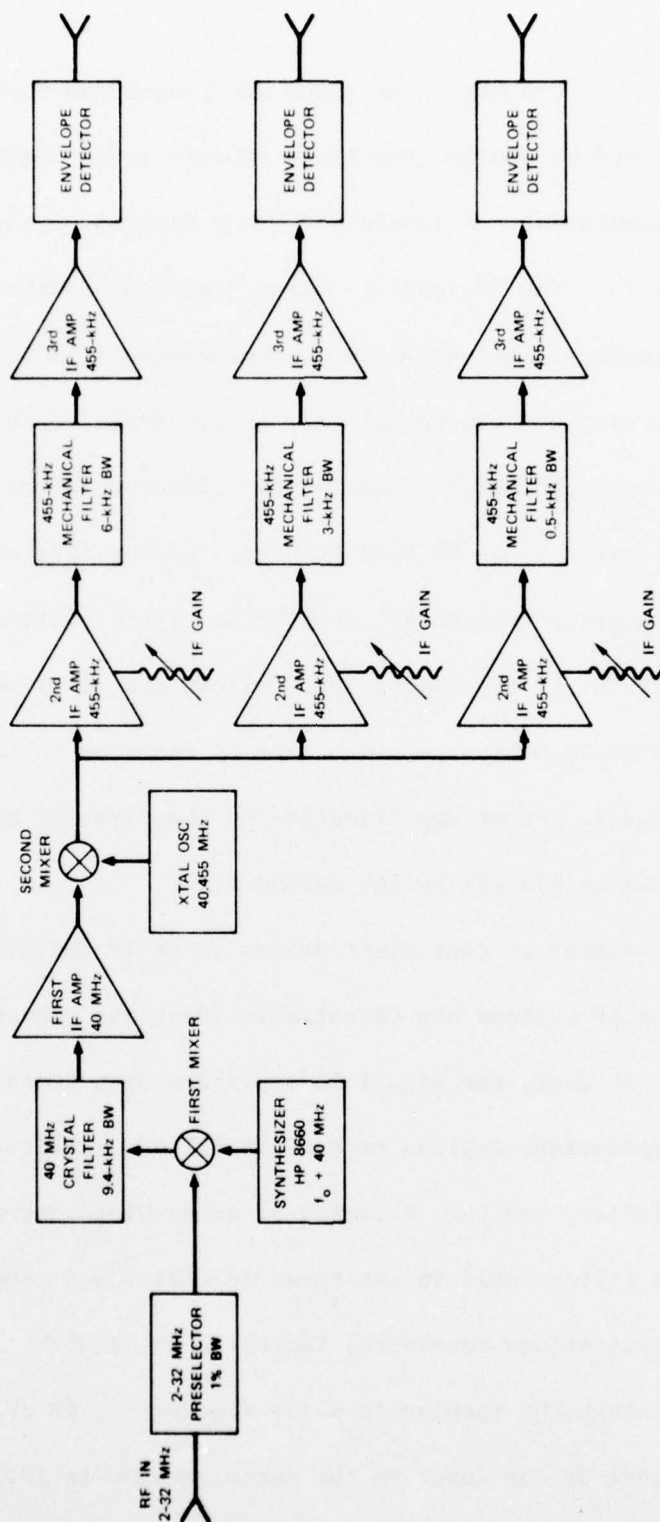
The noise measurement receiver we developed for this project covers the 2-to-32-MHz range and has three IF channels, with nominal 3-dB

* There were 10 binary digits ($2^{10}=1024$) in the digitized number. Thus there was a 60.2-dB range between the largest and the smallest digitized number.

bandwidths of 6, 3, and 0.5 kHz. The gains and bandwidths through the receiver were tailored to provide the large dynamic range required for impulsive-noise measurement. A simplified block diagram of the receiver is shown in Figure 13. The RF input is first bandwidth-limited and amplified by the preselector. Its bandwidth is approximately 1% of center frequency. The output from the preselector is converted to 40 MHz by a high-level double-balanced mixer. The local oscillator injection signal is supplied to the mixer by an HP 8600 Frequency Synthesizer at a frequency 40 MHz above the receiver frequency. The 40-MHz crystal filter (with bandwidth of 9.4 kHz at the -3 dB points) that follows the mixer output provides the further reduction in noise bandwidth that is required to maintain the system's dynamic range. After amplification by the first IF amplifier, the IF is converted down to 455 kHz by the second mixer.

The output of that mixer drives three IF amplifier systems in parallel. These IF systems are essentially identical except for the filter bandwidth. In each, the signal is amplified by a second IF amplifier, filtered by the appropriate Collins mechanical filter, amplified further by a third IF amplifier, and then detected by an envelope detector. The Collins mechanical filters used in the three IF chains are commonly used in many other communications receivers, including the R1051B.

Although the receiver's noise figure is 5 dB or less, the measured noise figure at the input to the entire system is 10.5 dB, because



SB-2997-12

FIGURE 13 SIMPLIFIED BLOCK DIAGRAM OF SRI NOISE MEASUREMENT RECEIVER

of the additional loss through the two hybrids in the antenna distribution system.

A plot of the peak output voltage of the receiver's envelope detector versus an input voltage from an impulse generator is shown in Figure 14 for the 500-Hz IF channel. The linearity of the curve is typical for any of the three IF bandwidths when the IF gain is adjusted to set the receiver's internal noise level to 10-mV peak at the output.

The time waveform of the detected envelope of the receiver's impulse response is shown in Figure 15 for each of the three IF bandwidths. Also shown there is the waveform of the detected envelope of the LSB output of the R1051B, which is described in the next section.

The impulse response photographs of Figure 15 can be used, by dividing the maximum amplitude by the area under the curve, to obtain the system impulse bandwidth as detailed in Ref. 30, where it is termed the video pulse technique. Another method, described in Eq. 4 of Ref. 30, for obtaining the impulse bandwidth uses a system gain measurement and the system's peak response to an impulse. The impulse bandwidths found by both methods, and some other bandwidth information, are shown in Table 1. The ringing in the Figure 15 impulse responses results in a greater area, and therefore a narrower impulse bandwidth when using the video pulse technique. The other technique provides impulse bandwidths closer to what we had expected.

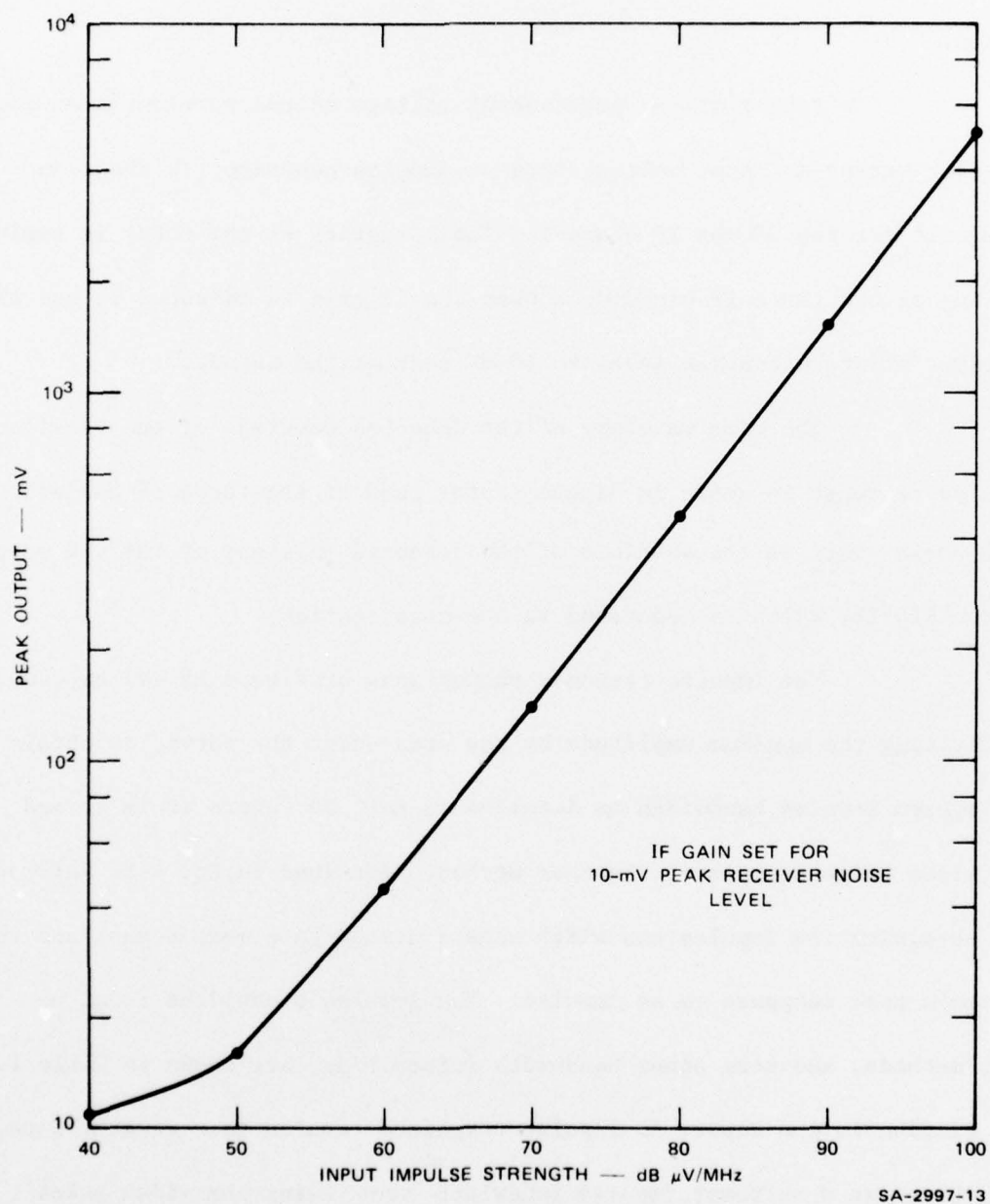
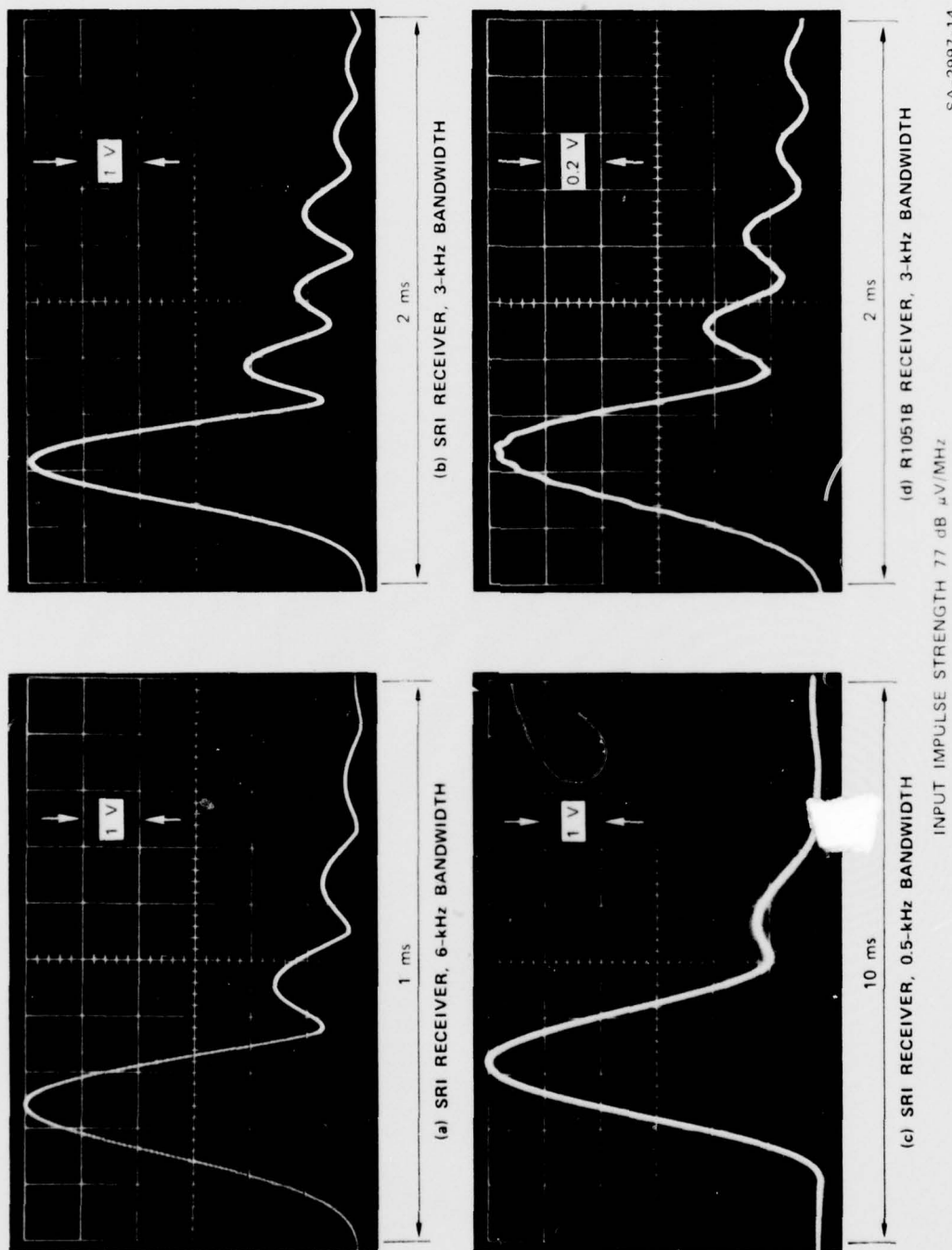


FIGURE 14 PEAK OUTPUT VOLTAGE VERSUS IMPULSE STRENGTH AT INPUT, SRI RECEIVER, 3.0-MHz, 0.5-kHz BANDWIDTH



SA-2997-14

FIGURE 15 IMPULSE RESPONSE OF SRI NOISE MEASUREMENT RECEIVER AND OF THE R1051B RECEIVER AT THE ENVELOPE DETECTOR OUTPUTS, 3.0 MHz

Table 1
MEASURED BANDWIDTHS OF THE VARIOUS RECEIVERS

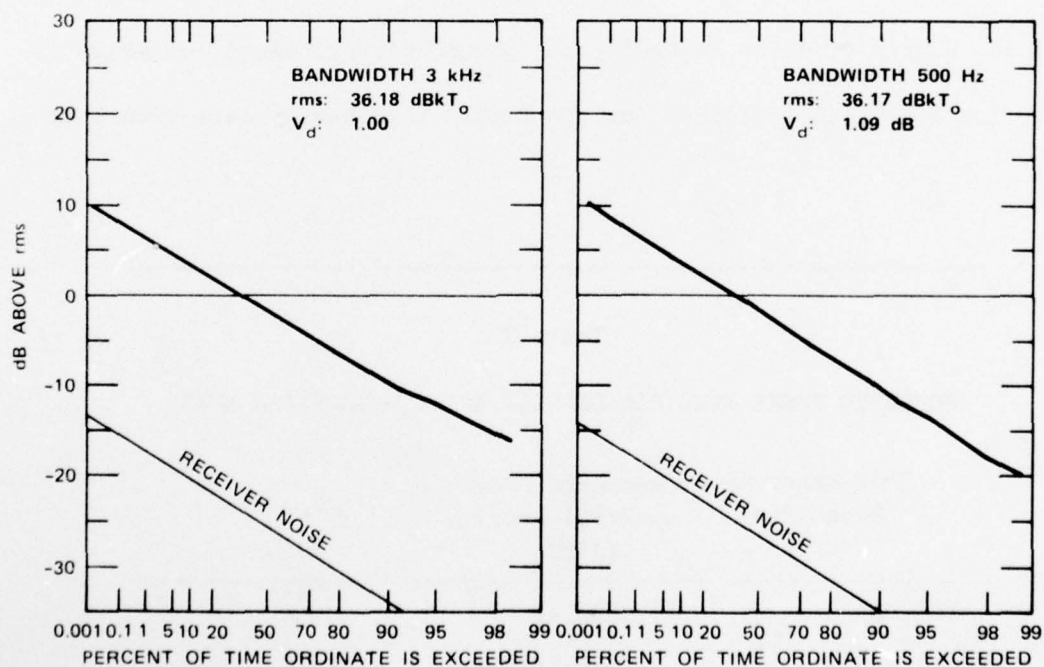
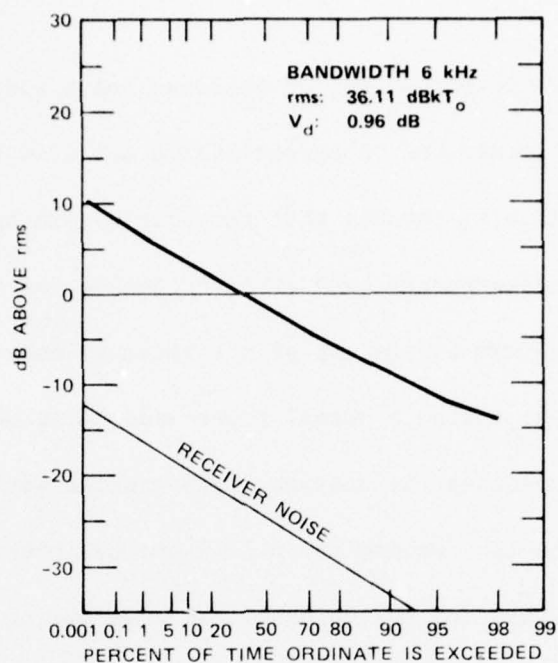
Receiver	3-dB Bandwidth (kHz)		6-dB Bandwidth (kHz)	60-dB Bandwidth (kHz)	Equivalent Noise-Power Bandwidth (kHz)	Impulse Bandwidth (kHz)	
	Nominal	Measured				Video Pulse Technique	Technique of Eq. 4, Ref. 30
SRI	6	5.9	6.1	-	-	4.0	5.9
SRI	3	3.8	4.0	-	-	2.2	3.5
SRI	0.5	0.38	0.40	-	-	0.40	0.46
R1051B	3	-	-	-	-	1.6	-
NM-26T	-	3.4	4.7	23.6	3.9	4.9	-

Figure 16 shows APDs of Gaussian noise made simultaneously using the three SRI receivers. A corresponding APD from the R1051B receiver is not available, because that receiver's gain had been adjusted for the error-rate measurements, and at that setting the noise from the Gaussian noise source was barely out of the receiver noise. These APD measurements were made during a normal power-line noise measurement session by simply replacing the antenna for 5 minutes with the same 36-dBkT_o Gaussian noise source that we use for a 1 minute calibration. The computer, which had been told that the rms value of the envelope of the 1 minute sample represented a power spectral density of 36 dBkT_o , identified the 5-minute sample of noise as having the power spectral densities shown in Table 2. The value indicated for the R1051B receiver is less than 3 dB

Table 2

COMPUTED POWER SPECTRAL DENSITY AND V_d --GAUSSIAN NOISE

3-dB Receiver Bandwidth (kHz)	Measured Power Spectral Density (dBkT_o)	V_d (dB)
6	36.11	0.96
3	36.18	1.00
0.5	36.17	1.09
3 (R1051B)	35.82	0.12



DATE: 21 MARCH 1975 DURATION: 5.0 min RUN CODE: 56

SA-2997-15

FIGURE 16 APDs OF GAUSSIAN NOISE AT 3.0 MHz—POWER SPECTRAL DENSITY 36.0 dBkT_o

above its computed receiver noise. Our V_d figures were calculated by the computer from the rms and average voltages, using the ratio

$$V_d = 20 \log \left(\frac{V_{rms}}{V_{avg}} \right) \text{dB.}$$

The computer uses the noise voltage samples to find the rms noise envelope voltage

$$V_{rms} = \sqrt{\frac{1}{N} \sum_{i=1}^N e_i^2} \text{ volts}$$

and the average noise envelope voltage*

$$V_{avg} = \frac{1}{N} \sum_{i=1}^N e_i \text{ volts,}$$

where e_i indicates the digitized i^{th} sample of the noise envelope. At 200 samples per second, the sample size is about $N = 60,000$. Thus V_{rms} and V_d represent an averaging over a 5-minute period.

The V_d ratio for Gaussian noise is approximately 1.05 dB, and Table 2 shows that reasonable V_d results were obtained, except for the

* This is a simplification over our previous method (Ref. 3), where the noise envelope was, itself, calculated from its quadrature components.

R1051B receiver. There the Gaussian noise was so low that many of the samples were digitized as either zeros or ones and, although a reasonable rms voltage was obtained, the calculated average voltage was almost the same as that rms value, and so an incorrectly low V_d ratio was obtained.

We have sketched the APD of the receiver noise on these and most of the other power-line noise APD plots. The rms value of the receiver noise was calculated and printed out by the computer. We know that the rms value of Gaussian noise is exceeded 36.8% of the time and that receiver noise is Gaussian-distributed thermal noise. Therefore, its envelope has a Rayleigh distribution, and its APD must be a straight line on Rayleigh paper, at the same slope as that of the noise from the 36-dBkT₀ noise source. From its rms value we can, therefore, draw the receiver noise APD in the appropriate place on the graph.

Figure 17 shows the APDs of the SRI receiver impulse response from impulses occurring 60 times per second. In these measurements the receiver gains were set so that the receiver noise did not exceed about 10 mV. Then the level of the impulse generator was adjusted so that the maximum output of the 6-kHz-bandwidth receiver was 5 V. At that impulse strength (85 dB μ V/MHz), the maximum output of the receiver with the 3-kHz bandwidth was about 4.2 V, and the maximum output of the 0.5-kHz bandwidth receiver was about 1.7 V. The computer processing indicated that the rms value of the receiver noise was far below that of the impulse noise (by from 24 to 38 dB, depending on the receiver) and it is sketched on the APD in approximately the correct location.

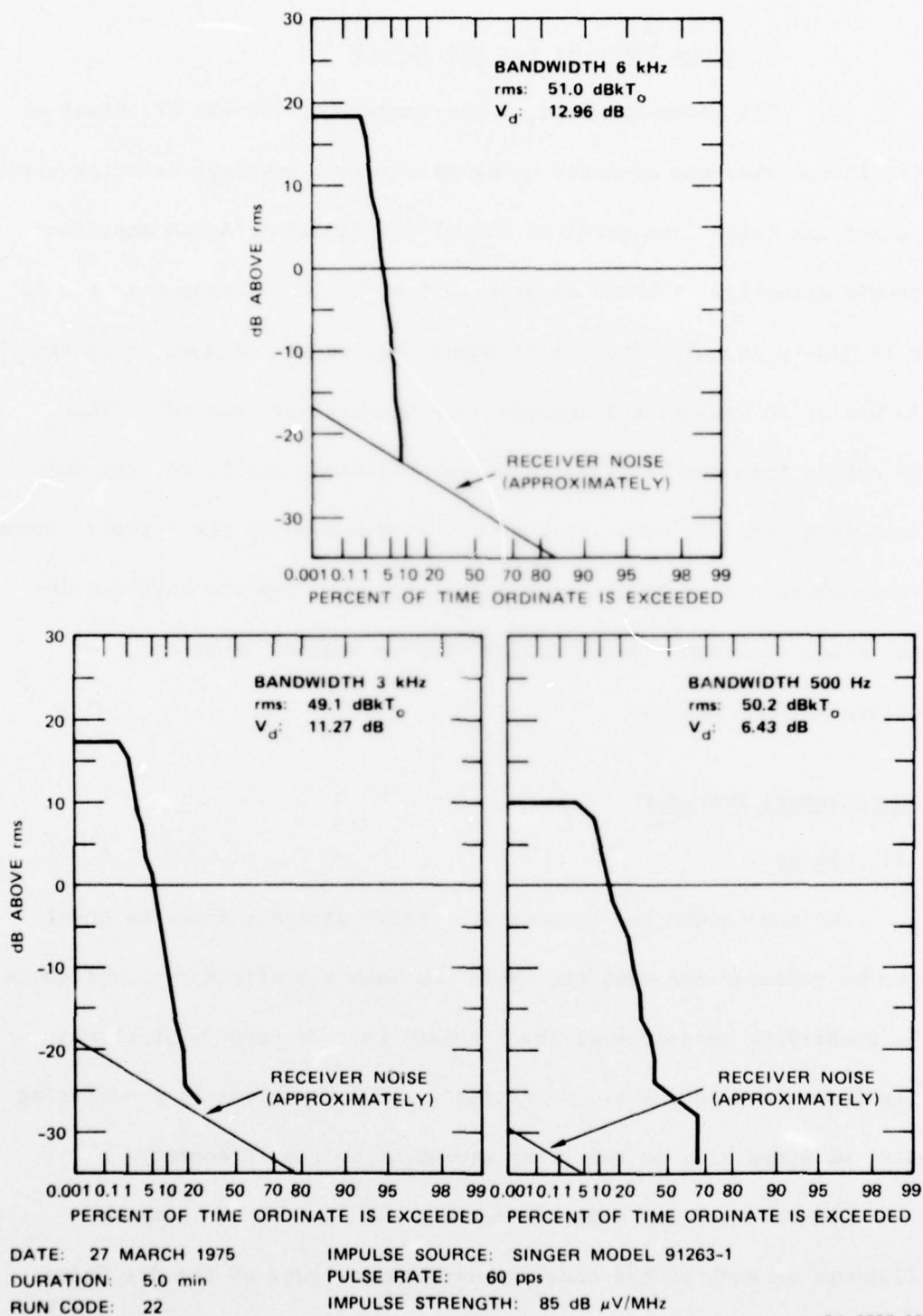


FIGURE 17 APDs OF THE IMPULSE RESPONSE OF THE SRI RECEIVERS AT 3.0 MHz

c. Envelope Detector for the R1051B

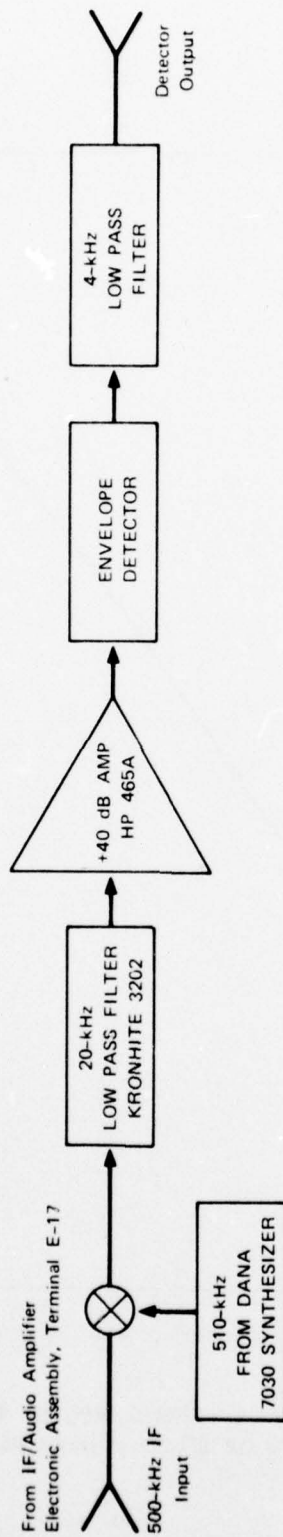
The lower-sideband, 3 kHz-bandwidth, 500-kHz IF output of the R1051B receiver was detected using an external envelope detector system. The output was taken from terminal E17 of the R1051B IF/Audio Amplifier Electronic Assembly. A block diagram of the envelope detector system is shown in Figure 18. The 500-kHz IF signal was converted down to 10 kHz to enable use of an operational amplifier as an envelope detector. That 10-kHz output from the mixer was low-pass filtered, amplified, and then envelope detected. A 4-kHz low-pass filter was used at the detector output. Figure 19 shows a plot of the peak output voltage from the envelope detector versus the input to the system from an impulse generator, for comparison with Figure 14.

C. Measurement Procedure

1. Setup

We positioned the antenna at a known distance from the power line to be measured and used the NM-26T to make a preliminary aural check of the power-line emissions at the proposed test frequency, which was usually very close to 3 MHz. Selecting a frequency clear of interfering signals, we tuned all the receiving equipment to that frequency.

We observed the noise from the power line on the monitor oscilloscope at each of the envelope detector outputs of the SRI Noise Measurement Receiver and adjusted the gain of each of the IF channels so that the noise being received was within that receiver's dynamic range (see



SA-2997-17

FIGURE 18 ENVELOPE DETECTOR FOR R1051B LOWER-SIDEBAND IF

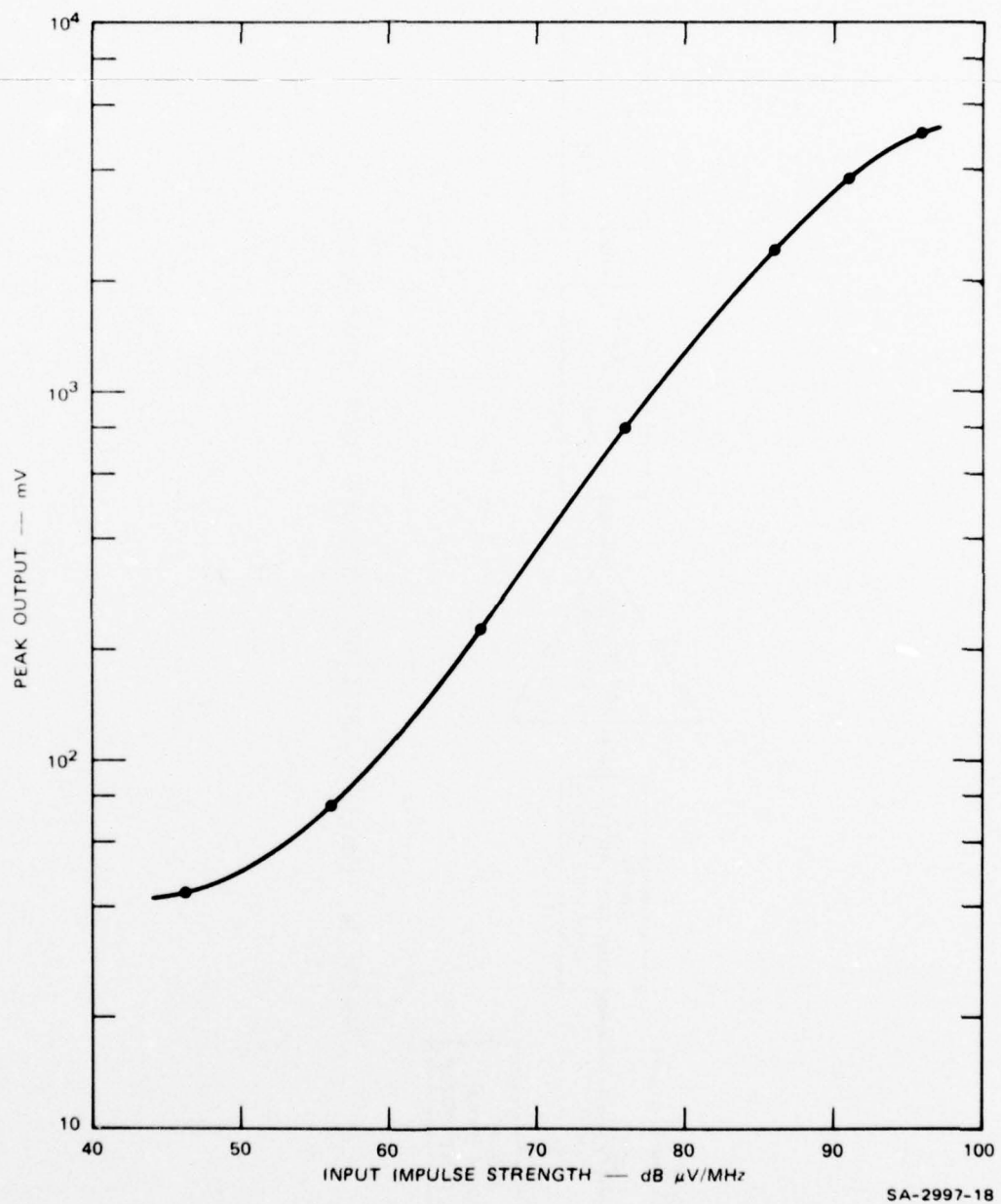


FIGURE 19 PEAK OUTPUT VOLTAGE VERSUS IMPULSE STRENGTH AT INPUT,
DETECTED ENVELOPE OF LOWER-SIDEBAND OF R1051B RECEIVER

Figure 12). We used the noise attenuator and the RF gain control of the R1051B, so that the noise into that receiver would be at the level required for the modem performance degradation test, to be performed later. We attempted to keep both the noise and the signal levels within the linear portion of the R1051B receiver's dynamic range. We measured the noise level at the R1051B upper sideband, using the USB rms voltmeter, and logged the readings for later reference.

2. Calibration

The system was calibrated for all tests in terms of the noise-power spectral density at the antenna terminals. Our calibration source was a Gaussian noise source--with power spectral density of 36 dBkT_0 into a $50\text{-}\Omega$ load--which was connected to the transmission line at the antenna terminals. Appendix A discusses theory.

To calibrate, we disconnected the feed cable from the antenna and substituted the Gaussian noise source. When power to the noise source is off, the source provides a $50\text{-}\Omega$ termination at room temperature for the receiving system. With the system terminated in this manner and with the RT618B transmitter turned off, the system noise levels--as measured by the NM-26T and by the LSB rms voltmeter--were indicated on the chart recording as receiver noise. The NM-26T and the USB rms voltmeter readings were recorded on a log sheet as rms receiver noise.

After setting the "site code"^{*} on the digital recording system to 00 as an indication to the computer that receiver noise was being recorded, we recorded the system receiver noise for 1 minute on the digital recording system. Then we switched on the power to the Gaussian noise source and changed the site (or run) code to 10 to indicate to the computer that noise from the calibration noise source was being injected into the system. The NM-26T rms and LSB rms voltmeter levels were identified as 36 dBkT_o on the chart recorder, and we logged the NM-26T rms and V_d readings and the reading of the USB rms voltmeter. We turned on the digital recording system for a period of 1 minute to record the calibration from the Gaussian noise source.

After that, we turned off the power to the Gaussian noise source and checked the noise level on the USB rms voltmeter with the previously logged reading, to make sure that they were identical. Then, with the RT618B transmitter on, we adjusted the signal attenuator for the signal-to-noise ratio required for the modem degradation test. The signal level was read from the USB rms voltmeter and logged as rms signal. The signal and noise attenuator settings were also logged.

This completed the calibration procedure, and so we then disconnected the Gaussian noise source and reconnected the antenna.

^{*} The site-code indicator on the receiver was originally intended to provide identification for tapes from numerous receiver sites. (See Ref. 7.) We used it to identify calibrations and so on and often refer to it as the run code.

3. Operation

With the RT618B transmitter off, we recorded on the log sheet the reading from the USB rms voltmeter as the power line's rms noise level. We used that and the previously logged rms signal levels to compute the USB SNR at the output of the predetection filter in the URA-17C. When the system was completely calibrated, it was ready for measurements of the degradation to the modem (error rate) and the APD of the noise; these could be done either independently or simultaneously. At most of the test sites, we made a group of error-rate measurements at a selected SNR simultaneously with the noise APD measurement.

The number of bits that the HP 1645 Data Error Analyzer uses in its calculation of the error rate can be adjusted in powers of ten. Error-rate measurements made simultaneously with the APD run usually used a sample size of 10^4 bits,* resulting in an integration time of 33.3 s for each measurement, and so error-rate measurements were printed by the digital printer at approximately 33-s intervals during a 5-minute APD measurement period.

After the APD recording had been completed, we continued to make error-rate measurements at a number of SNRs to construct an error-rate curve for that particular power-line noise source. The SNR was varied

* When this is done, the Data Error Analyzer gives error rates expressed in errors per 10^4 bits.

from the reference point by using the noise and signal attenuators. Generally, we used a 1- or 2-dB step on the signal attenuator and made about five error-rate measurements (each with a sample size of 10^4 bits) at the new SNR. We repeated that procedure at other selected attenuator settings, to obtain the required number of points for the error-rate curve. We generally measured error rates in the range from a low of about 2 or 3 in 10^4 to a high of about 1 in 10.

V TEST RESULTS

A. Error-Rate Measurements

1. Background

This chapter contains the error-rate data measured as described in Section IV-C and also the simultaneously measured APDs of the noise that was causing the errors. The noise was provided to the measurement systems by the same antenna. Such data were collected in the vicinity of several power lines, so we have modem performance degradation data from gap sources, from corona sources, and, possibly, from a mixture of both sources.

Our method of controlling the SNR at the output of the bandpass filter, just ahead of the detector, was to use individual attenuators for the signal and the noise before they were mixed to enter the receiver. (See Figure 12.) We adjusted this SNR, using the signal attenuator to obtain a binary error rate of a few errors in 10^3 . We logged the SNR obtained with these attenuator settings and then immediately made the simultaneous APD and error-rate measurements. Following that, we varied the attenuator settings to gather error-rate data at other SNRs. Removing 1 dB of signal attenuation was considered equivalent to increasing the SNR by 1 dB. Strictly speaking, this was true only when the rms value of the noise was relatively stable--such as when the noise was from a Gaussian noise diode, from an impulse

generator, or from certain power lines. Some power lines (for example, higher-voltage transmission lines) radiate noise that is sometimes very stable in its rms value over periods of many minutes; others (typically lower-voltage distribution lines) sometimes change in noise output by several decibels from one second to the next, as various gaps at various distances become active. Thus, for given attenuator settings, the SNR will not always be the same from one 10^4 -bit (33.3-s) sample to another, and the error rate will vary. We always plot all the error-rate samples in the graphs that follow, placing them at the SNR that corresponds to the attenuator settings. It is possible that ECAC's chart recordings of the time history of the rms value of the noise could be used to average the rms noise voltage over each 33.3-s sample, so as to determine the specific SNR applicable to each of these error-rate samples.

Figure 20 shows an error-rate curve made using noise from our Gaussian noise source. At each SNR the points clustered quite closely; the line is drawn through the median of these points. Also shown is a curve from measurements made previously (Ref. 3) in a similar manner but using different receivers, modems, and error-rate measuring equipment. The SNR was measured in the same manner at the same point in the URA-17, but the newer curve shows an apparent improvement of about 4 dB (that is, a given error rate is obtained at an SNR about 4 dB lower than before). We were aware of this discrepancy as the measurements were being made, and we checked and tested the equipment extensively, but were unable to determine the cause.

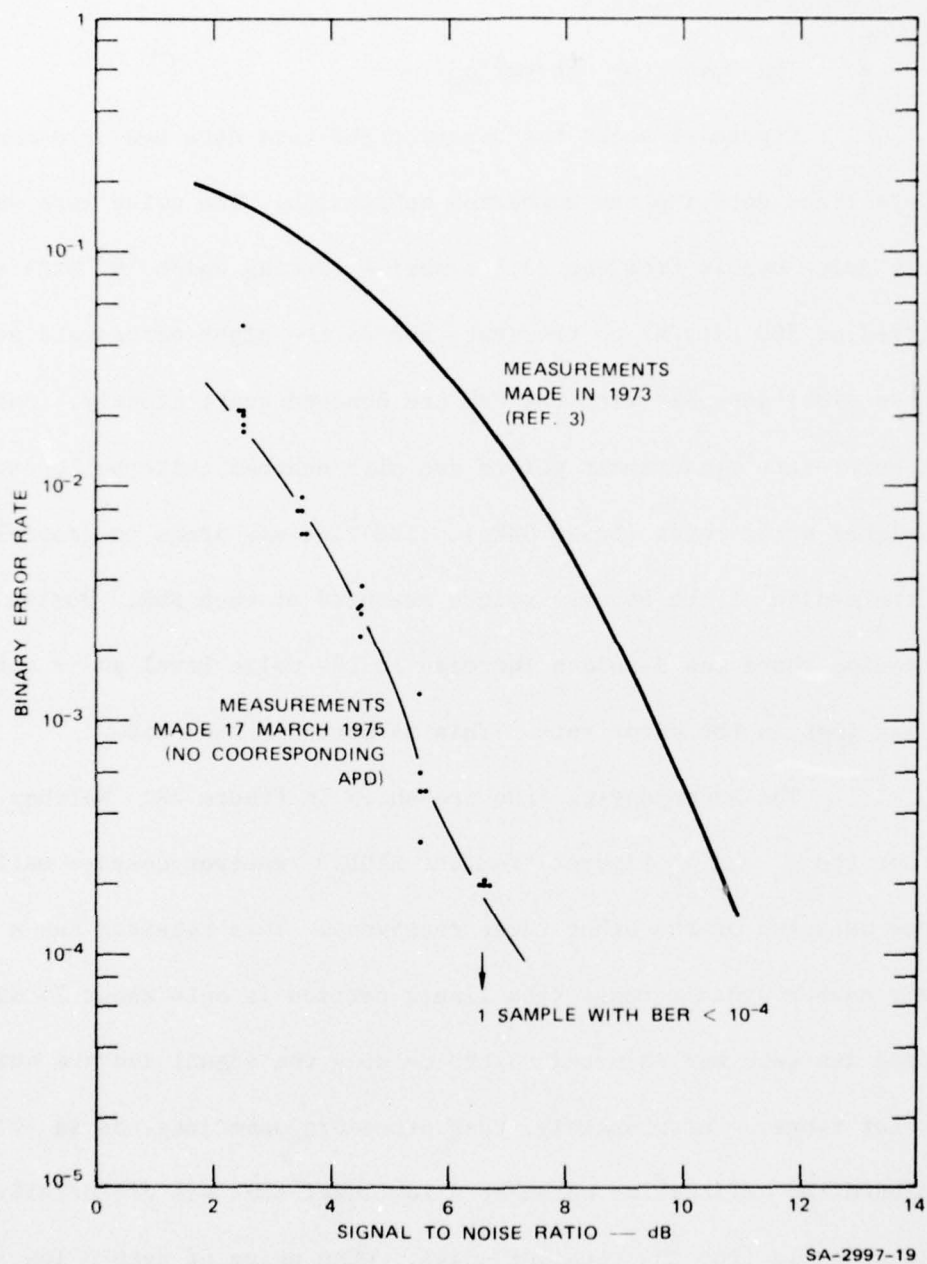


FIGURE 20 BINARY ERROR RATES CAUSED BY GAUSSIAN NOISE AT 3.0 MHz

2. Corona Noise Sources

a. The Dumbarton Substation

Figure 21 shows the binary error-rate data measured near the 230-kV lines entering the Dumbarton substation. The noise here was generally quite stable from one 33.3-s period (during which 10^4 bits were transmitted at 300 bits/s) to the next, and so the eight error-rate measurements made simultaneously with the APD are bunched quite closely. Subsequent error-rate measurement points are also bunched quite well, except at the higher error rates (lower SNRs). The line was drawn to generally follow the median of the several points measured at each SNR. During one 33.3-s period there was a sudden increase in the noise level and a corresponding jump in the error rate. This is noted on the plot.

The accompanying APDs are shown in Figure 22. Neither the APD nor the F_a and V_d figures from the R1051B receiver compare well with those measured on the other three receivers. This receiver has a comparatively narrow dynamic range (the linear portion is only about 25 dB wide), and its gain was adjusted to try to keep the signal and the noise within that range. Unfortunately, that procedure sometimes, as in this case, placed the calibrating noise at a low level that was essentially indistinguishable from the receiver noise. When noise of such a low level is digitized, the rms value of the calibrating noise falls somewhere between zero and 1, which is an infinite range when logged for conversion to decibels.

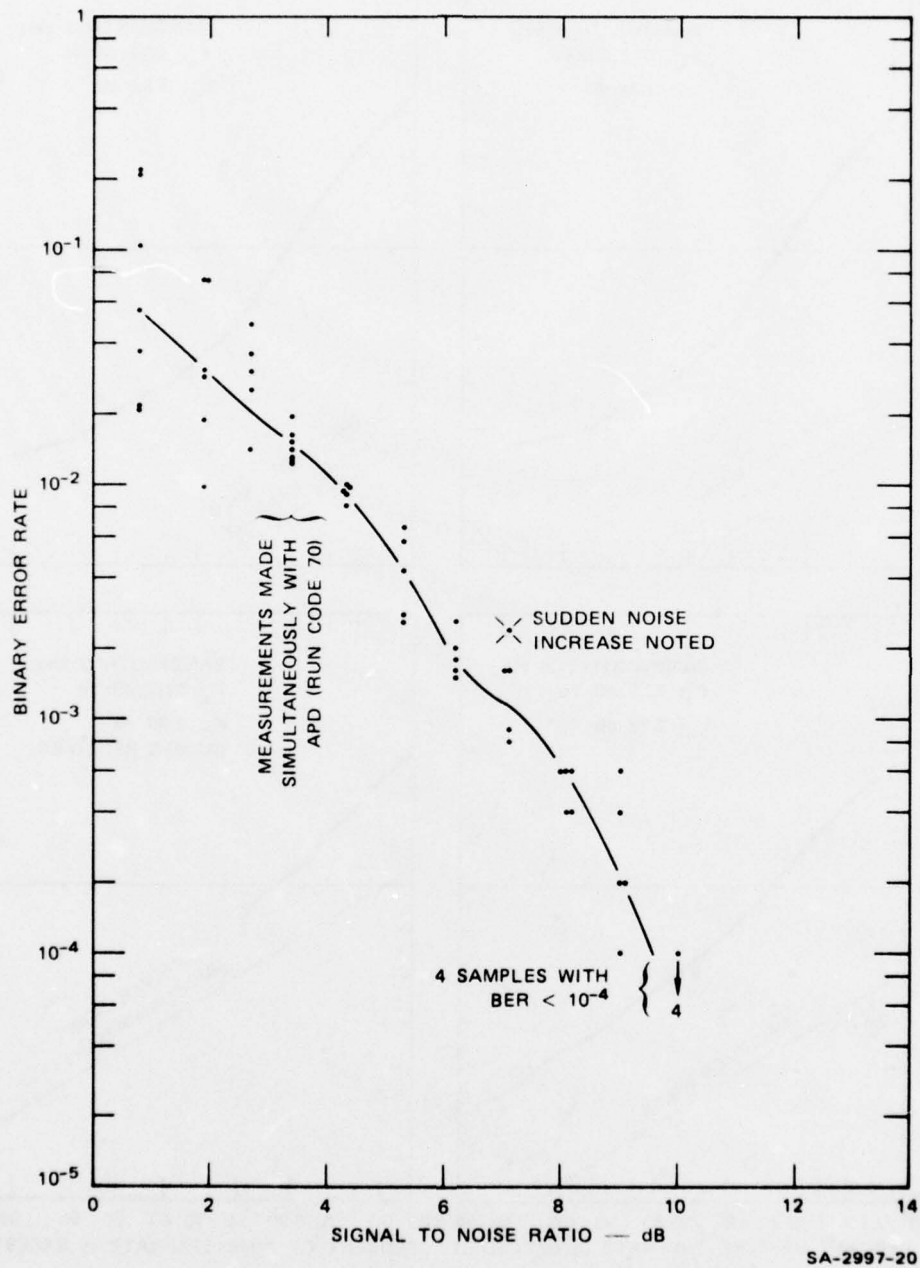
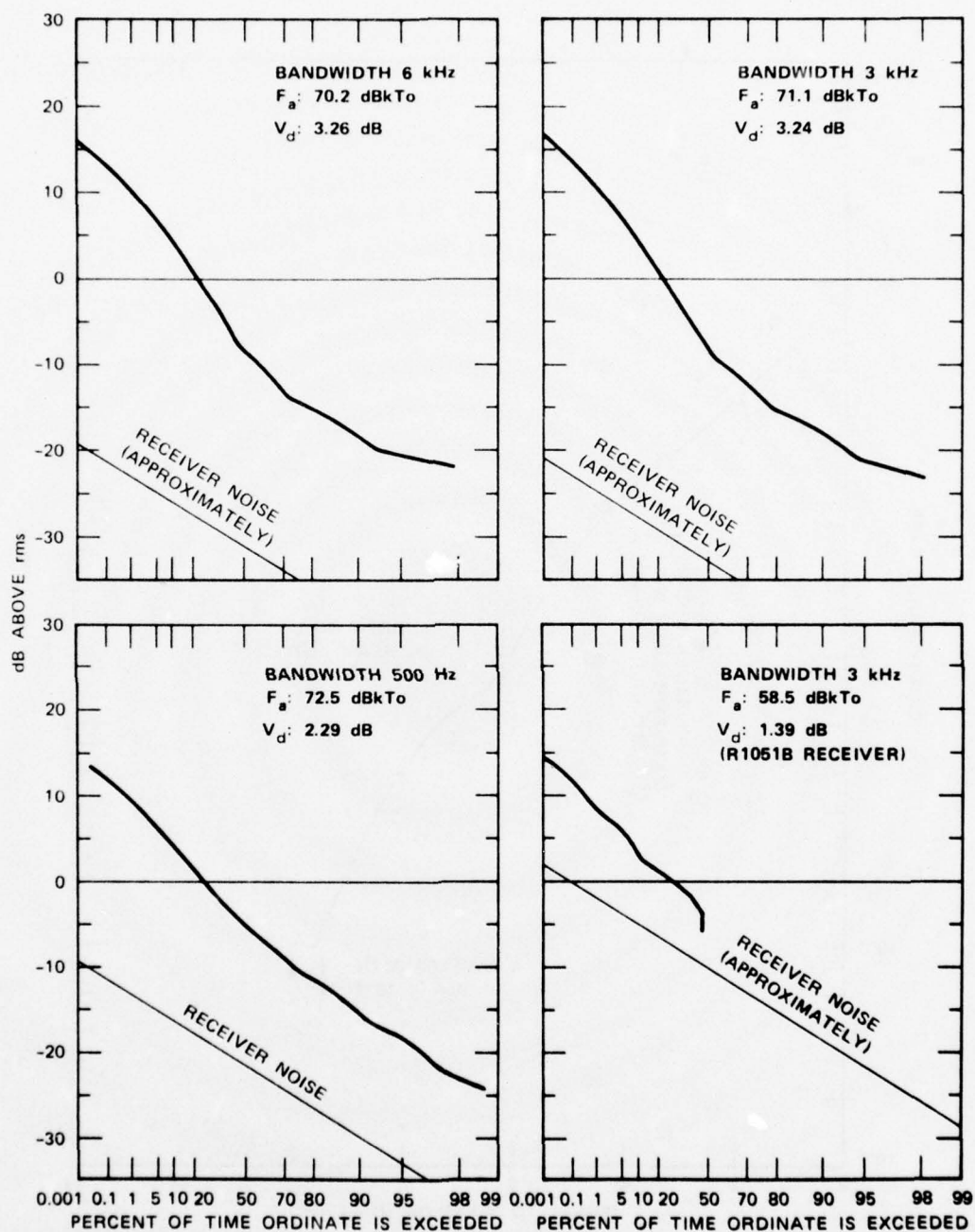


FIGURE 21 BINARY ERROR RATES CAUSED BY CORONA NOISE AT 3.0 MHz,
230-kV LINES, DUMBARTON SUBSTATION



DATE: 17 MARCH 1975 DURATION: 5.0 min WEATHER: SCATTERED CLOUDS
 TIME: 1537 PDT RUN CODE: 70 LOCATION: 50 ft FROM LINE
 SA-3930-41

FIGURE 22 APDs OF POWER LINE NOISE (CORONA) AT 3.0 MHz, NEAR 230-kV LINES AT DUMBARTON SUBSTATION

Thus, the number obtained there and identified as representing a power spectral density of 36 dBkT_0 at the antenna terminals was very inaccurately located, making the receiver calibration unreliable. This was never a problem with the other receivers.

b. The Cupertino Hillside

Figure 23 shows a plot of measurements of the binary error rate caused by corona noise from another pair of 230-kV lines. The noise was quite stable for the 5-minute period during which the simultaneous APD and error-rate measurements were made. However, when the same attenuator settings were used a half-hour or so later, it appeared that there had been a gradual increase in the noise, because the measured points were then clustered uniformly higher in error rate at supposedly the same SNR. The chart record of the rms value of the noise, which was supplied to ECAC, would indicate whether this was the case. Several high isolated impulses of unknown origin were observed while we were measuring the 5.6-dB SNR, and the error rate increased by more than an order of magnitude during that particular 33.3-s period. At the two higher SNRs we had several measurement periods in which no errors were measured in 10^4 bits. These are indicated on Figure 23 by small downward-pointing arrows; the associated numerals denote the number of sample periods having no errors.

The APDs of the power-line noise are shown in Figure 24. The power-line noise was 15 to 20 dB quieter during this period than previously measured here. The difference is attributable to the weather; most of our measurements at the Cupertino site were made during rain, but

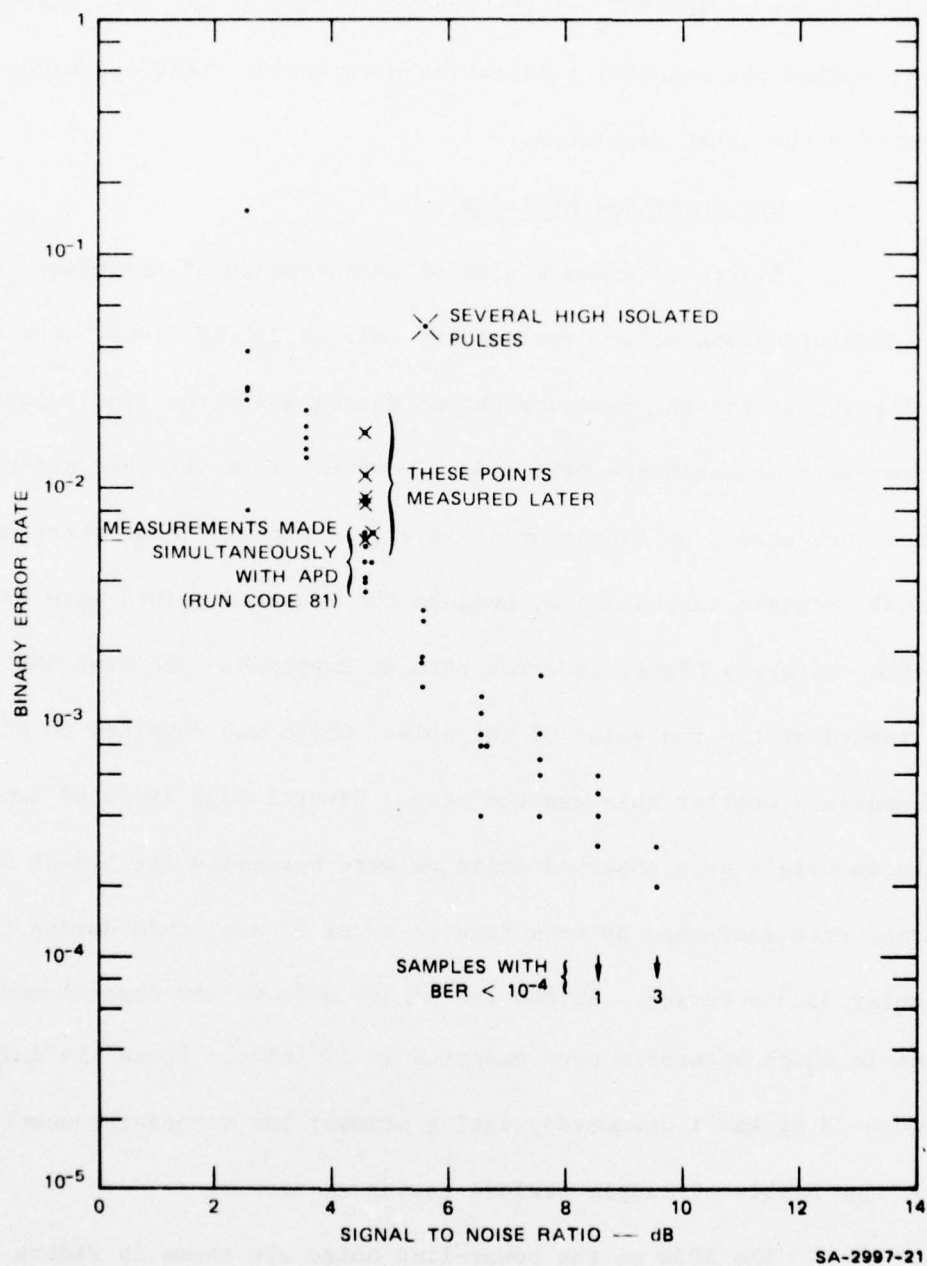
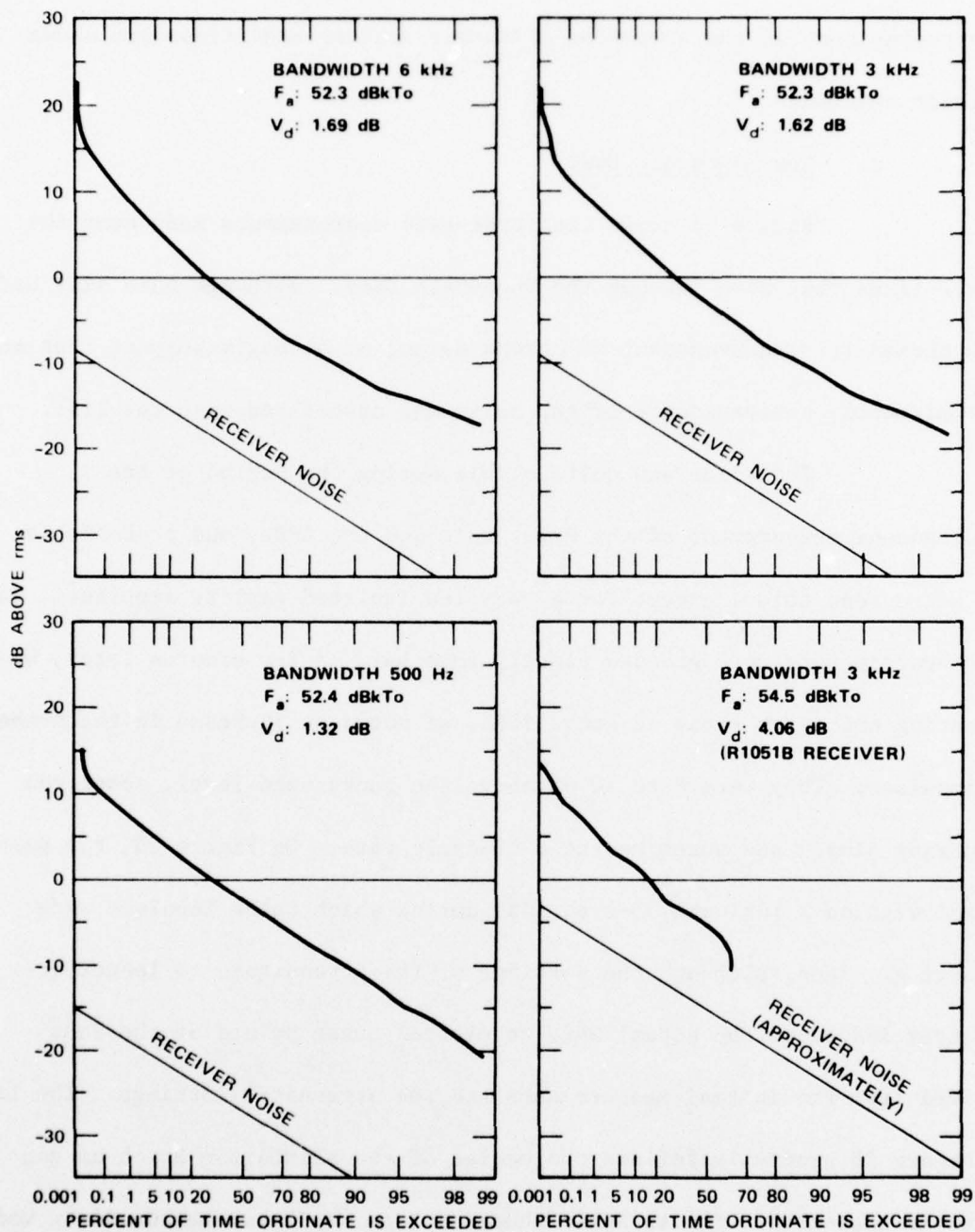


FIGURE 23 BINARY ERROR RATES CAUSED BY CORONA NOISE AT 3.0 MHz, 230-kV LINES, CUPERTINO HILLSIDE



DATE: 19 MARCH 1975 DURATION: 5.1 min WEATHER: CLOUDY, RAIN SEVERAL HOURS EARLIER
 TIME: 1553 PDT RUN CODE: 81 LOCATION: 60 ft FROM CENTERLINE

SA-3930-42

FIGURE 24 APDs OF POWER LINE NOISE (CORONA) AT 3.0 MHz NEAR 230-kV LINES IN CUPERTINO

these were not. Rain also seems to increase the V_d ratio--by about 1 dB. Some comparisons of the APDs from different weather conditions are shown in later sections.

c. The Sunnyvale Dump

Figure 25 shows the error-rate measurements made near the 115-kV lines that pass through the Sunnyvale Dump. Although this site had been chosen for measurement of corona noise, we strongly suspect that some intermittently active source of gap noise was associated with the line.

The noise was quite stable during the period of the simultaneous measurement of the error rate and the APDs, and probably it was all corona noise, except for a very few isolated gaplike impulses. The error-rate points were grouped closely together. A few minutes later, while measuring the error rates at other SNRs, we noted an increase in the number of impulses. They were 8 to 10 dB above the background level, sometimes occurring singly and sometimes at a 60-cycle rate. On Figure 25, the points marked with an X indicate 33-s periods during which these impulses were occurring. Then, although the settings of the attenuators no longer accurately indicated the actual SNR, we plotted these points at the SNRs derived from the initial measurements and the attenuator settings. The line on Figure 25 generally follows the median of the points for which no gap noise is suspected. The triangle-shaped points represent measurements made with the same attenuator settings as the measurements made simultaneously with the APD, but made perhaps 20 minutes later, when there was some of the gap type noise.

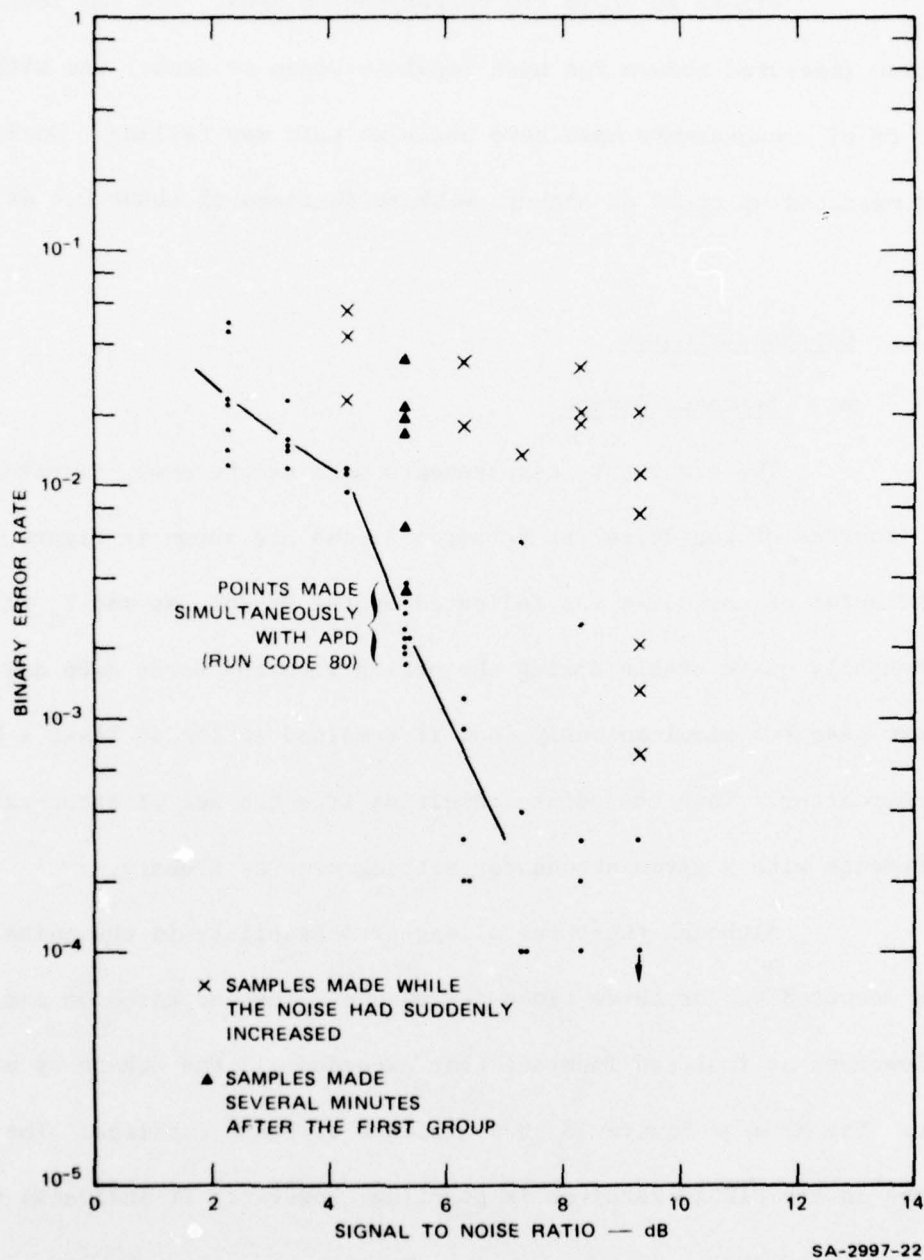


FIGURE 25 BINARY ERROR RATES CAUSED BY POWER-LINE NOISE AT 3.4 MHz, 115-kV LINES AT SUNNYVALE DUMP

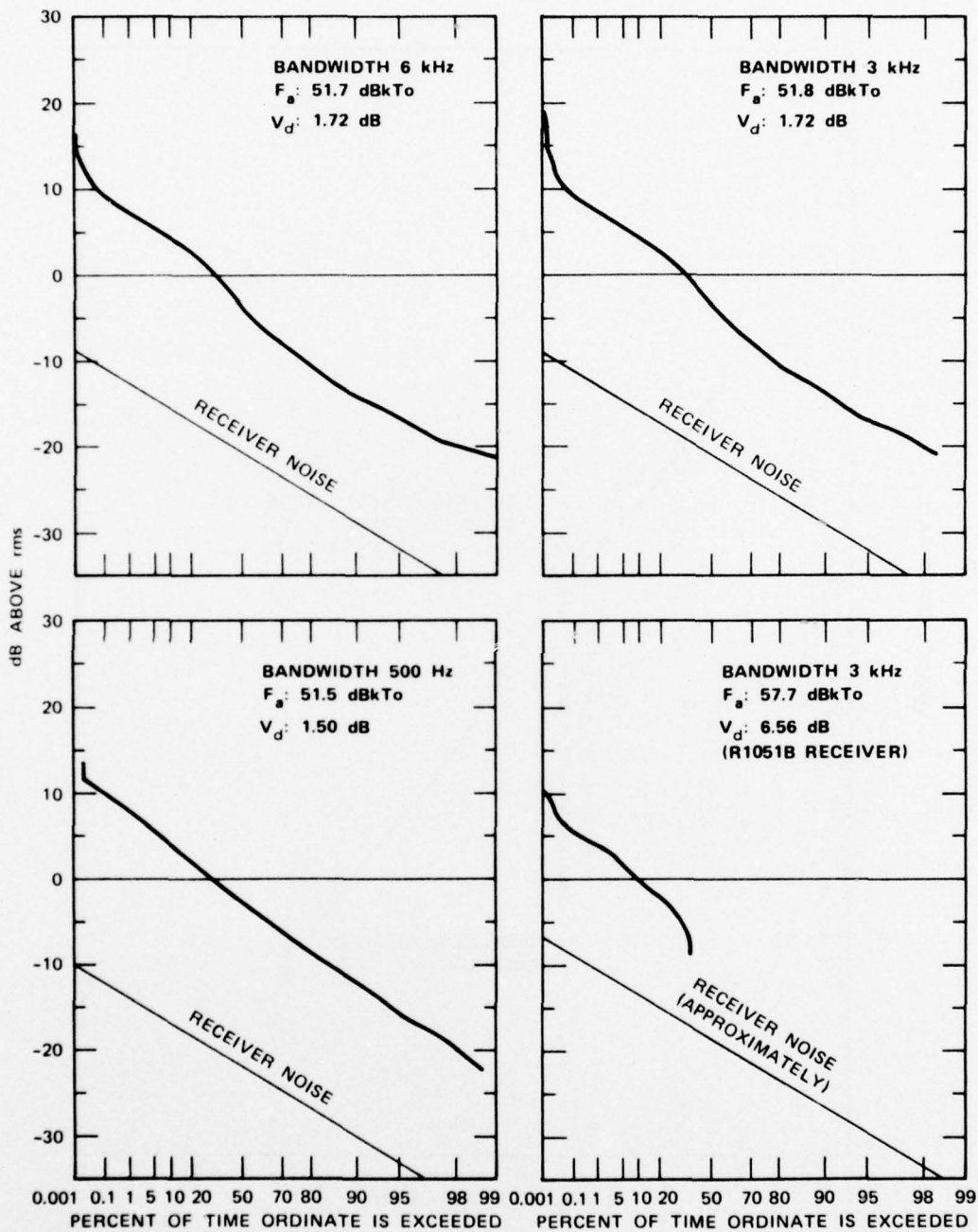
Figure 26 shows the corresponding APDs. The rms level of the noise (measured before the high impulses began to occur) was within 2 or 3 dB of measurements made here while no rain was falling. During rain we had measured up to 10 dB higher, with an increase of about 0.4 dB in V_d .

3. Gap Noise Source

a. Bernardo Avenue

The error-rate measurements made at the power distribution lines (sources of gap noise) at Bernardo Avenue are shown in Figure 27. The character of the noise (as indicated by the NM-26T rms and V_d meters) was generally quite stable during the period when the error rate and the APD were measured simultaneously, and it remained so for at least a half hour thereafter. Thus the points resulting from the set of error-rate measurements with a given attenuator setting cluster closely.

Although there was a long-term stability in the noise, high spikes occurred two or three times per minute. They appeared on the monitor oscilloscopes as isolated impulses that exceeded all the others by a great amount. The APDs of Figure 28 show evidence of these impulses. The APD measured in the R1051B receiver is puzzling, however: It indicates that



DATE: 19 MARCH 1975 DURATION: 5.3 min WEATHER: CLOUDY AND WINDY, THREATENING RAIN
 TIME: 1417 PDT RUN CODE: 80 LOCATION: 50 ft FROM CENTERLINE

SA-3930-43

FIGURE 26 APDs OF POWER LINE NOISE AT 3.4 MHz, 115-kV LINES AT SUNNYVALE DUMP

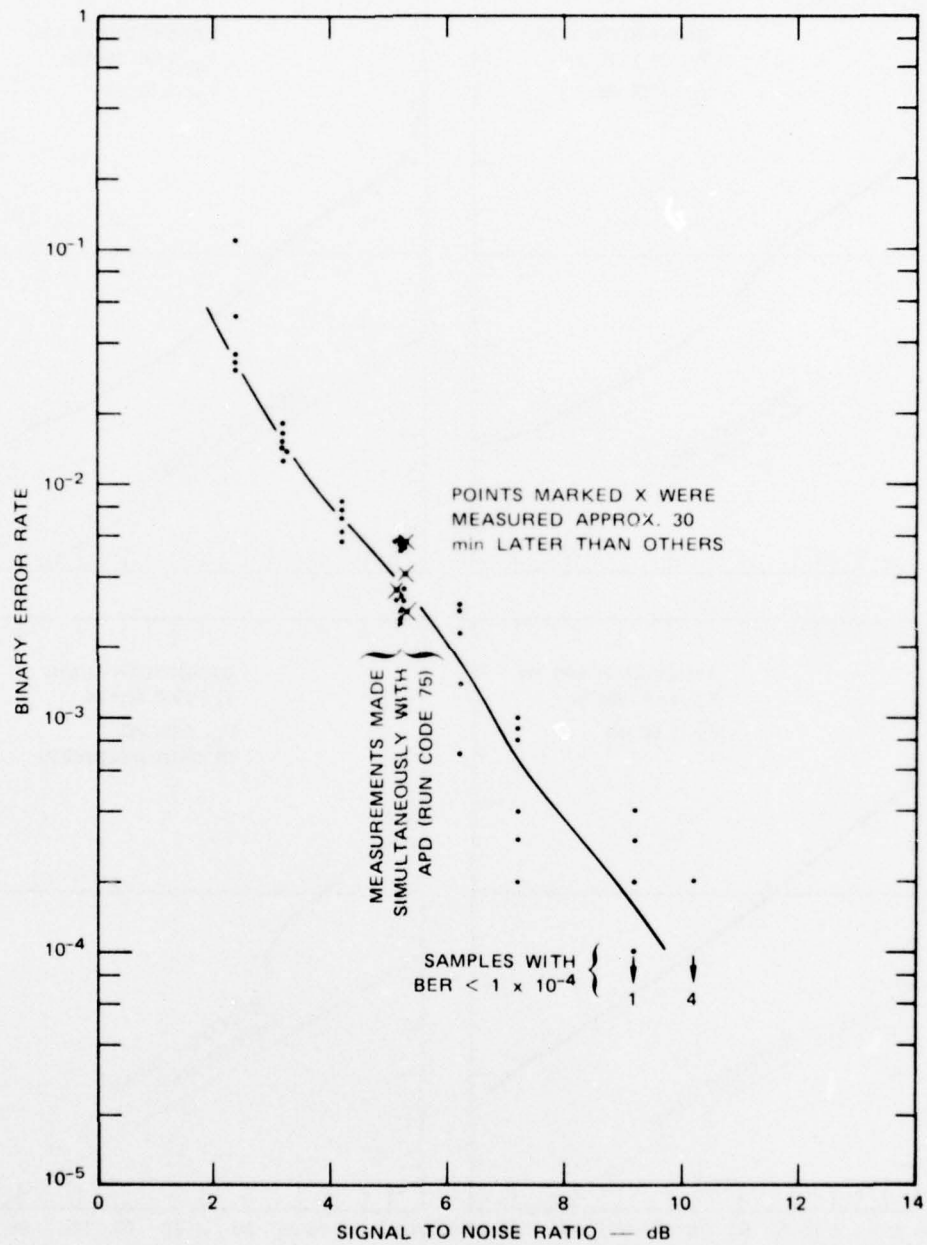
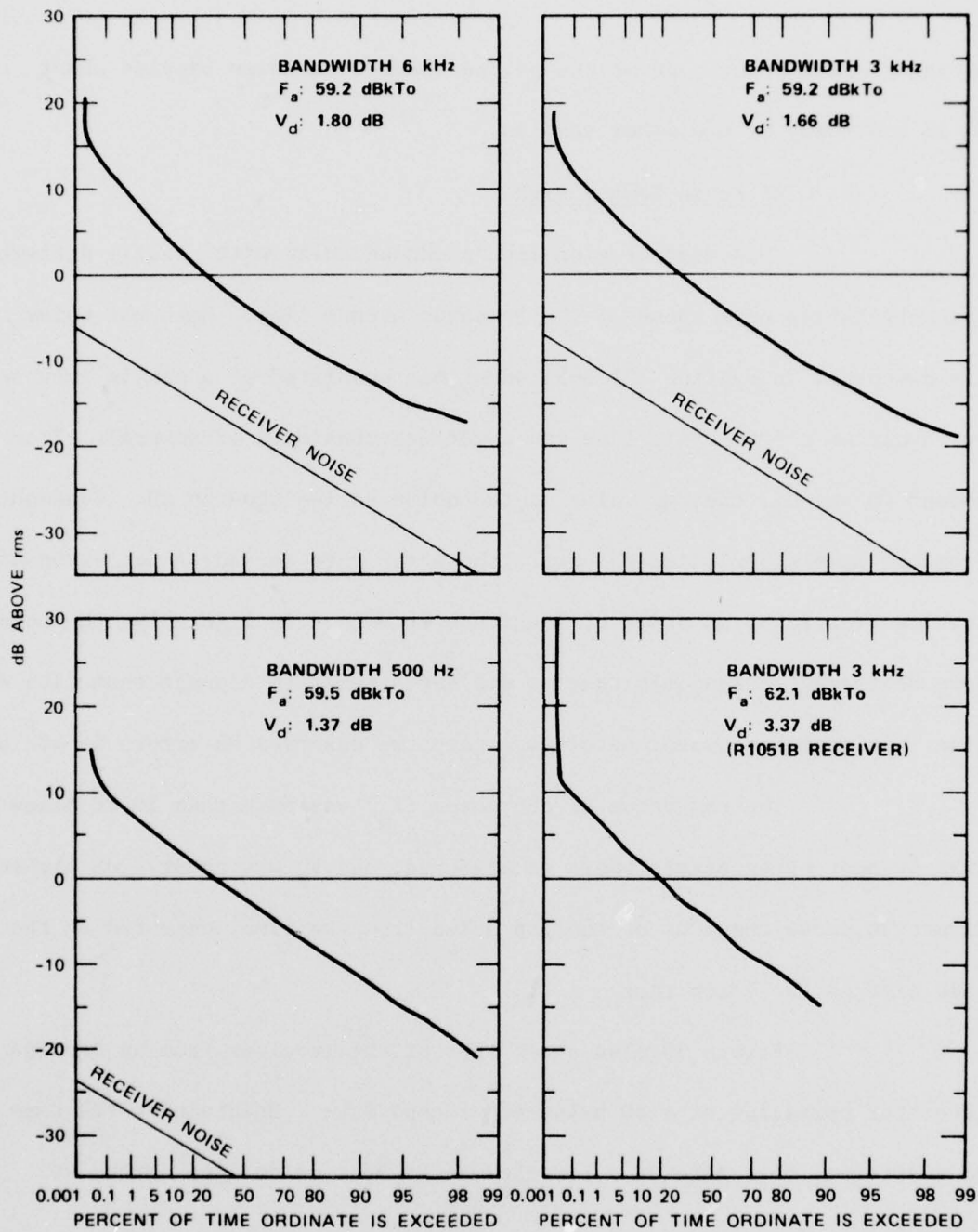


FIGURE 27 BINARY ERROR RATES CAUSED BY GAP NOISE AT 3.0 MHz, UNDER
LINE AT BERNARDO AVENUE



DATE: 18 MARCH 1975 DURATION: 5.5 min WEATHER: CLOUDY AND THREATENING RAIN, NO
 TIME: 1203 PDT RUN CODE: 75 RAIN FOR SEVERAL DAYS
 LOCATION: UNDER LINE ABOUT 50 ft FROM POLE
 WITH SUSPECTED SOURCES

SA-3930-44

FIGURE 28 APDs OF POWER LINE NOISE AT 3.0 MHz, UNDER DISTRIBUTION LINE
 ON BERNARDO AVENUE

during a small percentage of the period there were noise samples about 20 dB above any of the other samples.*

b. Ed Levin County Park

This distribution line produced noise with greatly different characteristics from those of the Bernardo Avenue line. Here the noise (as discussed in Section III-B-5) sometimes consisted of a single impulse per cycle on the 60-cycle line and sometimes consisted of several. From second to second, the rms value of the noise varied about 6 dB. Consequently, from one sample period to the next, the error rate for any given attenuator settings varied by an order of magnitude or more. On Figure 29, the points were scattered so randomly that we did not attempt to connect them with a line. At some attenuator settings, again, we observed no errors in 10^4 bits.

The rms value of the noise (F_a) was more than 10 dB below that at most other places where we measured, and V_d was about 1 dB higher. Figure 30 shows the APDs of the gap noise from the line, measured at the same time as the error rate.

Figure 30 also shows APDs of the impulses from an impulse generator operating at a 60 pulse-per-second rate. Maintaining the same gain settings that were used for the measurement of the gap noise, we

* According to the printout, this represented 10 samples out of approximately 66,000.

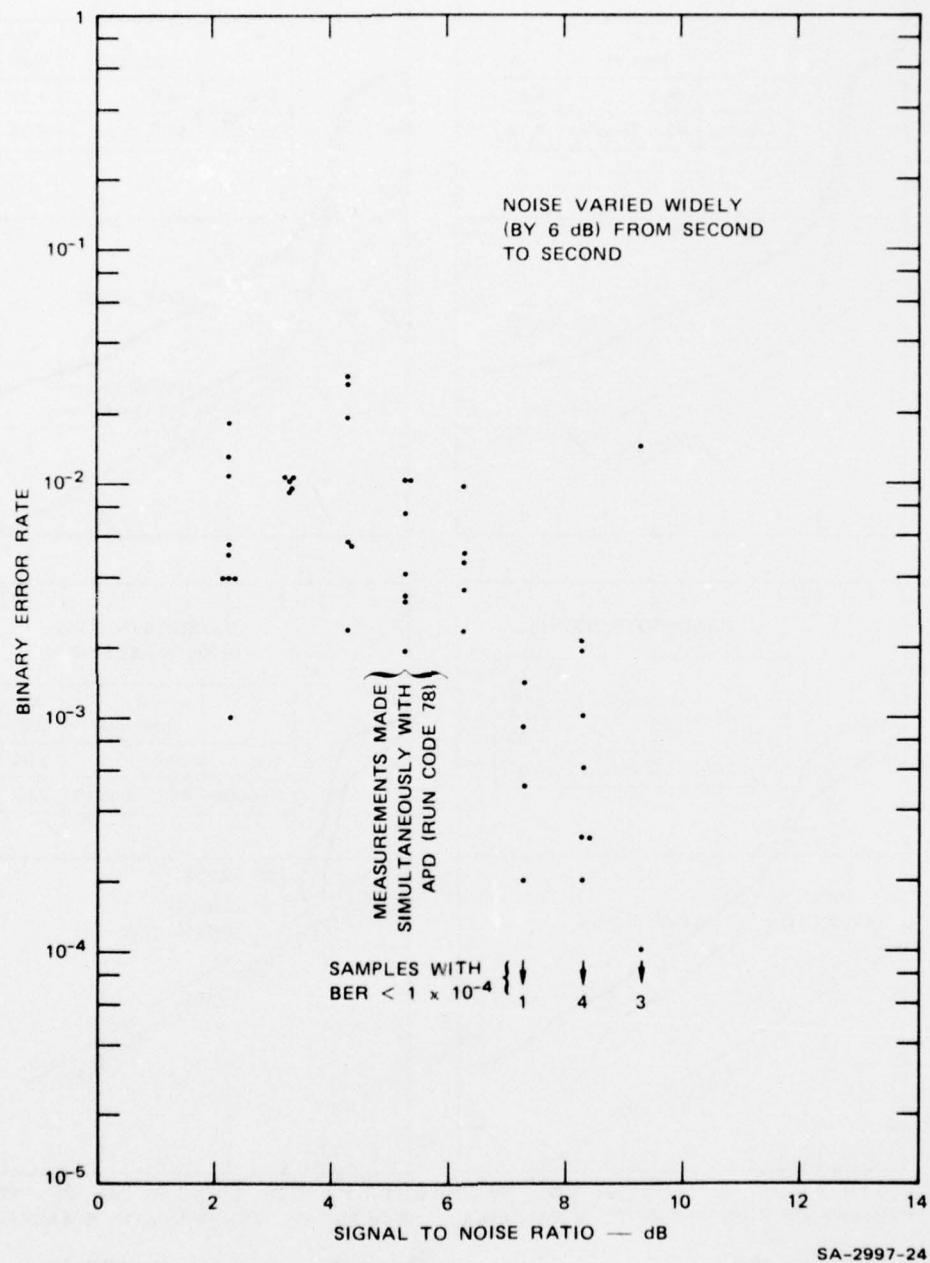
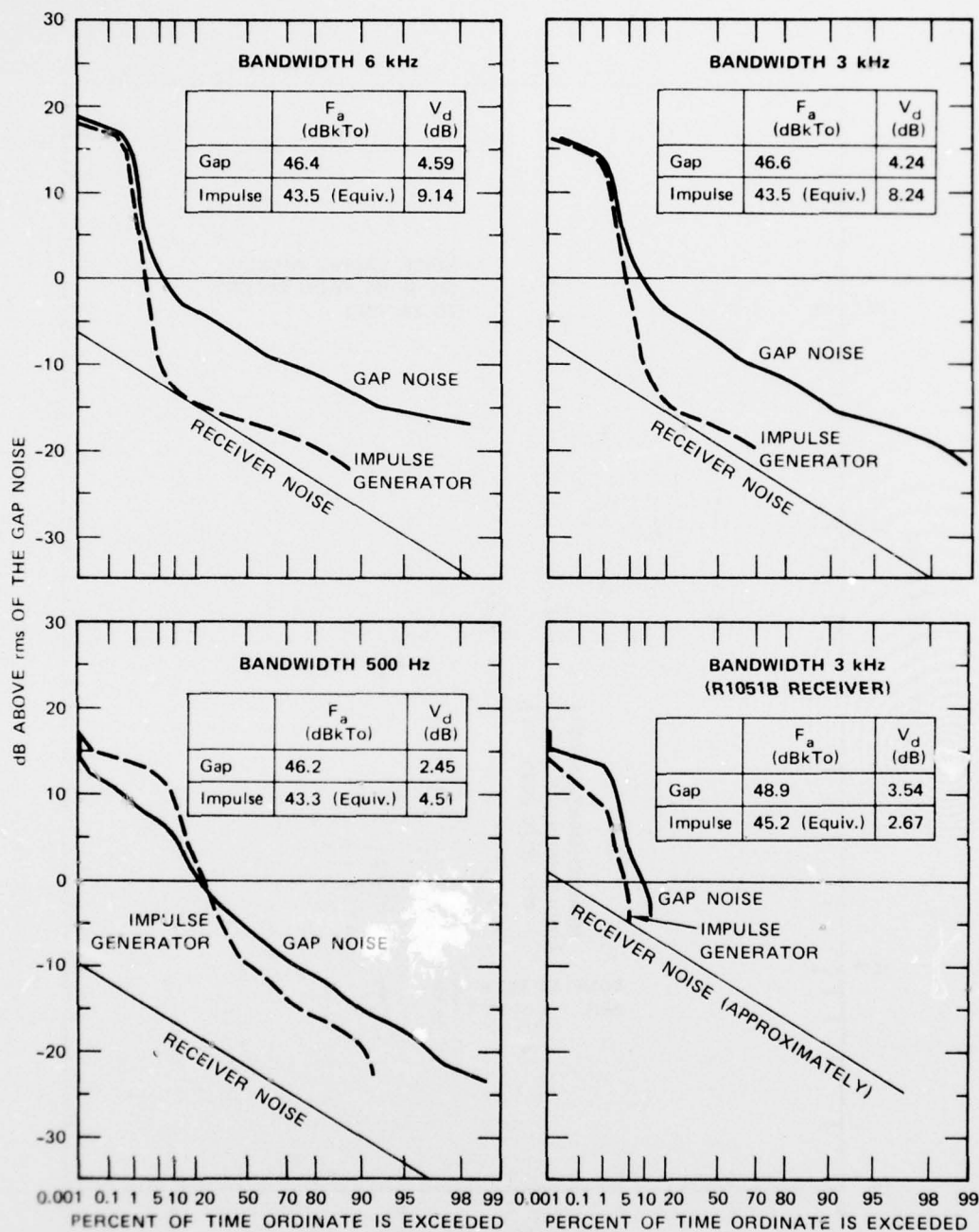


FIGURE 29 BINARY ERROR RATES CAUSED BY GAP NOISE AT 3.0 MHz,
ED LEVIN COUNTY PARK



DATE: 18 MARCH 1975

TIME: 1551 PDT

DURATION: 5.0 min (GAP), 4.9 min (IMPULSE)

RUN CODE: 78 (GAP), 79 (IMPULSE)

WEATHER: WARM AND SUNNY

LOCATION: ABOUT 6 ft FROM UNDER LINE

SA-3930-45

FIGURE 30 APDs OF (GAP) POWER LINE NOISE AT ED LEVIN PARK AND OF IMPULSE NOISE AT 62 dB μ V/MHz, 3.0 MHz

connected the impulse generator in place of the antenna and adjusted it so that it was providing pulses of the same height (on the oscilloscope) as the power line's gap source.* The APD measurement duration was 4.9 minutes. The rms value of the noise from the impulse generator was about 3 dB below that of the gap noise, while V_d was several dB higher (depending on the receiver bandwidth).

We measured the SNR and made error-rate measurements simultaneously with the impulse noise APD. The SNR was 8.3 dB, and the median of the ten closely grouped 33.3-s error-rate measurements was 4.2×10^{-3} --essentially the same as the median of the measurements made using the power line's gap noise at an SNR about 3 dB lower.

c. Agnews Hospital

The noise at the measurement site along the access road to Agnews Hospital seemed to come from many gaps, multiple gap breakdowns, or both. At times the noise looked as if it might be corona. It was very unstable, and from minute to minute the rms value changed by several decibels. We made measurements directly under the line and also at a distance of 50 ft (15.2 m).

Figure 31 shows the error-rate measurements, and Figure 32 shows the APDs made simultaneously when the antenna was under the line.

* The setting was 62 dB μ V/MHz.

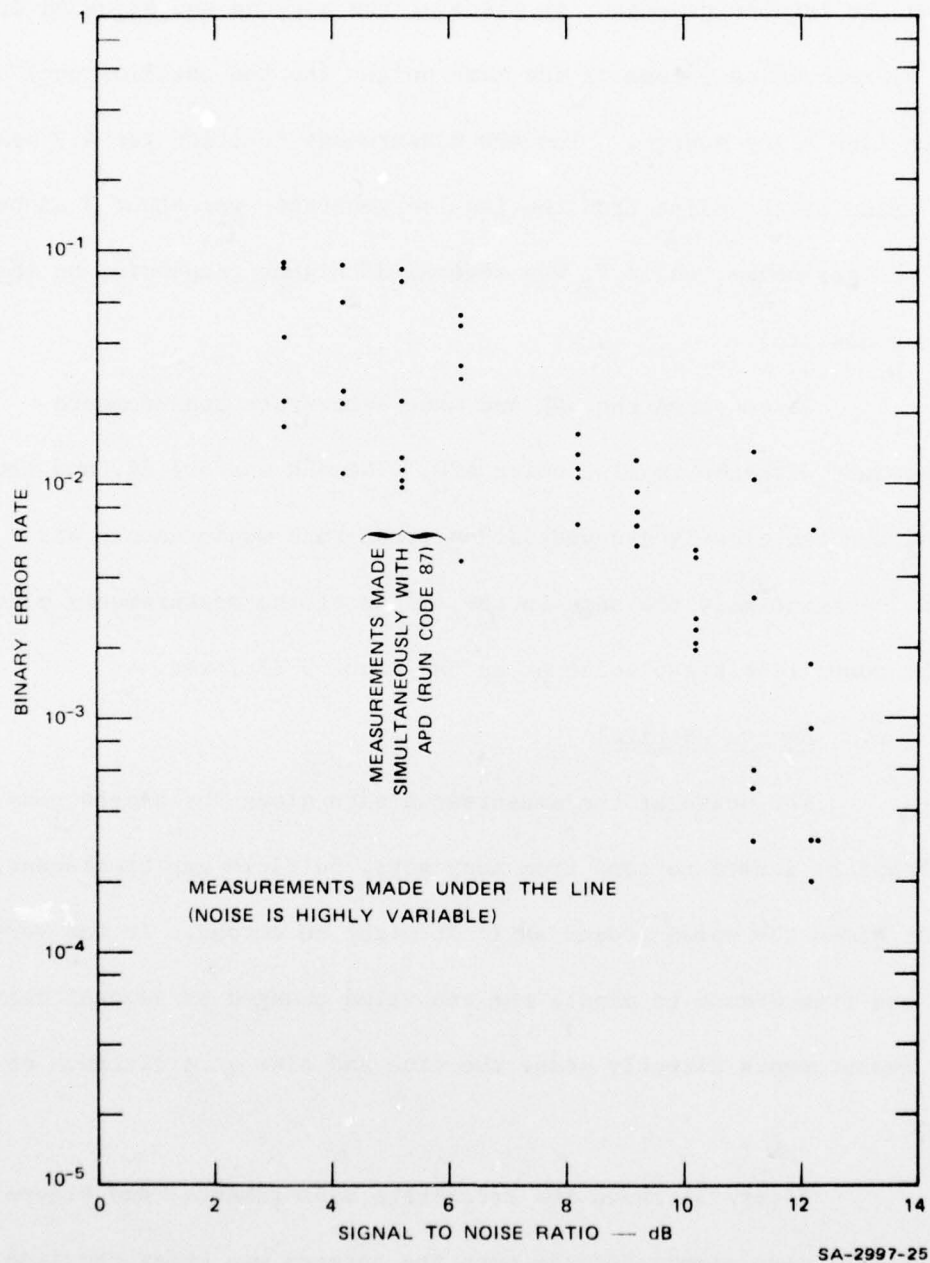
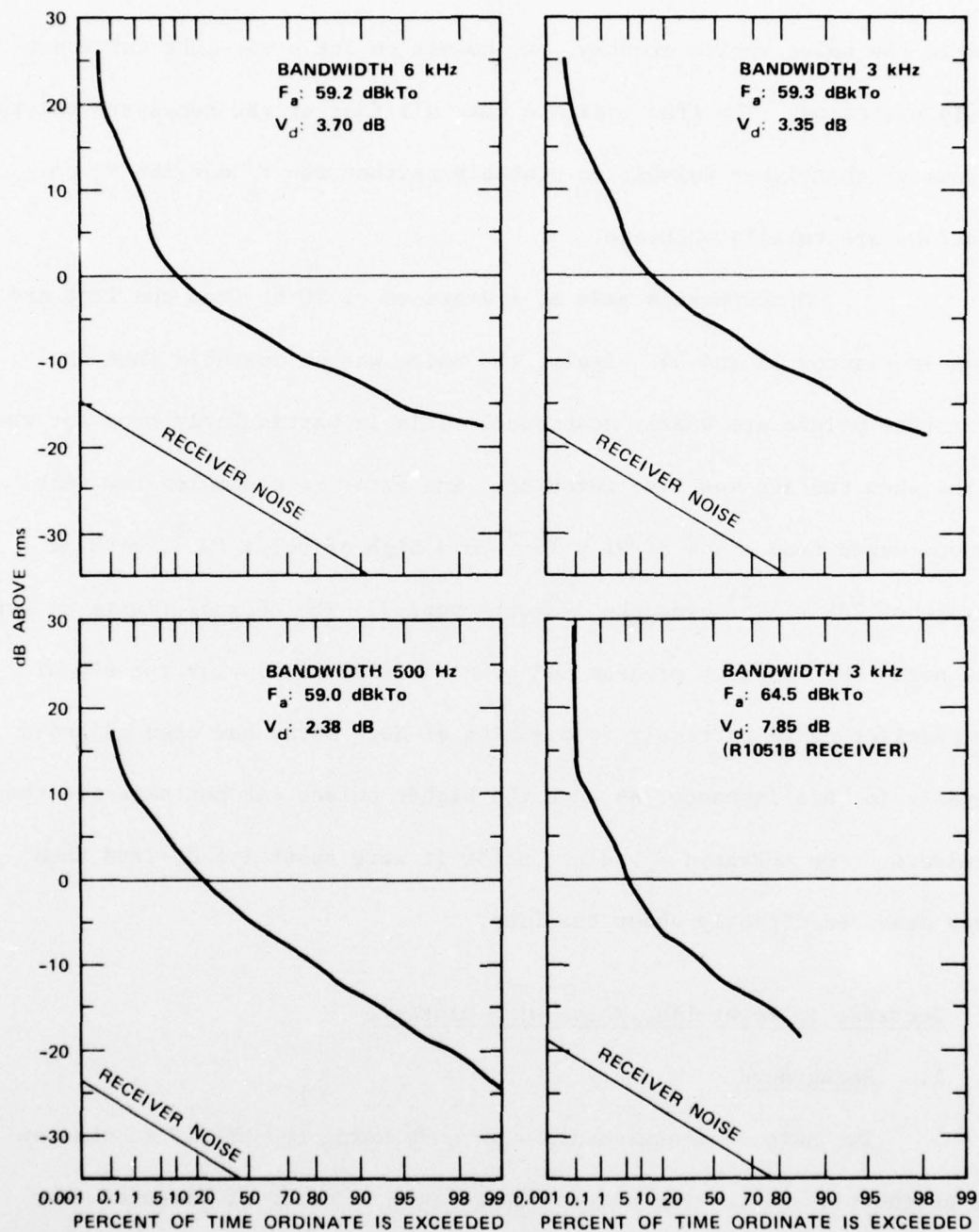


FIGURE 31 BINARY ERROR RATES CAUSED BY POWER-LINE NOISE AT 3.0 MHz, UNDER LINE AT AGNEWS HOSPITAL



DATE: 20 MARCH 1975 DURATION: 5.0 min WEATHER: SUNNY
 TIME: 1136 PDT RUN CODE: 87 LOCATION: DIRECTLY UNDER LINE
 SA-3930-46

FIGURE 32 APDs OF POWER LINE NOISE AT 3.0 MHz, UNDER DISTRIBUTION LINE AT AGNEWS HOSPITAL

Because the noise varied greatly, the points on the error-rate curve are widely scattered. The APDs indicate that all four of the receivers saturated on some of the higher pulses, so probably neither the F_a nor the V_d computations are totally accurate.

Measurements made at a distance of 50 ft from the line are shown in Figures 33 and 34. Again, the noise was so unstable that the error-rate points are widely scattered. This is particularly true for the period when the APD was also measured. The error rate samples for that period ranged from a low of 91×10^{-4} to a high of 960×10^{-4} , with an average of 232×10^{-4} over the 5-minute period. The APDs of Figure 34 were made after the computer program had been modified to display the APD of the receiver noise correctly as a series of Xs. Gains had been adjusted properly in this instance, so that the higher pulses did not saturate the receivers. The measured F_a values at 50 ft were about 1.5 dB less than those measured directly under the line.

B. Decrease in Power-Line Noise with Distance

1. Background

Two sets of measurements were made using the NM-26T to observe the attenuation of the rms noise voltage as a function of distance away from the power line. Although numerous such investigations have been made, the measurements have generally been done using either a peak or a quasi-peak detector (for example, see Ref. 9). Only a limited amount of distance

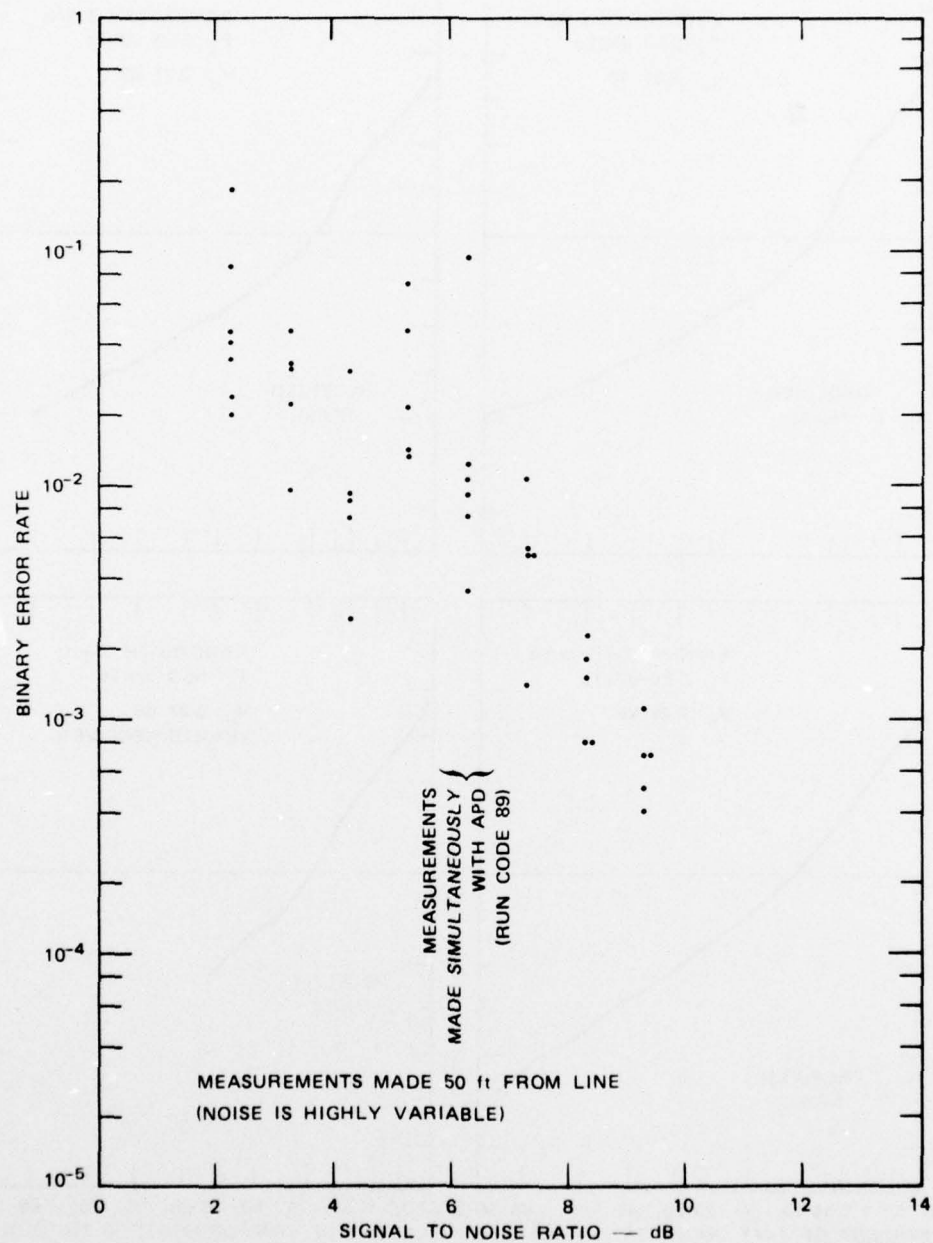


FIGURE 33 BINARY ERROR RATES CAUSED BY POWER-LINE NOISE AT 3.0 MHz,
NEAR LINE AT AGNEWS HOSPITAL

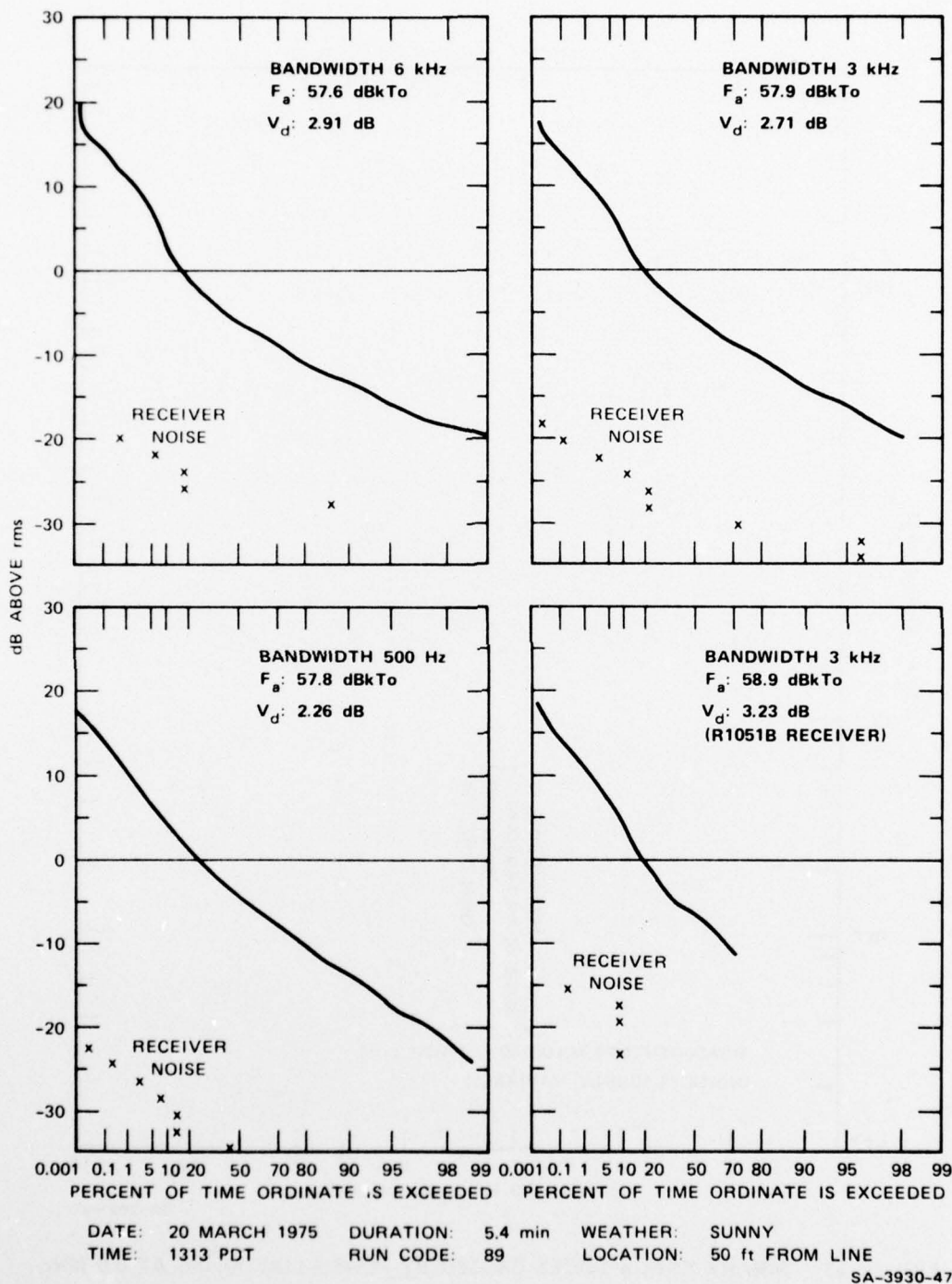


FIGURE 34 APDs OF POWER LINE NOISE AT 3.0 MHz, NEAR DISTRIBUTION LINE AT AGNEWS HOSPITAL

data are available from measurements made using an rms detector.^{13,14,27}

We made measurements at 3 MHz of the noise from the Bernardo Avenue power distribution line and the noise from the two 115-kV circuits at the Sunnyvale Dump.

2. General Procedure

Our procedure was to begin with the 9-ft rod antenna placed under the line and then to move away from the line, making measurements at various distances until we judged that the noise from the line had decreased to the level representative of the background. We used the NM-26T's short time constant, and at each location we usually made 11 measurements of both the rms noise voltage and the V_d at 15-s intervals, as suggested in Naval Shore Electronics Criteria.²⁸ The rms measurements were later converted to F_a , as discussed in Appendix A.

3. Bernardo Avenue

Figure 35 summarizes the measurements made at the Bernardo Avenue site. The measurement locations were in the field that can be seen in Figure 5. This field was covered with wet grass and mustard weeds growing about a foot high. Because the field was muddy, we could not drive a car into it, and so the 3-ft-square base-plate of the 9-ft rod antenna was placed directly on the wet grass. Individual measurements were shown as points on the graph, and the line connects the medians of the points measured at each distance.

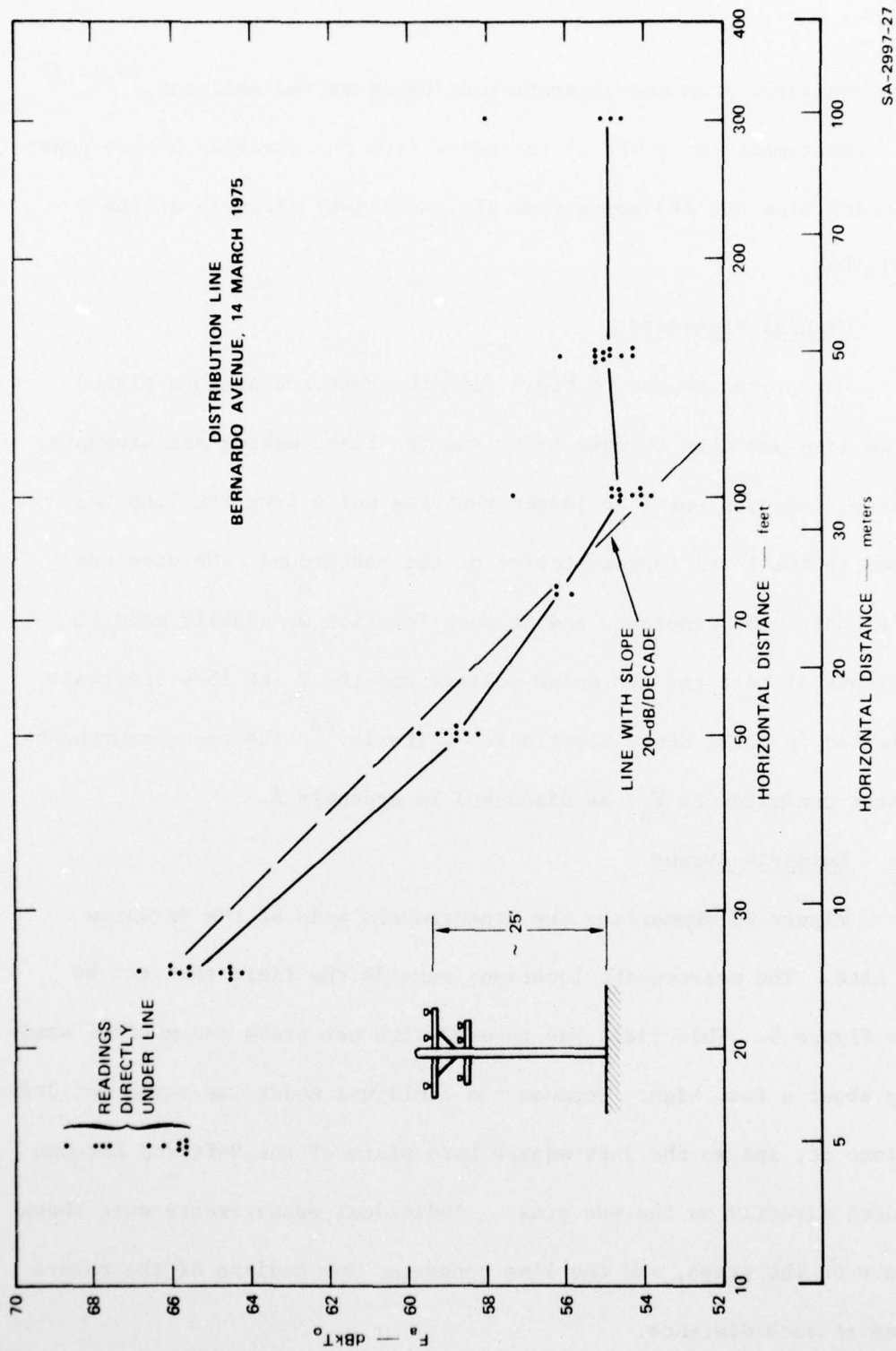


FIGURE 35 GAP NOISE AS A FUNCTION OF DISTANCE FROM LINE, 3.0 MHz

When under the line, we had listened to the NM-26T and had become accustomed to the sound of the noise from the line. Several times when we were out in the field, we noted an abrupt change in the sound of the noise, accompanied by increases of 15 dB or more in the rms value. Had our purpose been to document the radio-noise environment in the field, we would have included these samples. However, since we were measuring the falloff of the power-line noise, we excluded the samples where the character of the noise had changed abruptly for no known reason. The change may have been caused by noise from some other source entirely, or it may have been the result of a different gap source becoming active, as was observed at other places.

The noise from this line seemed to be reduced to the background noise level at about 100 ft from the line. The background level, 55 dBkT_0 , is within about 1 dB of the median level for a rural area at 3 MHz, as estimated by Spaulding and Disney.¹⁴ The samples discarded at 300 ft were about 60 dBkT_0 (6 dB above the background).

Lauber showed measurements of the noise from a 12.5-kV line at 2.5 MHz that agree very well with Figure 35.²⁷ He showed a level of about 59 dBkT_0 at 50 ft and the same falloff rate (20 dB per decade) to a background level of about 43 dBkT_0 at 300 ft. That level is appropriate for a quiet rural area.¹⁴

The V_d values were in the range 1.5 to 2.0 dB and did not show any noticeable trend as we moved away from the line and into the field.

4. Sunnyvale Dump

Figure 36 shows the distance attenuation measurements made at the 115-kV lines at the Sunnyvale Dump. The noise was about 10 dB higher than we had usually observed there, and it was very stable; the rms meter varied by 0.5 dB or less at each distance, and V_d remained at just over 1 dB. Aside from an exploratory day, before we began full-scale measurements, this was the only day that the weather was bright and sunny when we were at this location. On this clear day we would have expected the noise to be considerably lower than on the rainy days, rather than higher, this being a well-known characteristic of corona noise. Gap noise, on the other hand, is likely to be greatly decreased in damp weather. Although corona noise is prevalent on lines at this voltage and above, gap sources can exist. Possibly the major source here in rainy or damp weather was the corona, while on this sunny day, some gap noise sources became active. On lower-voltage lines with no accompanying corona, we had observed the phenomenon of gaps turning off and on.

The noise-power spectral density directly under the line was about 77 dBkT_0 and, with increasing distance, the noise appears to have been leveling out at about 59 to 61 dBkT_0 . This is higher by 5 or 6 dB than the noise levels we measured quite close to the line on some other days. A background of 40 to 50 dBkT_0 would be expected in this relatively rural area,¹⁴ and so we have to surmise that there were other, unrecognized, sources of noise in the area, such as activities in other parts of the dump.

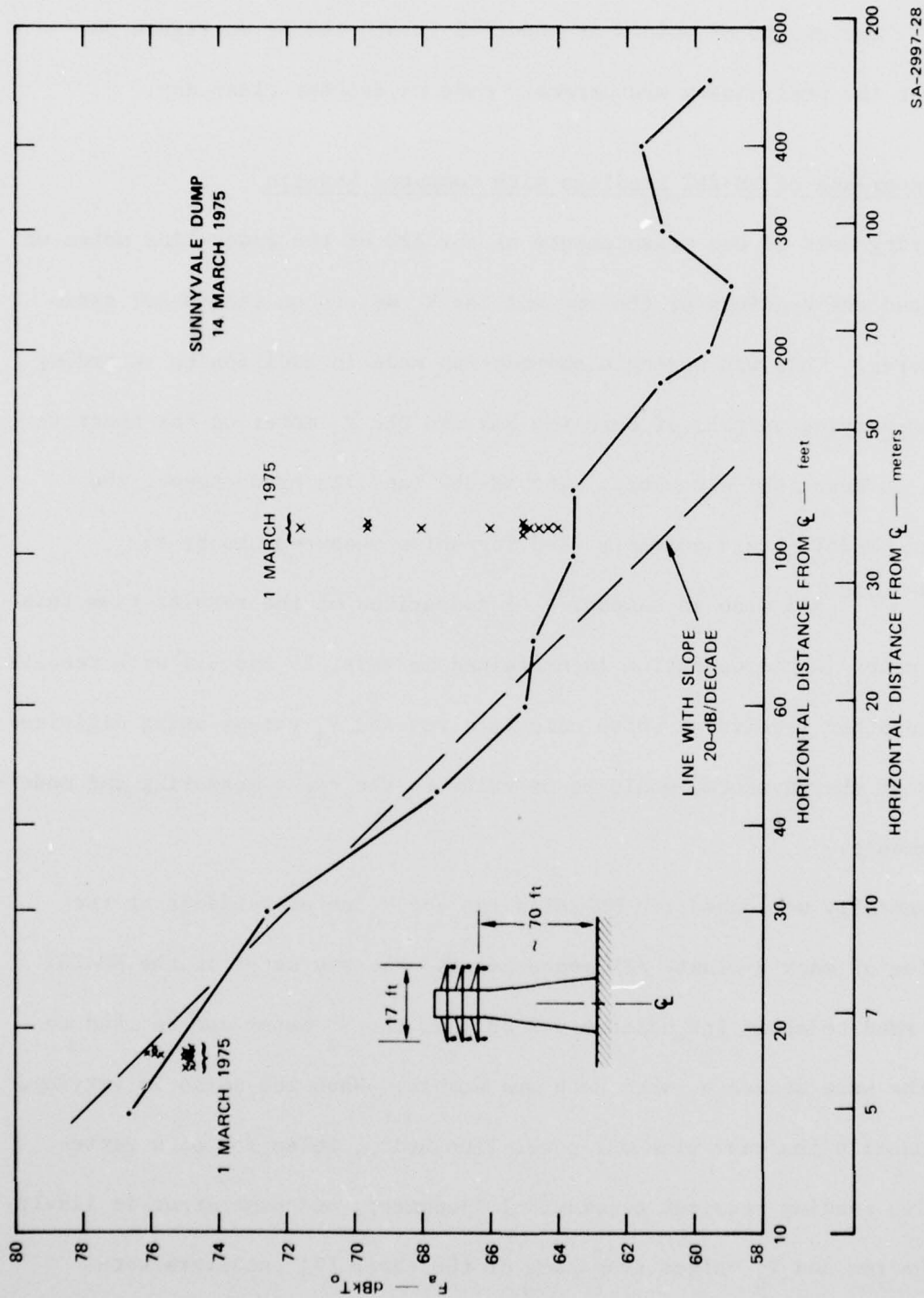


FIGURE 36 NOISE FROM 115 kV LINE AS A FUNCTION OF DISTANCE FROM LINE, 3.0 MHz

SA-2997-28

The groups of points at about 18 ft and 110 ft on Figure 36 represent the preliminary measurements made on another clear day.

C. Comparison of NM-26T Readings with Computed Results

During most of our measurements of the APD of the power-line noise we also noted the readings of the rms and the V_d meters on the NM-26T radio noise meter. This was a single observation made in addition to recording the time-varying outputs of both the rms and the V_d meter on the chart recorder, as described elsewhere. The NM-26T (and its predecessor, the modified NM-25T³¹) are commonly used for noise measurements by the Navy,^{23-26,28} and also in Canada.²⁷ A comparison of the results from this analog meter (whose operation is explained in Refs. 28 and 31) with results from the other receivers, which calculate rms and V_d values using digitized samples of the waveform, would be of value to the noise measuring and modeling community.

Generally we logged the NM-26T's rms and V_d meter readings at the beginning of each 5-minute APD measurement. The rms meter on the NM-26T can be read to about the nearest 0.2 dB, and the V_d meter can be read to about the same accuracy, when both are stable. When the noise is varying, as is usually the case with our power-line noise, selection of a representative reading requires considerable judgment, and some error is likely.

The rms and V_d values from each of the three SRI receivers were available only after computer processing, as discussed in Chapter IV.

Figure 37 is a scatter plot showing the rms noise voltages measured by both receiver systems and converted to actual F_a . The plot does not include F_a measurements made by digitizing the output of the R1051B receiver, because those measurements were generally far out of agreement with those made with the SRI receivers or the NM-26T. The plot shows three points (from three SRI receivers with different bandwidths) for each F_a reading from the NM-26T. Because we were measuring power spectral density (watts/Hz), all the receivers should have agreed, irrespective of bandwidth. The three SRI receivers agreed within a few tenths of a decibel, except for two very noisy instances (at the Dumbarton site), where the spread was slightly more than 2 dB. The same 9-ft vertical rod antenna was used for both systems, and they were calibrated using the same Gaussian noise source. This plot represents measurements from several power lines (with both gap noise and corona noise) at several distances. Most of the measurements were made at 3.0 MHz, but some were at 3.4 MHz. The agreement in F_a values is very good, considering that the NM-26T reading was made at the beginning of a 5-minute period, whereas the SRI receivers averaged over the entire 5-minute period, during which the noise would generally vary by several decibels.

Figure 38 shows the comparison of V_d readings of power-line noise made on the NM-26T with the computed value of V_d from one of the SRI receivers. The agreement was generally within 1 dB, and the points are so scattered that no clear trend of one system yielding larger values of V_d is noticeable. (We would expect a wideband system to provide greater V_d ratios than a

AD-A047 681

STANFORD RESEARCH INST MENLO PARK CALIF
MEASUREMENT OF THE APD AND THE DEGRADATION CAUSED BY POWER LINE--ETC(U)
APR 76 R A SHEPHERD, J C GADDIE

F/6 9/5

N00039-74-C-0077

UNCLASSIFIED

NL

2 OF 2

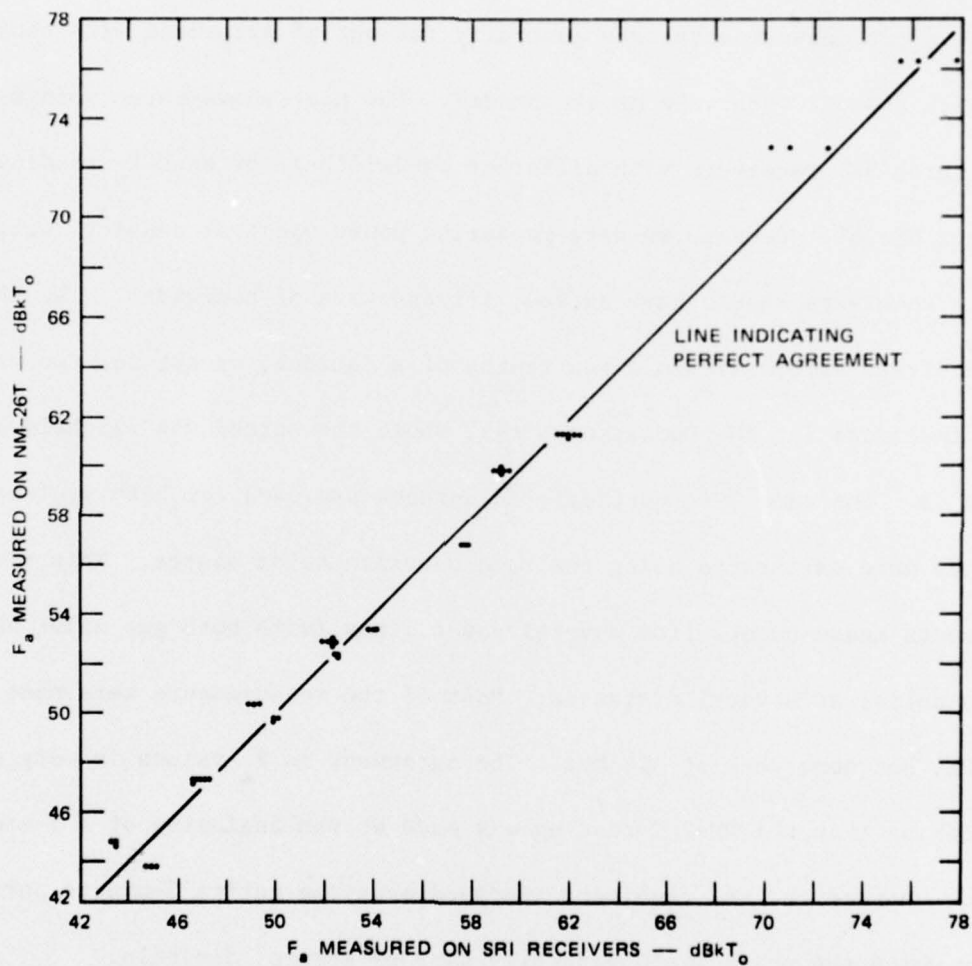
AD
A047681



END
DATE
FILMED

1 -78

DDC



SA-2997-29

FIGURE 37 COMPARISON OF POWER SPECTRAL DENSITY MEASUREMENTS MADE ON AN NM-26T RECEIVER WITH THOSE MADE ON SRI'S RECEIVERS—3.0 MHz

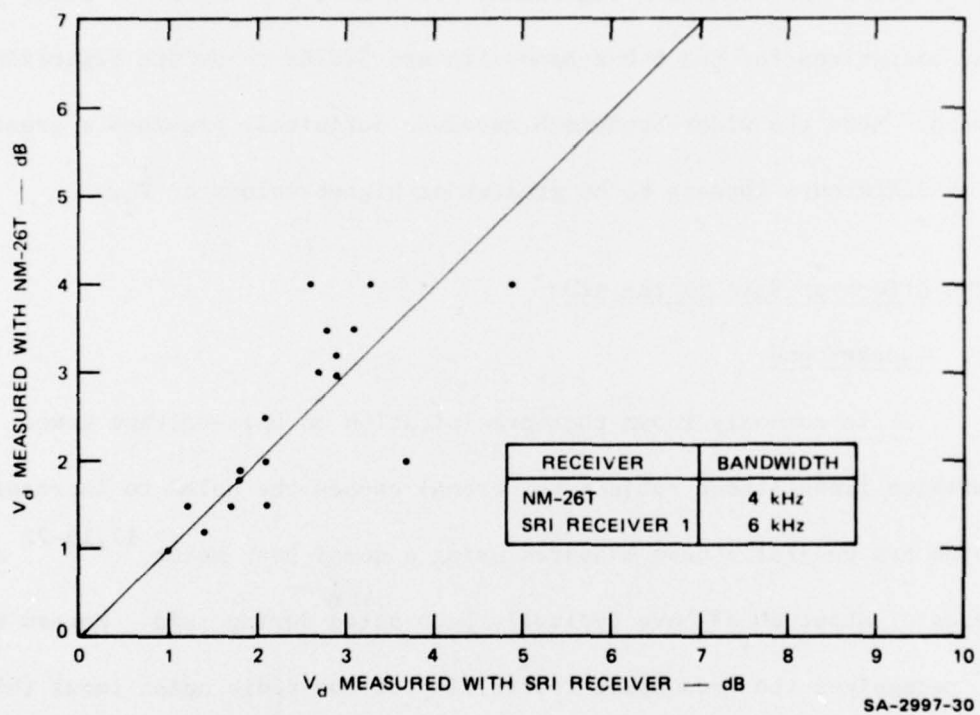


FIGURE 38 COMPARISON OF POWER-LINE V_d MEASUREMENTS—NM-26T AND SRI RECEIVER

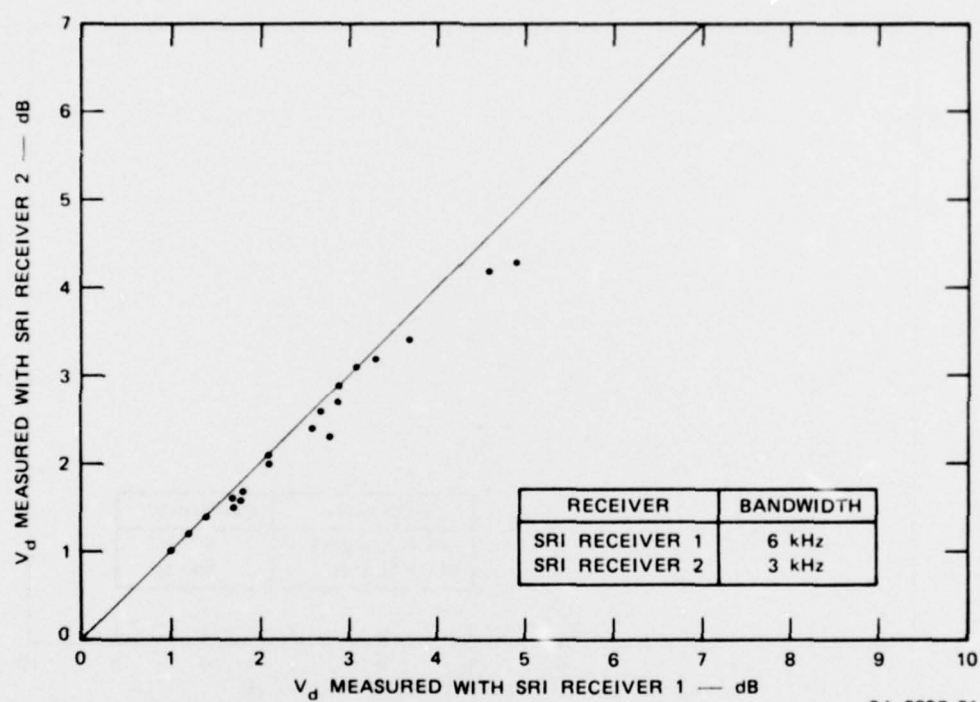
narrow-band system.) For the measurements shown in this comparison, our widest-bandwidth receiver (6 kHz) was used; a similar plot for measurements with our 3-kHz bandwidth receiver is almost identical and is not shown.

Figure 39 shows a comparison of the V_d values measured on the 6-kHz-bandwidth and 3-kHz-bandwidth digitizing receivers, and Figure 40 shows a similar comparison for the 6-kHz-bandwidth and 500-Hz-bandwidth digitizing receivers. Here the wider-bandwidth receiver definitely provides a greater V_d . The difference appears to be greater at higher values of V_d .

D. The Effect of Rain on the APDs

1. Background

It is commonly known that precipitation on high-voltage power transmission lines (those subject to corona) causes the noise to increase. The noise has generally been measured using a quasi-peak meter,^{17,19-22} and increases of about 20 dB have typically been noted during rain. Moreau and Gary³² recognized the "essential instability of the radio noise level (RI) generated by a transmission line," although they noted that a particular line's noise level during heavy rain is stable and reproducible for rain intensity greater than about 1 mm/hr. They considered the noise level under heavy rain--which is practically the maximum--to be the "basic level of a line" for use in making predictions. Although Hagn²³ made some measurements of the rms value of power-line noise from the same line in dry and rainy conditions, and Disney and Longley¹³ and Lauber¹⁵ have measured APDs



SA-2997-31

FIGURE 39 COMPARISON OF POWER-LINE V_d MEASUREMENTS—SRI RECEIVERS WITH 6-kHz AND 3-kHz BANDWIDTHS

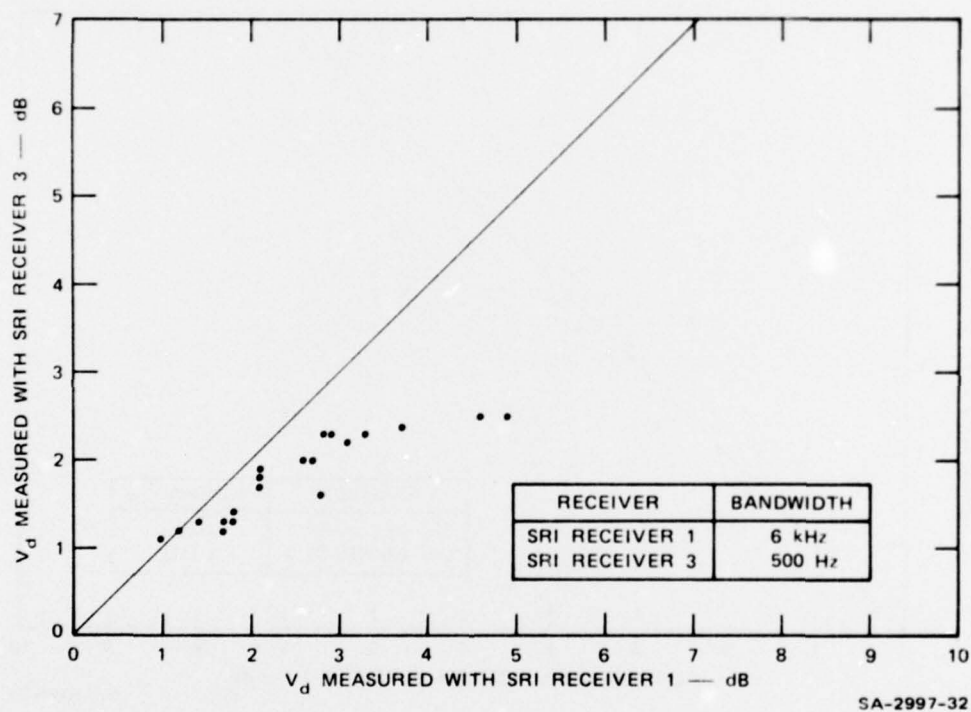


FIGURE 40 COMPARISON OF POWER-LINE V_d MEASUREMENTS—SRI RECEIVERS WITH 6-kHz AND 500-Hz BANDWIDTHS

of power-line noise, we believe that the following are the first reported measurements of power-line APDs and rms levels that enable comparisons to be made for dry and rainy weather.

2. 230-kV Lines at Cupertino

The APDs of Figure 41 were all made within about 2 ft of a spot 60 ft (about 18.3 m) from the centerline of the 230-kV lines at our Cupertino measurement location. We used our judgment in grading the rain intensity from no-rain through heavy rain; no measurements of rain intensity were made. All three SRI receivers indicated an increase of about 20 dB in F_a and an increase of about 1 dB in V_d from the no-rain sample of 19 March to the heavy-rain sample of 7 March.

Note that the no-rain sample does not represent a situation when the line could be considered completely dry and, therefore, possibly at its quietest state. The measurement was made in late afternoon during cloudy weather. There had been no rain since morning, but rain appeared likely at any moment; it is possible that rain was falling on portions of the line within a few miles. All the no-rain APDs indicate a sudden upturn (unusually high amplitudes for a small percentage of the time), but the RI051B receiver indicates that three samples out of approximately 60,700 (0.005%) were about 20 dB above what would be expected. We do not understand this, and we suspect some malfunction associated with that receiver, which had a relatively narrow dynamic range.

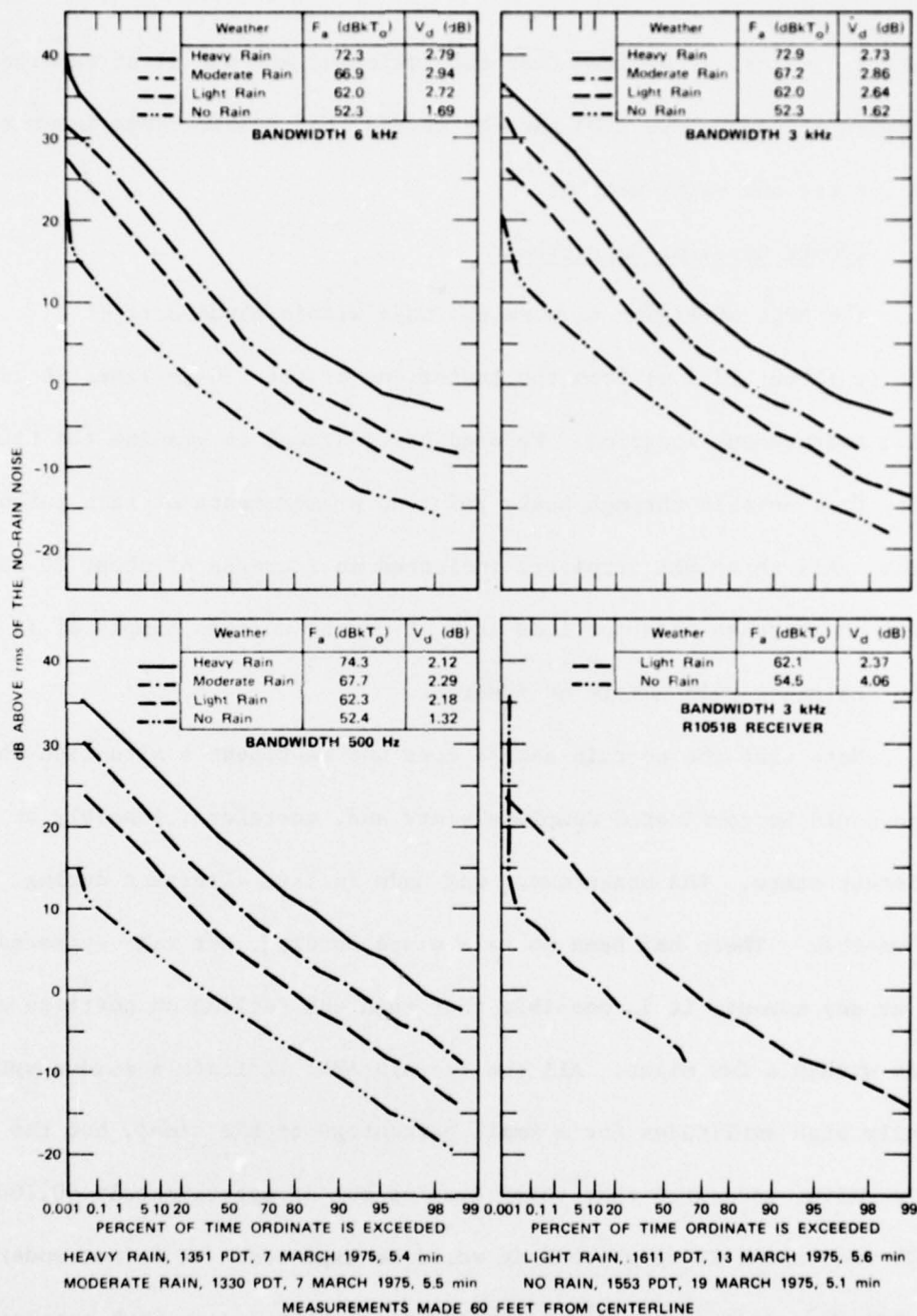


FIGURE 41 APDs OF CORONA NOISE NEAR 230-kV LINES (CUPERTINO) IN FOUR WEATHER CONDITIONS, 3.0 MHz

The light-rain measurement was taken when rain had begun to fall after a dry hour or so. Prior to making that data sample, we had watched the rms meter on the NM-26T steadily climb 3 or 4 dB within a period of about 10 minutes while rain appeared to be falling a mile or so away over the hill. This implies that the noise must propagate along the line from its actual source; the noise propagating through the intervening space would be greatly attenuated. As the rain began at our location, we observed, on the monitor oscilloscope, an increase in the rate of occurrence of received impulses. We could also watch the NM-26T's rms meter reading increase and decrease in correspondence with the intensity of the local rain. Instrumentation that would measure the instantaneous rain intensity could be used to determine the relationship between the rain intensity and F.
a

The heavy-rain sample was started about 10 minutes after the moderate-rain sample had been completed, and its rms value was about 6 dB higher. After we had made the first measurement, we noticed that both the rain intensity and the NM-26T's rms meter level had increased. Probably the level was changing during the 5-minute durations of both these APD measurements. At any rate, the values we report always represent integrations over the measurement time durations.

Figure 42 shows APD measurements made at a distance of 100 ft (30.5 m) from the same 230-kV power line; again, an increase of about 20 dB

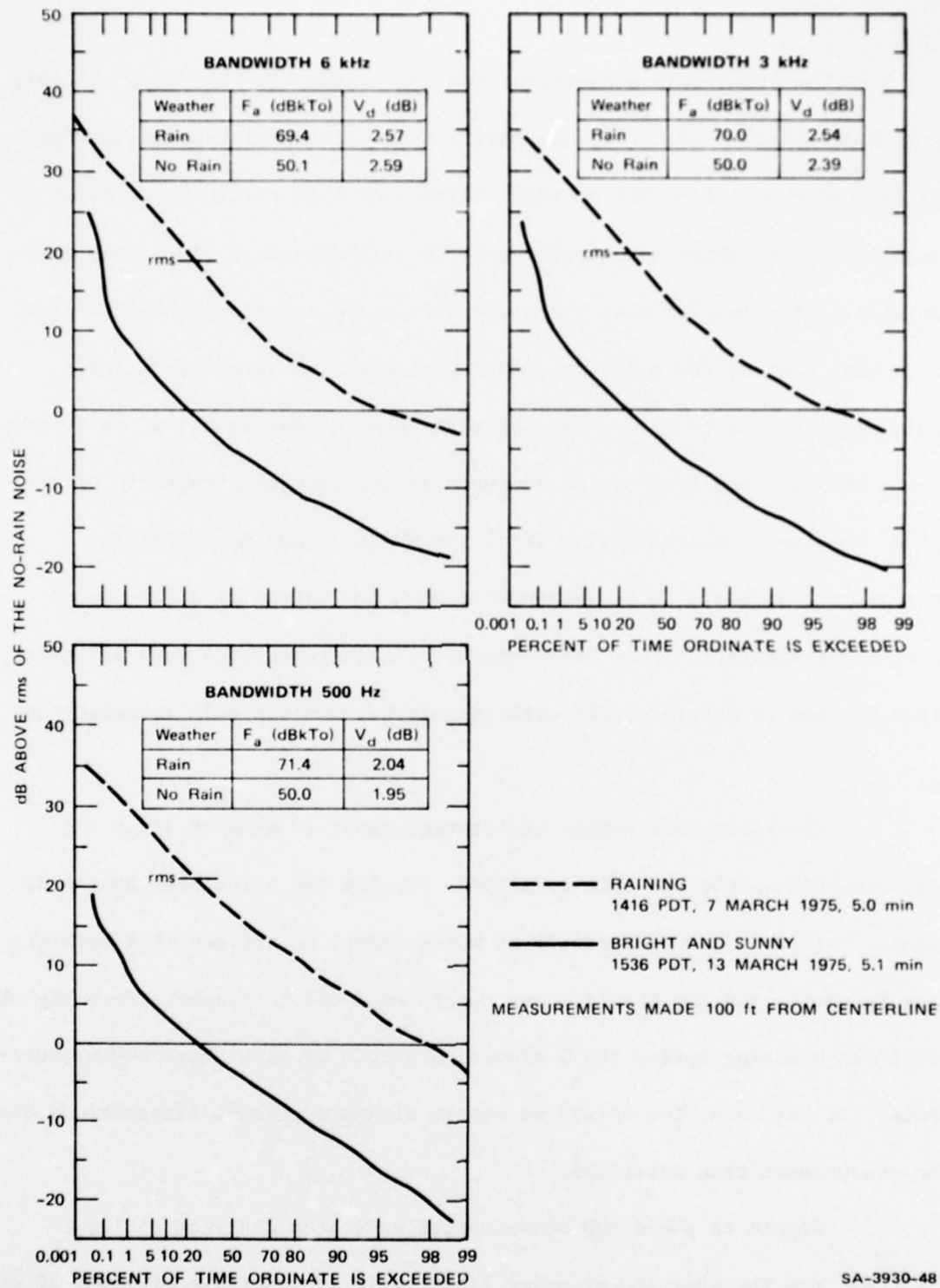
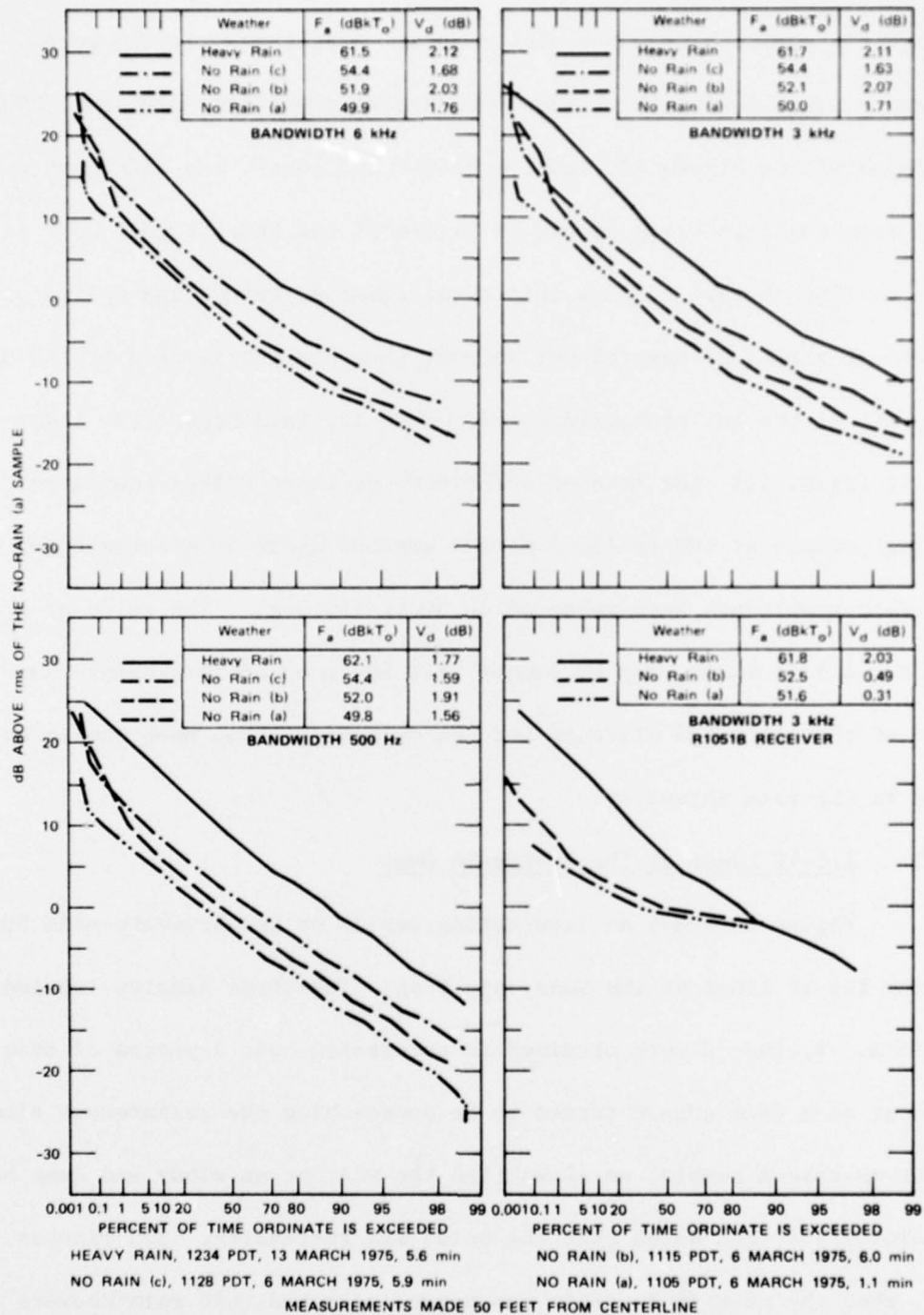


FIGURE 42 APDs OF CORONA NOISE NEAR 230-kV LINES (CUPERTINO) WITH AND WITHOUT RAIN, 3.0 MHz

in the F_a is apparent from no-rain to rain. Both these samples were measured on days for which we also had data at the closer distance. The no-rain sample on Figure 42, labeled bright and sunny, was made just a half-hour before the light-rain sample of Figure 41 and about a half hour following an earlier shower. During this measurement we noted high spikes occurring randomly at a rate of several per second; they are represented by the upturn in the APD at the low-probability end. When the rain began (the light-rain curve of Figure 41), the rate of occurrence of these spikes increased. The "raining" sample at 100 ft (30.5 m) was started about 20 minutes after the heavy-rain sample had been measured at 50 ft (18.3 m). The value of F_a was about 2.9 dB lower, but we cannot tell how much of that change was the result of the increased distance and how much might have been caused by a change in the rain intensity.

3. 115-kV Lines at the Sunnyvale Dump

Figure 43 shows an interesting series of measurements made 50 ft from the 115-kV lines at the Sunnyvale Dump. The three samples labeled no-rain-A, -B, and -C were obtained in succession over a period of about a half hour as a rain shower seemed to be approaching the measurement site. For the no-rain-A sample, we classified the weather as windy and damp but not raining and then noted that the noise was increasing. Ten minutes later, when the no-rain-B sample was begun, we noted that rain showers were falling on the line several miles away. The value of F_a increased by about



SA-2997-34

FIGURE 43 APDs OF NOISE NEAR 115-kV LINES (SUNNYVALE DUMP) IN SEVERAL WEATHER CONDITIONS, 3.0 MHz

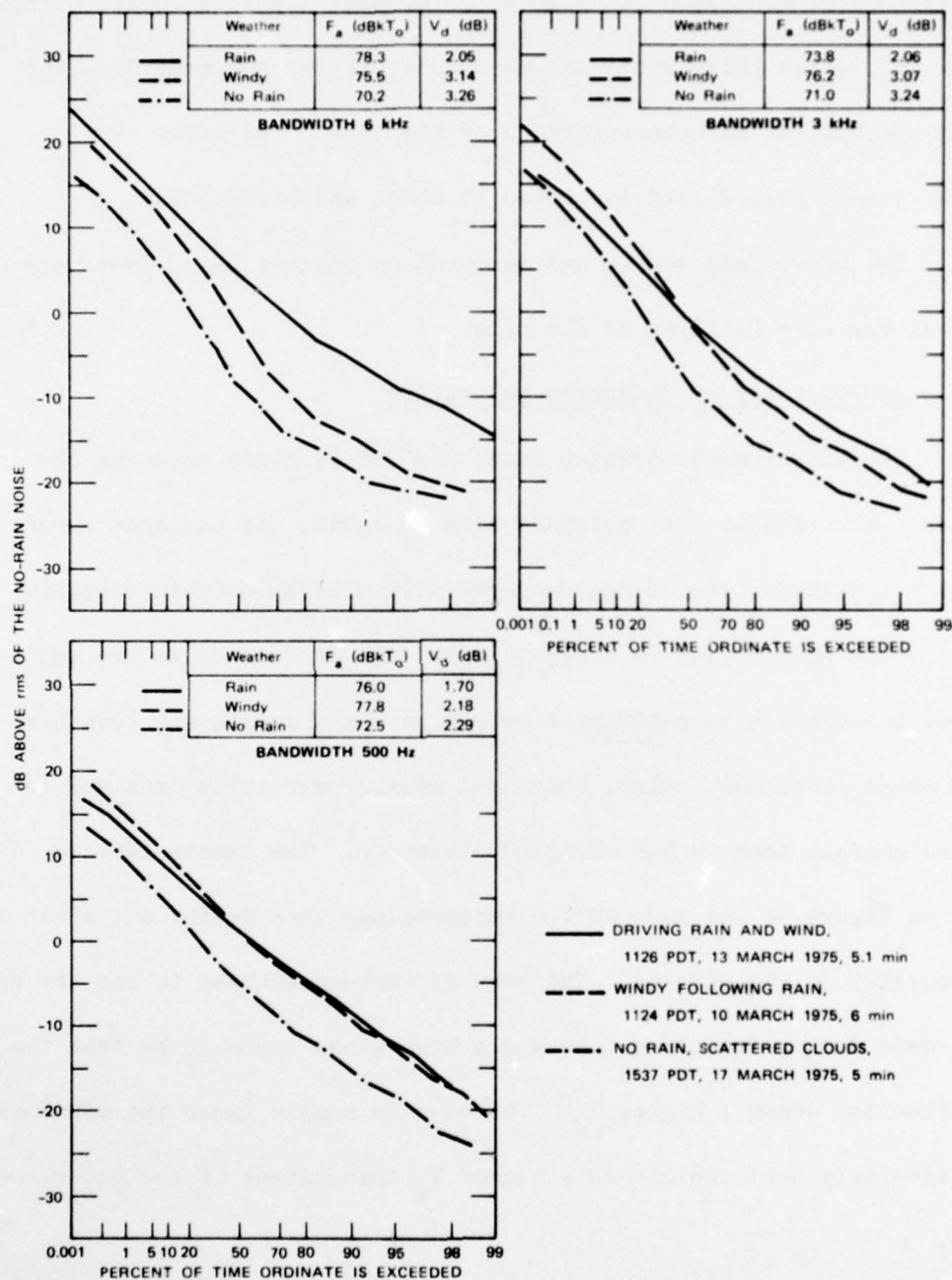
2 dB. The no-rain-C sample was started 13 minutes after the start of the previous one, while there still was no rain at the measurement location but rain was falling on other sections of the line. The value of F_a (over the sample period) had increased by about another 2.5 dB.

The heavy-rain sample was measured on another day. Some very small hail was also falling at the time.

4. 230-kV Lines at Dumbarton Substation

The measurement location under the 230-kV lines entering the Dumbarton Substation was the noisiest site we found. At our spot about 50 ft from the lines, the corona was generally clearly audible (that is, as audio noise in addition to radio noise). The difference in the radio-noise level between a no-rain and a very-heavy-rain sample was less here than at other locations. Also, there was greater variation from one receiver to another than we had observed elsewhere. The sample labeled "windy" on Figure 44 was made as the surroundings were drying out after a shower earlier in the morning. The main difference between it and the rain sample, made during drenching rain and a high wind, seems to be that the windy situation shows a higher V_d . The no-rain sample (when the wind was not particularly noticeable) has a higher V_d than either of the other two samples.

Elsewhere we had noticed that V_d was generally higher during rain and had found a much stronger correspondence between F_a and rain



SA-2997-35

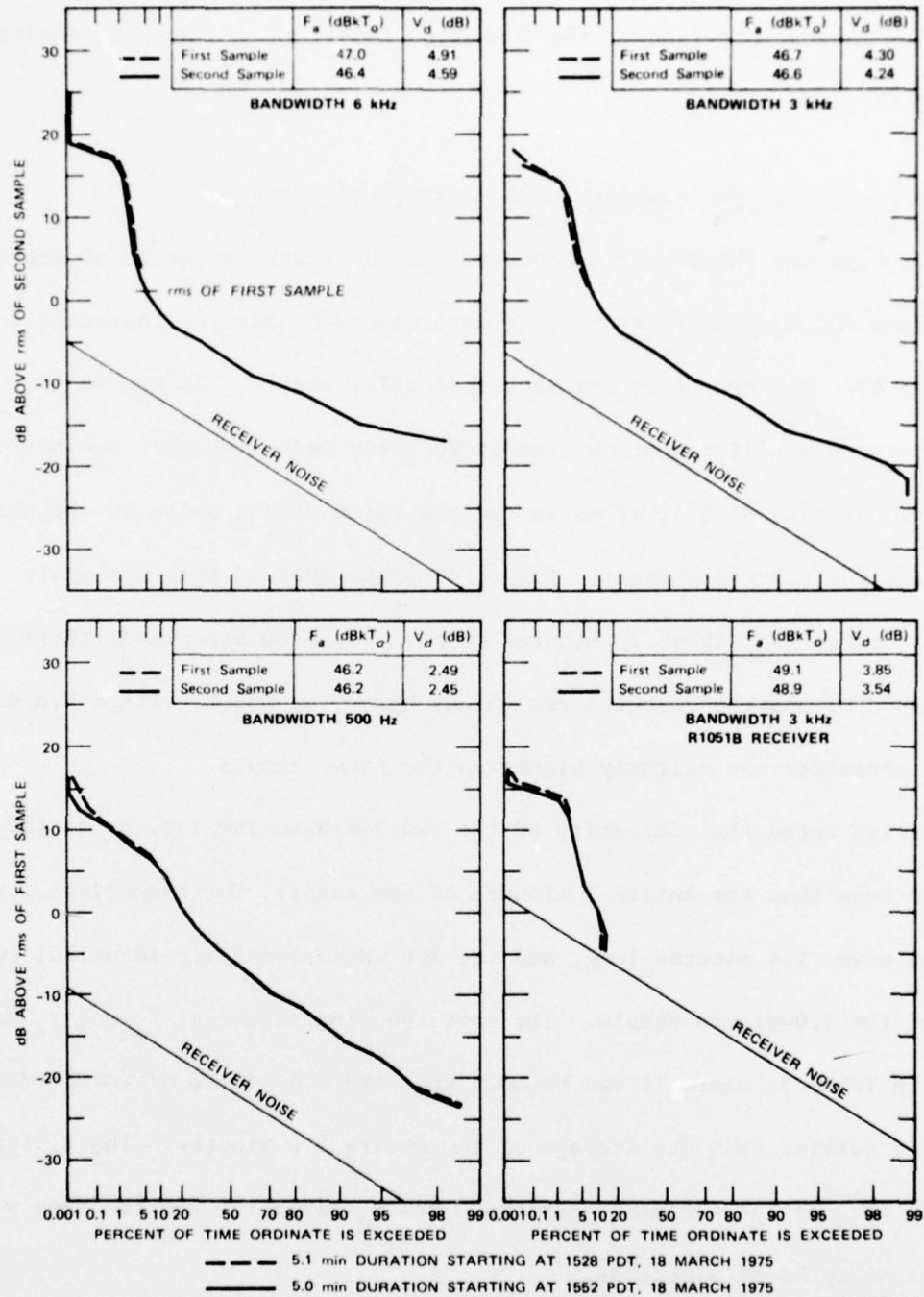
FIGURE 44 APDs OF CORONA NOISE UNDER 230 kV LINES (DUMBARTON SUBSTATION) IN SEVERAL WEATHER CONDITIONS, 3.0 MHz

intensity then we observed at the Dumbarton site. We do not yet understand these differences.

E. Comparison of Two Samples at Ed Levin County Park

Although the short-term (second-to-second) characteristics of gap-type power-line noise may vary widely, we have observed that the characteristics averaged over a longer term are sometimes quite stable. As mentioned before, the power distribution line at Ed Levin Park displayed second-to-second variations of 6 dB or so in the rms value of the noise as the number of active gap sources changed. Figure 45 shows APDs of that extremely variable noise made about 23 minutes apart. The APDs are almost totally superimposed, and the computed rms values agree, at worst, within 0.6 dB. The V_d parameter was slightly higher on the first sample.

Having noted the similarity of the two 5-minute samples, we decided to process less than the entire 5 minutes of one sample, for comparison. The subsample was 1.4 minutes long, and its APD was essentially identical to that of the 5.0-minute sample. The corresponding values of F_a and V_d are shown in Table 3, where it can be seen that the 1.4-minute subsample was slightly quieter than the average of the entire 5.0 minutes. The difference becomes less as the bandwidth narrows. The V_d parameter was the same within a few hundredths of a decibel.



SA-2997-36

FIGURE 45 APDs OF GAP NOISE DEMONSTRATING STABILITY OVER MANY MINUTES

Table 3

COMPARISON OF PARAMETERS FROM A 5.0-MINUTE
SAMPLE AND A 1.4-MINUTE SUBSAMPLE

Receiver 3-dB Bandwidth	F_a (dBkT _o)		V_d (dB)	
	Sample (5.0 min)	Subsample (1.4 min)	Sample (5.0 min)	Subsample (1.4 min)
6 kHz	46.4	45.4	4.59	4.50
3 kHz	46.6	45.7	4.24	4.11
500 Hz	46.2	45.8	2.45	2.50
3 kHz (R1051B)	48.9	48.0	3.54	3.35

Appendix A

CALIBRATION OF NOISE MEASUREMENTS TO OBTAIN F_a

PRECEDING PAGE BLANK-NOT FILMED

Appendix A

CALIBRATION OF NOISE MEASUREMENTS TO OBTAIN F_a

1. Introduction

All the noise measurements made with the NM-26T receiver and with the SRI Noise Measurement System involve rms voltage measurements using an electrically short vertical monopole. A very useful way to present such data is in terms of the power spectral density (watts per hertz) of the noise available from such an antenna. This appendix shows how we converted rms voltage measurements to the more universally useful power spectral density form.

Because we calibrated our system at the antenna terminals and because of the complexity of the combined hardware/software system, we divide this discussion into two parts. The first deals with calibration of the system from the antenna terminals inward; the second treats the system from the antenna terminals outward.

2. Calibration of the APDs from Antenna Terminals Inward

The noise envelope voltage from each of the four receivers was digitized at the rate of 200 times per second and placed on magnetic tape^{*}

^{*}This procedure and the equipment have been discussed at great length in Refs. 3 and 7. The computer program is listed in Appendix B.

for computer processing. As each noise envelope sample, e , was obtained by the computer, it was converted to a relative decibel figure by $E = 20 \log e$. A 5-minute data collection run results in 60,000 of these samples. A number of 2-dB-wide cells had been established, and each sample was then allocated to the appropriate cell. Dividing the number of counts in each cell by the total number of samples in the data collection run converts the data in the cells into a noise amplitude density array. The percentage of samples that fell within each cell is indicated. Starting at the high-amplitude end of the array of bins, the computer accumulates percentage proceeding in 2-dB steps to the low-amplitude end. After each 2-dB step, the percentage of samples that are above that level is known; by the time the low-amplitude end is reached, 100% of the samples have been accumulated, and the data for an as-yet-uncalibrated APD are available.

Only one point must be calibrated to calibrate the entire APD. By finding the E (relative dB) that our system computes for some signal of known power spectral density, all other points on the APD can be related to that known point. For calibration, we used a Gaussian noise source whose power spectral density into a 50Ω load was 36 dBkT_0 . Connecting this noise source in place of the antenna and recording data for a minute or so gives about 12,000 samples, from which we can compute a relative dB number, E_{36} , representing the rms value of the sampled envelope of the noise source. So

$$E_{36} = 20 \log e_{\text{rms}} = 10 \log \left(\frac{1}{N} \sum_{i=1}^N e_i^2 \right) \quad (\text{A-1})$$

corresponds to a noise-power spectral density of 36 dBkT_0 at the antenna terminals.* We use the known input power spectral density, $P_k = 36 \text{ dBkT}_0$, and the system's relative dB, E_{36} , to find a calibration factor $K \text{ dB}$ from

$$K = E_{36} - 36. \quad (\text{A-2})$$

Then K can be used to convert any other relative dB reading E to dBkT_0 at the antenna terminals by

$$P = E - K \quad \text{dBkT}_0, \quad (\text{A-3})$$

thus calibrating the APD from the antenna terminals inwards.

When measuring the power-line noise, the computer also calculates the rms value of that noise and converts it to a power spectral density, P_{nc} , at the antenna coupler, according to Eq. (A-3) above. Subtracting the rms value from each point of the APD enabled us to plot the APD in dB relative to its own rms value. That rms value can also be converted to the effective noise factor F_a , as described in the next section of this appendix.

* Strictly speaking, this is not at the antenna terminals, but at the antenna coupler terminals.

3. Determination of F_a from our Calibrated Measurements

The noise power spectral density in watts per hertz^{*} available from an equivalent loss-free antenna can be expressed in terms of an effective noise factor:³³

$$F_a = 10 \log f_a = 10 \log \left(\frac{p_{na}}{kT_o} \right) \text{ dBkT}_o, \quad (\text{A-4})$$

where

p_{na} = the mean noise power spectral density available from a short lossless vertical antenna, in watts per hertz

k = Boltzmann's constant = 1.38×10^{-23} joules per °K

T_o = reference temperature = 288 °K

(a) F_a on the APD

When measuring the APD of the noise, we calibrate at the output terminals of the antenna coupler using a Gaussian noise source with known power spectral density and then actually measure p_{nc} , the noise power spectral density at the terminals of the antenna coupler circuit. At 3 MHz, according to the antenna manufacturer's literature, the coupler insertion loss is

* F_a is also commonly used to represent the noise power in a 1-kHz bandwidth. That F_a is numerically 30 dB greater than our noise power spectral density.

$$AF = 10 \log \left(\frac{P_{na}}{P_{nc}} \right) = 16.3 \text{ dB}, \quad (\text{A-5})$$

so

$$F_a = 10 \log \left(\frac{P_{nc}}{kT_o} \right) + 16.3 \text{ dBkT}_o. \quad (\text{A-6})$$

The quantity $10 \log \left(\frac{P_{nc}}{kT_o} \right)$ dB, or $P_{nc} \text{ dBkT}_o$, is available from the computer as the rms value of the APD, and so we must add 16.3 dB to convert that value to the actual F_a for our antenna. The antenna itself, a 9-ft (2.74-m) rod, is short compared to a wavelength ($\lambda = 100 \text{ m}$ at 3 MHz); therefore our corrected F_a values are appropriate for a short vertical antenna.

(b) F_a from the NM-26T

We can convert rms noise readings made on the Singer NM-26T receiver in exactly the same manner if it is calibrated using the Gaussian noise source. However, when the NM-26T is used without that calibration source, a different approach is needed. Equation (A-4) can be rewritten (see Refs. 23 through 29) as

$$F_a = E_{nl} - 20 \log f_{\text{MHz}} + 95.5 \text{ dBkT}_o, \quad (\text{A-7})$$

where

E_{nl} = equivalent vertically polarized groundwave rms noise field strength, dB > 1 μ V/m in a 1-Hz bandwidth

f_{MHz} = measurement center frequency in megahertz.

Because we do not generally measure the noise in a 1-Hz bandwidth, a conversion factor is required to account for the measurement bandwidth, b Hz.

Therefore

$$E_{nl} = E_n - 10 \log b \quad \text{dB} > \mu\text{V/m} , \quad (\text{A-8})$$

where

E_n = equivalent vertically polarized groundwave rms noise field strength, dB > 1 μ V/m, in the measurement bandwidth b.

Typically an equivalent noise power bandwidth $b = 4$ kHz is considered appropriate^{23,24,27} for the NM-26T (and modified NM-25Ts) and our measurements indicated a 3.9-kHz noise power bandwidth, so we evaluate Eq. (A-8) as

$$E_{nl} = E_n - 36 \quad \text{dB} > \mu\text{V/m} . \quad (\text{A-9})$$

Now we have to account for the effects of all the hardware items interposed between the electromagnetic field and the voltage that we read on the NM-26T's meter. We use a number of factors thus:

$$E_n = MR + AF - EH + CL \quad \text{dB} > \mu\text{V/m} , \quad (\text{A-10})$$

where:

MR = NM-26T meter reading in dB \geq 1 μ V (including the effect of the internal attenuators)

AF = antenna coupler insertion loss in dB

EH = antenna effective height factor in dB/m

CL = cable insertion loss in dB.

As mentioned above, at 3 MHz, AF = 16.3 dB for the 9-ft rod antenna we used. At 3 MHz, the loss (CL) in our 30-ft RG58 feedline is about 0.2 dB. The effective height factor for the 9-ft rod is approximately EH = 2.8 dB above 1 m; this is the theoretical figure (based on half the physical height) for a short vertical monopole above an infinite, perfectly conducting ground plane. On the basis of measurements by Hagn²⁴ and by Lauber²⁷ this is a reasonable EH to use when the antenna is placed atop an automobile, as it was in almost all our tests. Therefore we evaluate Eq. (A-10) as

$$E_n = MR + 13.7 \quad \text{dB}\mu\text{V/m} \quad (\text{A-11})$$

Then we can combine Eqs. (A-7), (A-9), and (A-11) to obtain

$$F_a = MR + 73.2 - 20 \log f_{\text{MHz}} \quad \text{dBkT}_o \quad (\text{A-12})$$

We made our measurements at 3.0 MHz, so for our uncalibrated NM-26T measurements

$$F_a = MR + 63.7 \quad \text{dBkT}_o \quad (\text{A-13})$$

Appendix B

COMPUTER PROGRAM LISTINGS FOR SRI NOISE MEASURING SYSTEM

PRECEDING PAGE BLANK-NOT FILMED

CDC 6700 FTN V3.C-355C OPT=1 75/04/04, 09.08.13.

CDC 6700 FTN V3.C-355C OPT=1 75/04/04, 09.08.13.

117

PRECEDING PAGE BLANK-NOT FILMED

BEST AVAILABLE COPY

```

C
COMMON /RECORD/ INFO(4), INFO(R,R), ISAVST, LREAL(2048),
1 LRFC, NDATA
A 88
A 90
C ..... A 91
C ..... A 92
C ..... A 93
C ..... A 94
C ..... A 95
C ..... A 96
C ..... A 97
C ..... A 98
C ..... A 99
C ..... A 100
C ..... A 101
C ..... A 102
C ..... A 103
C ..... A 104
C ..... A 105
C ..... A 106
C ..... A 107
C ..... A 108
C ..... A 109
C ..... A 110
C ..... A 111
C ..... A 112
C ..... A 113
C ..... A 114
C ..... A 115
C ..... A 116
C ..... A 117
C ..... A 118
C ..... A 119
C ..... A 120
C ..... A 121
C ..... A 122
C ..... A 123
C ..... A 124
C ..... A 125
C ..... A 126
C ..... A 127
C ..... A 128
C ..... A 129
C ..... A 130
C ..... A 131
C ..... A 132
C ..... A 133
C ..... A 134
C ..... A 135
C ..... A 136
C ..... A 137
C ..... A 138
C ..... A 139
C ..... A 140
C ..... A 141
C ..... A 142
C ..... A 143
C ..... A 144
C ..... A 145
C ..... A 146
C ..... A 147
C ..... A 148
C ..... A 149
C ..... A 150
C ..... A 151
C ..... A 152
C ..... A 153
C ..... A 154
C ..... A 155
C ..... A 156
C ..... A 157
C ..... A 158
C ..... A 159
C ..... A 160
C ..... A 161
C ..... A 162
C ..... A 163
C ..... A 164
C ..... A 165
C ..... A 166
C ..... A 167
C ..... A 168
C ..... A 169
C ..... A 170
C ..... A 171
C ..... A 172
C ..... A 173

```

BEST AVAILABLE COPY

```

180 WRITE (A, 50)
      FORMAT (9H TAPE EOF)
      ICHG = 1
      ICFE = 1
      IF (ISCODE .GT. 1PRCS) GO TO 120
      GO TO 20
190 IF (LREF .LT. 415) GO TO 150
      ISCODE = INFO(1)
      IF (NCALL .GT. 1 .AND. INIL .NE. ISCODE) ICHG = 1
      IF (ICMG .EQ. 1) WRITE (A, 50) NCALL
      IF (ICMG .EQ. 0) GO TO 80
      IF (INIL .GT. 1PRCS) GO TO 120
      IF (INIL .EQ. 1) GO TO 110
      IF (INIL .EQ. 0) GO TO 100
      GO TO 90
195 80 IF (ISCODE .GT. 1PRCS) GO TO 120
      IF (ISCODE .EQ. 10) GO TO 110
      IF (ISCODE .EQ. 0) GO TO 100
      IF (ICALH2 .EQ. 0) GO TO 140
      IF (ICALH2 .EQ. 1) CALL CALH2 (ICMG)
      IF (ICALH2 .EQ. 2) CALL CALH3 (ICMG)
      GO TO 140
200 100 IF (INITS .EQ. 0) GO TO 140
      CALL PNOISE (ICMG)
      GO TO 120
      IF (ICALH1 .EQ. 0) GO TO 140
      CALL CALH1 (ICMG)
      GO TO 140
205 120 CALL DATPRC (ICMG, INIL)
      IF (NCALL .LT. NSETS) GO TO 130
      IF (ICMG .EQ. 1) GO TO 24
      ICHG = 1
      IF (ISCODE .EQ. 0) GO TO 100
      GO TO 120
210 130 IF (LREF .EQ. 1) GO TO 20
      GO TO 140
      IF (ICMG .EQ. 0) GO TO 100
      ICHG = 0
      GO TO 80
215 140 IF (NCALL .LT. NSETS) GO TO 170
      ICHG = 1
      IF (ISCODE .GT. 1PRCS) GO TO 120
      GO TO 20
      INIL = ISCODE
220 170 ICHG = 0
      GO TO 20
      STOP
      END

```

```

A 174
A 175
A 176
A 177
A 178
A 179
A 180
A 181
A 182
A 183
A 184
A 185
A 186
A 187
A 188
A 189
A 190
A 191
A 192
A 193
A 194
A 195
A 196
A 197
A 198
A 199
A 200
A 201
A 202
A 203
A 204
A 205
A 206
A 207
A 208
A 209
A 210
A 211
A 212
A 213
A 214
A 215
A 216
A 217
A 218
A 219
A 220
A 221-

```

```

SUBROUTINE RYTMK
C .....
C RYTMK REVISED 05/07/74 KSH
C THIS SUBROUTINE UNPACKS BYTES IN THE BUFFER, INUF, STORING
C THE RESULT IN ARRAY IN.
C .....
C RYTMK VARIABLES
C INTR = MASKED CONTENTS OF INUF
C NMOV = NUMBER OF BITS TO SHIFT INTR
C NM = NUMBER OF BYTE BEING UNPACKED
C .....
C COMMON / BYTES / IR, LOC, LAST, MASK, IN(15), MR(15), INUF(512)
C .....
C BYTES COMMON VARIABLES
C IR = INDEX OF PACKED WORD IN BUFFER
C INUF = ARRAY INTO WHICH DATA IS BUFFERED
C IN = ARRAY OF UNPACKED BYTES
C LAST = NUMBER OF BYTES TO BE UNPACKED
C LOC = LOCATION OF FIRST BYTE TO BE UNPACKED
C MASK = 1777
C MR = ARRAY CONTAINING APPROPRIATE MASK FOR EACH OF THE 15
C FOUR-BIT BYTES IN A WORD
C .....

```

```

H 1
H 2
H 3
H 4
H 5
H 6
H 7
H 8
H 9
H 10
H 11
H 12
H 13
H 14
H 15
H 16
H 17
H 18
H 19
H 20
H 21
H 22
H 23
H 24
H 25
H 26
H 27
H 28
H 29
H 30
H 31
H 32
H 33
H 34
H 35
H 36
H 37
H 38
H 39

```

```

40      DO 20 NM = 1, LAST
        MOVE = (LOC - 15) * 4
        INTR = TRUE (IR) .AND. MR(LOC)
        INTRM = MAX(1, INTR, MOVE)
        IF (LOC.EQ. 15) GO 20
45      10 LOC = 0
        IR = IR + 1
        20 LOC = LOC + 1
        RETURN
        END
        SUBROUTINE CALIRI (ICMG)
C .....
C CALIRI      REVISED 05/07/74 KSM
C THIS PROGRAM COMPUTES CONSTANTS FOR EACH FREQUENCY TO
C ACCOUNT FOR DECIMALS (DB) ABOVE THE REFERENCE NOISE POWER (KTOW).
C .....
10      DIMENSION SUMDB(8), AVMSOL(8)
C .....
15      CALIRI VARIABLES
C AVMSOL = CALIBRATION OF PREVIOUS RECEIVER
C DB = DB INPUT TO SYSTEM FOR CALIBRATION
C EP = .001
C ICMG = SITE CHANGE FLAG (0 = SAME SITE, 1 = CHANGE IN SITE)
C IENTRY = NUMBER OF RECORDS PROCESSED
C LDCVRS = NUMBER OF RECEIVERS BEING SAMPLED
C SNCRAL = NUMBER OF POINTS PER RECEIVER IN EACH RECORD
25      C SUMDB = SUM OF SQUARES OF AMPLITUDE FOR ONE RECEIVER
C SUMDB = SUM OF SQUARES OF AMPLITUDE FOR ALL RECEIVERS
C .....
30      COMMON / CALIR / AVMSQ(8), FDB(8)
C .....
C CALIR COMMON VARIABLES
35      C AVMSQ = CALIBRATION OF RECEIVER
C FDB = NOISE BAND WIDTH IN HERTZ
C .....
40      COMMON / CONST / P104
C .....
45      CONST COMMON VARIABLES
C P104 = ONE-FOURTH PI
C .....
50      COMMON / CONTRL / IPPIN
C .....
55      CONTRL COMMON VARIABLES
C IPPIN = PRINT FLAG (0 = NO HEADINGS PRINTED, 1 = PRINT HEADINGS)
C .....
60      COMMON / PLOT / NOP, NTL, RECNSE(50, 8)
C .....
65      PLOT COMMON VARIABLES
C NOP = NUMBER OF RING IN SCALE
C NTL = NUMBER OF POINTS PER RECEIVER IN EACH RECORD ON DATA TAPE
C RECNSE = RECEIVER NOISE APP
70      C .....
C .....
75      COMMON / RECORD / INFO(9), IDRC(8,4), ISAVST, LREAL(2048),
        I LREC, NDATA
C .....

```


BEST AVAILABLE COPY

```

C.....
C
C          RECORD COMMON VARIABLES
C
40 C IDRC  = ARRAY CONTAINING PREAMBLE VALUES PERTAINING TO EACH RECEIVER
C INFO  = ARRAY CONTAINING PREAMBLE VALUES PERTAINING TO SITE, EXACT
C       TIME, RATE AND NUMBER OF RECEIVERS
C ITRAVS = SAVED PREVIOUS SITE
C LREAL = UNPACKED REAL DATA
45 C LREC  = LENGTH OF RECORD
C NDATA = NUMBER OF SAMPLES
C.....
C
90 C      COMMON / SAMPLE / ARF(512, R), AMPSQ(512, R), N, NRC, NCALL, MON
C      ITM, IDAY, I HOUR, MINIT, ISEC, RATE, MPTS, ARSQ(512, R)
C.....
C
95 C          SAMPLES COMMON VARIABLES
C
C AMPSQ = SQUARE OF AMPLITUDE
C ARF   = ARRAY CONTAINING REAL DATA VALUES
C ARSQ  = SUM OF SQUARES OF CORRECTED REAL VALUES
100 C IDAY = -1
C I HOUR = -1
C ISEC  = -1
C MINIT = -1
C MONTH = -1
105 C MPTS = 12H
C N      = NUMBER OF COMPLEX DATA POINTS DESIRED IN FOURIER PROCESSING
C NCALL  = COUNTER INDICATES NUMBER OF TIMES SUBROUTINE FINDATA HAS
C        BEEN CALLED
C NRC    = RECEIVER NUMBER
110 C RATE = 50
C.....
C
C          DATA ENTRY/0/
C
115 C
C      IF (IENTRY .GT. 0) GO TO 40
C.....
C
120 C READ DECIMAL INPUT TO SYSTEM
C.....
C
125 C READ (5, 10) DB
C      10 FORMAT (PF10.0)
C      WRITE (6, 20) DB
C      20 FORMAT (35H DB INPUT TO SYSTEM, FOR CALIBRATION, E10.3)
C      EP = 1.0E - 3
C      DO 30 J = 1, R
C      30 SUMDH(J) = 0.0
C      SMCAL = 0.0
130 C
C      40 CONTINUE
C      IENTRY = IENTRY + 1
C      IF (ICRG .EQ. 1) GO TO 70
C      LRCVRS = INFO(R)
C      DO 60 J = 1, LRCVRS
C      60 IF (IENTRY .GT. 1 .AND. ABS(AVRMSQ(J) - AVMSQ(J)) .LT. EP) GO
C      TO 60
C      SUMDH = 0.0
C      DO 50 I = 1, NTL
C      50 IF (J .EQ. 1) SMCAL = SMCAL + 1.
C      SUMDH = SUMDH + AMPSQ(I, J)
140 C
C      60 CONTINUE
C      SUMDH(J) = SUMDH(J) / SMCAL
C      AVMSQ(J) = AVMSQ(J)
C      AVRMSQ(J) = SUMDH(J) / SMCAL
145 C
C      70 CONTINUE
C      RETURN
C      DO 80 J = 1, LRCVRS
C      80 AVRMSQ(J) = 10. * ALOG10(AVRMSQ(J)) - DB
150 C
C      90 CONTINUE
C      WRITE (6, 90) (AVRMSQ(J), J = 1, LRCVRS)
C      90 FORMAT (5H KTOR, RE10.3)
C      IENTRY = 0
C      RETURN
155 C
C      END
C      SUBROUTINE CALIP2 (ICRG)
C.....
C
5 C      CALIP2      REVISED 05/07/74 KSH
C.....
C      THIS SUBROUTINE COMPUTES THE CALIBRATION OF THE RECEIVER.
C.....
C.....

```

```

10      C      DIMENSION CWER(1), SUMDR(16)
      C      .....
      C      CALIBR VARIABLES
15      C      .....
      C      COMMON / CALIB / AVERMSQ(8), BDN(16)
      C      .....
      C      CALIB COMMON VARIABLES
      C      AVERMSQ = CALIBRATION OF RECEIVER
      C      BDN = NOISE BAND WIDTH IN HERTZ
20      C      .....
      C      COMMON / CONST / PI04
      C      .....
      C      CONST COMMON VARIABLES
      C      PI04 = ONE-FOURTH PI
      C      .....
50      C      COMMON / CONTRL / IPRIN
      C      .....
      C      CONTRL COMMON VARIABLES
      C      IPRIN = PRINT FLAG (0 = NO HEADINGS PRINTED, 1 = PRINT HEADINGS)
      C      .....
60      C      COMMON / PLOT / NOP, NTL, RECNSE(50, 8)
      C      .....
      C      PLOT COMMON VARIABLES
      C      NOP = NUMBER OF PINS IN SCALE
      C      NTL = NUMBER OF POINTS PER RECEIVER IN EACH RECORD ON DATA TAKE
      C      RECNSE = RECEIVER NOISE AREA
70      C      .....
      C      COMMON / RECORD / INFO(9), TORC(8,8), ISAVST, LREAL(2048),
      C      1 LREFC, NDATA
      C      .....
75      C      RECORD COMMON VARIABLES
      C      .....
      C      INFO = ARRAY CONTAINING PREAMBLE VALUES PERTAINING TO EACH RECEIVER
      C      IMAG = UNPACKED IMAGINARY DATA
      C      INFO = ARRAY CONTAINING PREAMBLE VALUES PERTAINING TO SITE, EXACT
      C      TIME, RATE AND NUMBER OF RECEIVERS
      C      ISAVST = SAVED PREVIOUS SITE
      C      LREAL = UNPACKED REAL DATA
45      C      LREFC = LENGTH OF RECORD
      C      NDATA = NUMBER OF SAMPLES
      C      .....
90      C      COMMON / SAMPLE / ARF(512, 8), AMPSD(512, 8), N, NRC, NCALL, MON
      C      1TH, IDAY, ITHUR, IINIT, ISEC, RATE, MPTS, ARSQ(512, 8)
      C      .....
95      C      SAMPLE COMMON VARIABLES
      C      .....
      C      AMPSD = SQUARE OF AMPLITUDE
      C      ARF = ARRAY CONTAINING REAL DATA VALUES
      C      ARSQ = SUM OF SQUARES OF CORRECTED REAL VALUES

```

BEST AVAILABLE COPY

```

100 C IDAY = -1
C ITHOUR = -1
C ISEC = -1
C MINIT = -1
C MONTH = -1
105 C NPTS = 12H
C N = NUMBER OF COMPLEX DATA POINTS DESIRED IN FOURIER PROCESSING
C NCALL = COUNTER INDICATES NUMBER OF TIMES SUBROUTINE FINDATA HAS
C BEEN CALLED
C NRC = RECEIVER NUMBER
110 C RATE = 50

C .....
C .....
C DATA ENTRY/0/
115 C .....
C .....
C IF (IENTRY .GT. 0) GO TO 30
C READ (5, 10) INSITE, INDIN, CW(INDIN), ROW(INDIN)
120 C FORMAT (2110,2F10.0)
C SUMDL(INDIN) = 0.0
C SNCL = 0.0
C CON = CW(INDIN) * 10. * ALOG10(ROW(INDIN)) * 174.
C WRITE (6, 20) INSITE, INDIN, CW(INDIN), ROW(INDIN), CON
125 C FORMAT (5H 10.15,4H RECV#,15.3H C#,F10.3,2H R#,F10.3,4H CON#,F10.3
C 1)
C 70 CONTINUE
C IENTRY = IENTRY + 1
C IF (ICMG .EQ. 1) GO TO 70
C IF (INFO(1) .EQ. INSITE) GO TO 50
130 C WRITE (6, 40) INFO(1), INSITE
C 40 FORMAT (20H RECVR NUMBERS ARE INCORRECT,215)
C NCALL = 100000
C RETURN
C 50 CONTINUE
C SNCL = SNCL + 256.
135 C SUMDL = 0.0
C DO 60 I = 1, NTL
C SUMDL = SUMDL + AMPSQ(I, INDIN)
C 60 CONTINUE
C SUMDL(INDIN) = SUMDL(INDIN) + SUMDL
140 C RETURN
C 70 CONTINUE
C IF (SNCL .EQ. 0) GO TO 80
C AVMSQ(INDIN) = 10. * ALOG10(SUMDL(INDIN) / SNCL) - CON
145 C WRITE (6, 90) INDIN, AVMSQ(INDIN), IENTRY
C 90 FORMAT (4H RECV#,15.12H CALIBRATION#,F10.3,20H NUMBER OF RECORDS PR
C 1)
C IENTRY = 0
C RETURN
150 C END

C .....
C .....
C SUBROUTINE CALIB3 (ICMG)
C .....
C .....
C CALIB3 REVISED 05/07/74 KSH
C .....
C THIS SUBROUTINE COMPUTES THE CALIBRATION OF THE RECEIVER.
C .....
10 C .....
C .....
C DIMENSION CW(8), SUMDL(8)
C .....
C .....
15 C .....
C .....
C CALIB3 VARIABLES
C CON = CW SIGNAL
C CW = CW SIGNAL IN DECIBELS
C ICMG = SITE CHANGE FLAG (0 = SAME SITE, 1 = CHANGE IN SITE)
20 C IENTRY = NUMBER OF RECORDS PROCESSED
C INDIN = RECEIVER NUMBER
C INSITE = SITE IDENTIFICATION
C SNCL = NUMBER OF POINTS PER RECEIVER IN EACH RECORD
C SUMDL = SUM OF SQUARES OF AMPLITUDE FOR ONE RECEIVER
25 C SUMDL = SUM OF SQUARES OF AMPLITUDE FOR ALL RECEIVERS
C .....
C .....
C COMMON / CALIB / AVMSQ(8), ROW(8)
30 C .....
C .....
C CALIB COMMON VARIABLES
C .....
35 C AVMSQ = CALIBRATION OF RECEIVER
C ROW = NOISE BAND WIDTH IN HERTZ
C .....
C .....

```

BEST AVAILABLE COPY

```

40      COMMON / CONST / PI04
      .....
45      CONST COMMON VARIABLES
      PI04 = ONE-FOURTH PI
      .....
50      COMMON / CONTRL / IPRIN
      .....
55      CONTRL COMMON VARIABLES
      IPRIN = PRINT FLAG (0 = NO HEADINGS PRINTED, 1 = PRINT HEADINGS)
      .....
60      COMMON / PLOT / NOP, NTL, RECNSF(50, R)
      .....
65      PLOT COMMON VARIABLES
      NOP = NUMBER OF HINS IN SCALE
      NTL = NUMBER OF POINTS PER RECEIVER IN EACH RECORD ON DATA TAPE
      RECNSF = RECEIVER NOISE APO
      .....
70      COMMON / RECORD / INFO(9), INRC(R,R), ISAVST, LREAL(204R),
      1 LREC, NDATA
      .....
75      RECORD COMMON VARIABLES
      INRC = ARRAY CONTAINING PREAMBLE VALUES PERTAINING TO EACH RECEIVER
      IMAG = UNPACKED IMAGINARY DATA
      INFO = ARRAY CONTAINING PREAMBLE VALUES PERTAINING TO SITE, EXACT
      TIME, DATE AND NUMBER OF RECEIVERS
      ISAVST = SAVED PREVIOUS SITE
      LREAL = UNPACKED REAL DATA
      LREC = LENGTH OF RECORD
      NDATA = NUMBER OF SAMPLES
      .....
90      COMMON / SAMPLE / ARF(512, R), AMPSQ(512, R), N, NRC, NCALL, MON
      1 TH, IDAY, THOUR, MINIT, ISEC, RATE, MPTS, ARSQ(512, R)
      .....
95      SAMPLE COMMON VARIABLES
      AMPSQ = SQUARE OF AMPLITUDE
      ARF = ARRAY CONTAINING REAL DATA VALUES
      ARSQ = SUM OF SQUARES OF CORRECTED REAL VALUES
      INAY = -1
      INOUR = -1
      ISEC = -1
      MINIT = -1
      MONTH = -1
      MPTS = 12H
      N = NUMBER OF COMPLEX DATA POINTS DESIRED IN FOURIER PROCESSING
      NCALL = COUNTER INDICATES NUMBER OF TIMES SUBROUTINE FINDATA HAS
      BEEN CALLED
      NRC = RECEIVER NUMBER
      RATE = 50
      .....
110     DATA ENTRY/0/
      .....
115     IF (IENTRY .GT. 0) GO TO 30
      READ (5, 10) INSITE, INDIN, CW(INDIN), ROW(INDIN)
      10 FORMAT (2I10,2F10.0)
      SUMRCL(INDIN) = 0.0
      SNCF = 0.0
      CCON = CW(INDIN)
      WRITE (6, 20) INSITE, INDIN, CW(INDIN), ROW(INDIN)
      20 FORMAT (5H ID,15.6H RECVR,15.3H DR,E10.3,5H RCNRD15,E10.3)
      30 CONTINUE
      IENTRY = IENTRY + 1
      IF (ICNG .EQ. 1) GO TO 70
      IF (INFO(1) .EQ. INSITE) GO TO 40
      WRITE (6, 40) INFO(1), INSITE

```


BEST AVAILABLE COPY

```

130      40 FORMAT (2RH RECVR NUMBERS ARE INCORRECT,215)          F 128
      NCAL = 100000                                              F 129
      RETURN                                                    F 130
135      50 CONTINUE                                              F 131
      SNCAI = SNCAI * 25A,                                       F 132
      SUMH = 0.0                                                 F 133
      DO 40 I = 1, NTL                                           F 134
      SUMH = SUMH + AMPSQ(I, INFIN)                               F 135
      40 CONTINUE                                              F 136
      SUMHL(INFIN) = SUMHRL(INFIN) + SUMH                       F 137
      RETURN                                                    F 138
140      70 CONTINUE                                              F 139
      IF (SNCAI .EQ. 0.) GO TO 40                                F 140
      AVHMSQ(INFIN) = 10. * ALOG10(SUMHRL(INFIN) / SNCAI) = CCON F 141
      80 WRITE (6, 90) INFIN, AVHMSQ(INFIN), IENTHY             F 142
145      90 FORMAT (6H RECVR,15,12H CALTRATION,F10.3,2RH NUMBER OF RECORDS PW F 143
      LOCESSED,110)                                             F 144
      IENTHY = 0                                                 F 145
      RETURN                                                    F 146
      END                                                        F 147-

      SUBROUTINE COMPRS (X, NOLD, NNEW, XOLD, XNEW)              F 1
C .....                                                    F 2
C .....                                                    F 3
C .....                                                    F 4
5      C COMPRS          REVISED 05/07/74 KSH                  F 5
C .....                                                    F 6
C      THIS SUBROUTINE COMPRESSES THE GRAPH BY REMOVING EMPTY BINS F 7
C      AT THE BOTTOM AND TOP OF SCALE.                          F 8
C .....                                                    F 9
10     C .....                                                    F 10
C      DIMENSION X(1), XOLD(1), XNEW(1)                        F 11
C .....                                                    F 12
C .....                                                    F 13
15     C .....                                                    F 14
C .....                                                    F 15
C      COMPRS VARIABLES                                         F 16
C .....                                                    F 17
C      IROT = NEW BOTTOM BIN                                     F 18
C      IROT = ONE BIN BELOW BOTTOM                               F 19
C      ITOP = NEW TOP BIN                                       F 20
C      NNEW = NEW NUMBER OF BINS                                 F 21
C      NOLD = PREVIOUS NUMBER OF BINS                           F 22
C      NPOLD = PREVIOUS NUMBER OF BINS PLUS ONE                 F 23
C      X = NUMBER OF POINTS IN EACH BIN                         F 24
25     C XNEW = NEW SCALE                                         F 25
C      XOLD = OLD SCALE                                         F 26
C .....                                                    F 27
C .....                                                    F 28
30     C .....                                                    F 29
C .....                                                    F 30
      DO 10 I = 1, NOLD                                           F 31
      IF (X(I) .EQ. 0.0) GO TO 10                                F 32
      IROT = I                                                    F 33
      GO TO 20                                                    F 34
35     10 CONTINUE                                              F 35
      20 CONTINUE                                              F 36
      NPOLD = NOLD + 1                                           F 37
      DO 30 I = 1, NOLD                                           F 38
      K = NPOLD - I                                               F 39
40     IF (X(K) .EQ. 0.0) GO TO 30                               F 40
      ITOP = K                                                    F 41
      GO TO 40                                                    F 42
      30 CONTINUE                                              F 43
      40 CONTINUE                                              F 44
      NNEW = ITOP - IROT + 1                                       F 45
      IROT = IROT - 1                                             F 46
      DO 50 I = 1, NNEW                                           F 47
      II = I + IROT                                              F 48
      X(I) = X(II)                                                F 49
50     XNEW(I) = XOLD(II)                                         F 50
      50 CONTINUE                                              F 51
      RETURN                                                    F 52
      END                                                        F 53-

      SUBROUTINE RAYLEE (DUM1, DUM2, DUM3, KA, OFFX, OFFY, SC1, SC2, SIZ I 1
      IF, DUM4, IO, IH, SC, IO, DUM5)                           I 2
C .....                                                    I 3
C .....                                                    I 4
5      C .....                                                    I 5
C      RAYLEE          REVISED 05/07/74 KSH                  I 6
C .....                                                    I 7
C      THIS SUBROUTINE IS CALLED BY THE LIBRARY ROUTINE GRAPH4 TO MAKE A
C      RAYLEIGH SCALE ON THE X-AXIS OF THE GRAPH PRODUCED.
10     C .....                                                    I 8
C .....                                                    I 9
      DIMENSION ST(13), SL(13)                                   I 10
      DIMENSION R(2), R2(2, 2), XR(2), YR(2)                   I 11
C .....                                                    I 12

```

BEST AVAILABLE COPY

```

15 C ..... I 13
C ..... I 14
C ..... I 15
C ..... I 16
C ..... I 17
20 C ..... I 18
C ..... I 19
C IR = LABEL INDICATOR (0 = NO SCALE LABELS, 1 = LABEL SCALE) I 20
C IC = FLAG X OR Y VALUES (1 = X, 2 = Y) I 21
C ID = INDICATOR FOR X OR Y SCALE (0 = X AXIS, 1 = Y AXIS) I 22
25 C ID = INDICATOR FOR RIGHT OR SIDE READING PLOT (0 = SIDE READING, I 23
C ..... I 24
C NENTRY = SUBROUTINE ENTRY COUNTER I 25
C NA = NUMBER OF CHARACTERS IN LABEL I 26
C OFFX = X-DISTANCE TO ORIGIN I 27
30 C OFFY = Y-DISTANCE TO ORIGIN I 28
C Q = GRID SIZE I 29
C RA = LENGTH OF PLOT IN LINEAR UNITS I 30
C RASAV = I 31
C SAV = I 32
35 C SC = HEIGHT OF CHARACTER INPUT I 33
C SC1 = SIZE OF LARGE TIC MARK I 34
C SC2 = SIZE OF SMALL TIC MARK I 35
C SIZE = LENGTH OF AXIS I 36
C SI = PERCENT SCALE I 37
40 C ST = I 38
C X = X-COORDINATE OF STARTING POSITION OF LABEL I 39
C XR = I 40
C Y = Y-COORDINATE OF STARTING POSITION OF LABEL I 41
C YR = I 42
45 C ..... I 43
C ..... I 44
C ..... I 45
C ..... I 46
C ..... I 47
50 DATA (SL(I), I=1, 13)/0.001, 0.1, 1, 5, 10, 20, 50, 70, 80, 90, 95, 98 I 48
1., 99, / I 49
DATA NENTRY/0/ I 50
C ..... I 51
C ..... I 52
85 C ..... I 53
C ..... I 54
C IF (NENTRY .GT. 0) GO TO 20 I 55
DO 10 I = 1, 13 I 56
ST(I) = ALOG(ALOG(100. / SL(I))) I 57
IF (I .EQ. 1) SAV = ST(I) I 58
ST(I) = ST(I) - SAV I 59
10 CONTINUE I 60
RASAV = ST(13) I 61
NENTRY = 1 I 62
65 20 CONTINUE I 63
X = OFFX I 64
Y = OFFY I 65
NA = 0 I 66
RA = RASAV I 67
Q = SIZE / RA I 68
70 IF (ID) 30, 30, 60 I 69
30 IF (ID) 40, 40, 50 I 70
40 XR(1) = X I 71
XR(2) = X I 72
75 YR(1) = Y + SC1 I 73
YR(2) = Y + SC2 I 74
IC = 1 I 75
AA = X I 76
GO TO 90 I 77
80 XR(1) = Y - SC1 I 78
XR(2) = X - SC2 I 79
YR(1) = Y I 80
YR(2) = Y I 81
IC = 2 I 82
85 AA = Y I 83
GO TO 90 I 84
90 IF (ID) 70, 70, 80 I 85
70 XR(1) = X + SC1 I 86
XR(2) = X + SC2 I 87
90 YR(1) = Y I 88
YR(2) = Y I 89
IC = 2 I 90
AA = Y I 91
GO TO 90 I 92
95 30 XR(1) = X I 93
XR(2) = X I 94
YR(1) = Y + SC1 I 95
YR(2) = Y + SC2 I 96
IC = 1 I 97
100 AA = X I 98
Q = - Q I 99
90 CONTINUE I 100
K = 1 I 101
DO 120 I = 1, 13 I 102
105 R(IC) = AA + ST(I) * Q I 103
R2(1, IC) = R(IC) I 104
R2(2, IC) = R(IC) I 105
IF (IR) 110, 110, 100 I 106
110 CALL PENS (I) I 107
CALL LRLAADD (X, Y, SL(I), SC, ID, IO, NN) I 108

```

BEST AVAILABLE COPY

```

110 CALL PENS (0)
      CALL PLOT (X, Y, 3)
      CALL PLOT (XMIN, YMIN, 2)
120 CONTINUE
      RETURN
      END
115
      SUBROUTINE HAYLF2 (AMAS, XMS, AX, BX, CX, DX, EX)
      .....
      HAYLF2      REVISED 05/07/74 KSH
      .....
      THIS SUBROUTINE IS CALLED BY THE LIBRARY ROUTINE GRAPH4 TO MAKE A
      HAYFLEIGH SCALE ON THE X-AXIS OF THE GRAPH PRODUCED.
      .....
      HAYLF2 VARIABLES
      .....
      AX = MINIMUM X VALUE
      BX = 0.0
      CX = MAXIMUM X VALUE
      DX = 0.0
      EX = EXPONENT FOR AXIS SCALING (0.0)
      XMAX =
      XMIN =
      .....
      ENTRY SLOGAND
      .....
      BY = 0.0
      DX = 0.0
      EX = 0.0
      XMAX = 1. / ALOG(1. / .99)
      XMIN = -1. / ALOG(100. / .01)
      WRITE (6, 10) XMIN, XMAX
10 FORMAT (2F20.13)
      AX = XMIN
      CX = XMAX
      RETURN
      END
      SUBROUTINE DATPRC (ICMG, INIL)
      .....
      DATPRC      REVISED FEB. 1975 JRW
      .....
      THIS SUBROUTINE PRODUCES THE FOLLOWING PLOTS
      1. AMPLITUDE PROBABILITY DISTRIBUTION OF AUTOMOBILE
      IGNITION NOISE
      .....
      THIS SUBROUTINE IS ENTERED FOR SITE 0 AND
      SITES ABOVE 10 (ALL WITH TEST DATA).
      IT IS NOT ENTERED FOR SITE 10 WHICH IS A
      FIXED GAUSSIAN NOISE.
      .....
      DIMENSION IPLOT(7), LABEL1(24), LABEL2(24), LABEL3(24), SCAPD(50),
      1 PRCAPD(50, 8), LABEL4(24), HSCAPD(50), D
      2PLOT(57), SAVAL(50), SCAPL(50), XPDHMS(8), APDRMS(8), ABSXPD(8),
      3JLRI(20), RECVRY(50, 8), RECVY(50)
      .....
      DATPRC VARIABLES
      .....
      ABSXPD = SUM OF REAL VALUES FOR EACH RECEIVER
      AMPTRM = AMPLITUDE SQUARED
      APRHMS = SUM OF SQUARES OF AMPLITUDE FOR RECEIVER
      ARTEMP = REAL DATA VALUES
      DIF1 = DIFFERENCE BETWEEN CURRENT HOUR AND PREVIOUS HOUR
      DIF2 = DIFFERENCE BETWEEN CURRENT MINUTE AND PREVIOUS MINUTE
      DIF3 = DIFFERENCE BETWEEN CURRENT SECOND AND PREVIOUS SECOND
      DPLOT = NEW PLOT SCALE
      FA = AVERAGE POWER
      FR = FREQUENCY TO WHICH RECEIVER IS TUNED
      ICMG = SITE CHANGE FLAG (0 = SAME SITE, 1 = CHANGE IN SITE)
      IN = SITE IDENTIFICATION CODE
      JENTRY = NUMBER OF RECORDS PROCESSED
      JLRI = TEN BLANK CHARACTERS
      JMIN = NEGATIVE CALIBRATION OF RECEIVER
      JNWHR = HOUR OF CURRENT RECORD
      JNMIN = MINUTE OF CURRENT RECORD
      JNSEC = SECOND OF CURRENT RECORD

```

```

45 C IPLOT = ARRAY CONTAINING PLOTTING OPTIONS * G 45
C ICAVME = HOUR OF PREVIOUS SITE * G 46
C ICAVME = MINUTE OF PREVIOUS SITE * G 47
C ICAVSE = SECOND OF PREVIOUS SITE * G 48
C JRL = GATE LABEL ARRAY * G 49
50 C JRI = INCREMENT FROM WHICH DATA POINTS WILL BE TAKEN FROM INPUT * G 50
C JRI = ARRAYS FOR PLOTTING * G 51
C LABEL1 = LABEL FOR PLOT 1 (AMPLITUDE PROBABILITY DISTRIBUTION OF * G 52
AUTOMOBILE IGNITION NOISE) * G 53
C LABEL2 = LABEL FOR PLOT 2 (XPD DISTRIBUTION OF THE REAL PART OF * G 54
AUTOMOBILE IGNITION NOISE) * G 55
65 C LABEL3 = LABEL FOR PLOT 3 (XPD DISTRIBUTION OF THE IMAGINARY PART OF * G 56
AUTOMOBILE IGNITION NOISE) * G 57
C LABEL4 = LABEL FOR PLOT 4 (JOINT DISTRIBUTION OF AMPLITUDE AND PHASE * G 58
FOR IGNITION NOISE) * G 59
C LOT = NUMBER OF NON-EMPTY BINS IN PLOT 4 * G 60
C LDCVME = NUMBER OF RECEIVERS * G 61
C LDCVME = NUMBER OF BINS * G 62
C LDCVME = INDEX OF FIRST AMPLITUDE OF AMPTEMP * G 63
C LDCVME = INDEX OF FIRST POINT OF AMPTEMP * G 64
65 C PTSARD = ARRAY INDICATING AMPLITUDE PROBABILITY DISTRIBUTION OF * G 65
AUTOMOBILE IGNITION NOISE * G 66
C RECVRY = RECEIVER NOISE FOR Y AXIS * G 67
C RECVY = Y AXIS FOR RECEIVER NOISE WITH CALIBRATION ADJUSTMENT, * G 68
RECVRY = SCALE VALUES * G 69
70 C SAVG = ARRAY OF PERCENTAGE VALUES FOR TABLE PRINTOUT * G 70
C SAVG = AMPLITUDE PROBABILITY DISTRIBUTION (APD) * G 71
C SAVG = ADDRESS OF FIRST Y COORDINATE OF DATA TO BE PLOTTED * G 72
C SECS = SECONDS BETWEEN PREVIOUS TIME AND PRESENT TIME * G 73
C SPS = NUMBER OF POINTS PER FREQUENCY * G 74
75 C SPS1 = ONE LESS THAN NUMBER OF POINTS PER FREQUENCY * G 75
C SUM = TOTAL NUMBER OF POINTS IN PLOT * G 76
C TBASE = PHASE * G 77
C VAL = RATIO OF ACCUMULATED NUMBER OF POINTS TO TOTAL NUMBER OF * G 78
POINTS * G 79
80 C VAVG = AVERAGE VALUE OF ENVELOPE * G 80
C VD = IMPULSIVENESS MEASURE OF NOISE ENVELOPE * G 81
C VMS = VMS VALUE OF NOISE ENVELOPE OVER PERIOD DURING WHICH DATA * G 82
IS COLLECTED * G 83
C VMSD = VMS VALUE SQUARED * G 84
85 C XMAX = MAXIMUM VALUE OF X AXIS * G 85
C XMIN = MINIMUM VALUE OF X AXIS * G 86
C XDRMS = SUM OF SQUARES OF REAL VALUES FOR RECEIVER * G 87
C YMAX = MAXIMUM VALUE OF Y AXIS * G 88
90 C YMIN = MINIMUM VALUE OF Y AXIS * G 89
C * G 90
C * G 91
C * G 92
C * G 93
C * G 94
95 C * G 95
C * G 96
C * G 97
C * G 98
C * G 99
C * G 100
C * G 101
C * G 102
C * G 103
C * G 104
105 C * G 105
C * G 106
C * G 107
C * G 108
C * G 109
C * G 110
C * G 111
C * G 112
C * G 113
C * G 114
115 C * G 115
C * G 116
C * G 117
C * G 118
C * G 119
C * G 120
120 C * G 121
C * G 122
C * G 123
C * G 124
C * G 125
C * G 126
C * G 127
C * G 128
C * G 129
130 C * G 130
C * G 131
C * G 132
C * G 133

```



```

135 ..... G 134
C ..... G 135
COMMON /RECORD/ INFO(9), THRC(R,R), ISAVST, LREAL(2048),
1 LREC, NDATA
C ..... G 137
140 ..... G 138
C ..... G 139
C ..... G 140
C ..... G 141
C INFO = ARRAY CONTAINING PREAMBLE VALUES PERTAINING TO EACH RECEIVER G 142
C IMAG = UNPACKED IMAGINARY DATA G 143
145 C INFO = ARRAY CONTAINING PREAMBLE VALUES PERTAINING TO SITE, EXACT G 144
C TIME, RATE AND NUMBER OF RECEIVERS G 145
C ISAVST = SAVED PREVIOUS SITE
C LREAL = UNPACKED REAL DATA G 146
C LREC = LENGTH OF RECORD G 147
150 C NDATA = NUMBER OF SAMPLES G 148
C ..... G 149
C ..... G 150
C ..... G 151
155 COMMON /SAMPLES/ AMP50(512, R), AMP50(512, R), N, NRC, NCALL, MON
1TH, IDAY, THOUR, MINIT, ISEC, RATE, MPTS, ARSQ(512, R)
C ..... G 152
C ..... G 153
C ..... G 154
C ..... G 155
C ..... G 156
160 C ..... G 157
C ..... G 158
C AMP50 = SQUARE OF AMPLITUDE G 159
C ARF = ARRAY CONTAINING REAL DATA VALUES G 160
C ARSQ = SUM OF SQUARES OF CORRECTED REAL VALUES G 161
165 C IDAY = -1 G 162
C THOUR = -1 G 163
C ISEC = -1 G 164
C MINIT = -1 G 165
C MONTH = -1 G 166
C MPTS = 12H G 167
170 C N = NUMBER OF COMPLEX DATA POINTS DESIRED IN FOURIER PROCESSING G 168
C NCALL = COUNTER INDICATES NUMBER OF TIMES SUBROUTINE FINDATA HAS G 169
C BEEN CALLED G 170
C NRC = RECEIVER NUMBER G 171
C RATE = 50 G 172
175 C ..... G 173
C ..... G 174
C ..... G 175
C ..... G 176
C DATA ILHL/1CH / G 177
DATA IENTRY,NGP/0.40/ G 178
180 DATA JLHL(1),JLHL(5),JLHL(6),JLHL(7),JLHL(8),JLHL(12),JLHL(16),JLH
11(17),JLHL(18),JLHL(19),JLHL(20)/40HPERCENT OF TIME ORIGINATE IS EX G 179
2CEDED, 10HMMH ABOVE 1CH RMS, 10HMMH FREQ, 40H COMPONENT G 180
3 RELATIVE TO ITS RMS, 40HPROBABILITY X/XRMS LESS THAN ARE G 181
4CTSSA, 10HXPDP FREQ, 10HY COMPONENT, 10HY Y/YRMS 1, 10HYDP FREQ G 182
185 50HMMH FREQ/ G 183
DATA (RSCAPD(I),I=1,40)/4.,0.,4.,6.,8.,10.,12.,14.,16.,18.,20.,22
1.,24.,26.,28.,30.,32.,34.,36.,38.,40.,42.,44.,46.,48.,50.,52.,54.,
256.,58.,60.,62.,64.,66.,68.,70.,72.,74.,76.,78.,/ G 184
190 ..... G 185
C ..... G 186
C ..... G 187
C ..... G 188
C NOTE ARRAYS ARE OUT OF SYNCH DUE TO REVERSE SUMMING IN CALCULATION G 189
C OF ARF --- SC/PO(I) = 10. * (RSCAPD(I+1)/10.) G 190
C ..... G 191
C ..... G 192
195 DATA (SCAPD(I),I=1,40)/1.0,2.512,3.981,6.310,1.0E+1,1.585E+1,2.512
1E+1,3.981E+1,6.31E+1,1.0E+2,1.585E+2,2.512E+2,3.981E+2,6.31E+2,1.0
2E+3,1.585E+3,2.512E+3,3.981E+3,6.31E+3,1.0E+4,1.585E+4,2.512E+4,3.
3981E+4,6.31E+4,1.0E+5,1.585E+5,2.512E+5,3.981E+5,6.31E+5,1.0E+6,1.
4585E+6,2.512E+6,3.981E+6,6.31E+6,1.0E+7,1.585E+7,2.512E+7,3.981E+7
200 5.6,31E+7,1.0E+8/ G 198
C ..... G 199
C ..... G 200
C IF (IENTRY .GT. 0) GO TO 80 G 201
IENTRY = 1 G 202
205 ..... G 203
C ..... G 204
C ..... G 205
C INITIALIZE DATA ARRAYS FOR PLOTTING G 206
C ..... G 207
C ..... G 208
C ..... G 209
C ..... G 210
210 ..... G 211
DO 10 I = 1, 50 G 212
DO 10 J = 1, R G 213
PTRAPD(I, J) = 0.0 G 214
RECHSF(I, J) = 0.0 G 215
10 CONTINUE G 216
215 DO 20 J = 1, R G 217
XPDHMS(J) = 0.0 G 218
APDHMS(J) = 0.0 G 219
ARXPD(J) = 0.0 G 220
IF (RDP(J) .EQ. 0.0) RDP(J) = 1. G 221
220 20 CONTINUE G 222

```

```

      SAV = 0.0
      WRITE (6, 30) (SCAPD(I), I = 1, NCP)
30  FORMAT (10H AND SCALE,10E10.3)
      DO 40 I = 1, 24
        LABEL1(I) = TMR
        LABEL2(I) = TMR
        LABEL3(I) = TMR
225  40 LABEL4(I) = TMR
        IF = INFO(1)
        LCVRS = INFO(4)
        ENCODE (16, 40, LABEL1(3), INFO(2), INFO(3))
        40  ENCODE (12, 142, 12, 142, 4475 I)
        ENCODE (16, 50, LABEL1(2), INFO(4), INFO(5))
        TCVMRP = INFO(4)
        TCVMIN = INFO(5)
        TCVSEC = INFO(6)
        NTL = (1024, / FLOAT(LCVRS) * 1.0E = 9)
        WRITE (6, 70) NTL
        70  ENCODE (41H NUMBER OF POINTS PER RECEIVER PER RECORD,15)
240  70 CONTINUE
        IF TENTRY = TENTRY + 1
        IF (ICRG .EQ. 1) GO TO 117
C.....
C
245  C STORE DATA FROM RECORD FOR PLOTTING
C.....
        TTSVST .NE. 10) GO TO 84
        TO = INFO(1)
250  TCAVER = INFO(4)
        TCVMIN = INFO(5)
        TCVSEC = INFO(6)
        84  TCAVER = INFO(4)
        TCVMIN = INFO(5)
        TCVSEC = INFO(6)
        DO 100 J = 1, NTL
          IND = 0
          ARTEMP = ARS(I, J)
          AMPRMP = ARSQ(I, J)
          CALL FNDRT (CAMPMP, SCAPD, NPAMP)
          ARPRMS(J) = ARPRMS(J) + AMPRMP
          XPRMS(J) = XPRMS(J) + ARSQ(I, J)
          PISCAPD(NPAMP, J) = PISCAPD(NPAMP, J) + 1.
          IF (ARTEMP .LT. 0.0) ARTEMP = - ARTEMP
          ABSXPD(J) = ABSXPD(J) + ARTEMP
        100 CONTINUE
        100 CONTINUE
        CND = CND + FLOAT(NTL)
        RETURN
270  110 CONTINUE
C.....
C
C PLOT 1
C AMPLITUDE PROBABILITY DISTRIBUTION OF AUTOMOBILE IGNITION NOISE
C.....
        JLI = 1
        TPLT(2) = 0
        TPLT(4) = 1
        TPLT(6) = 1
        TPLT(8) = 0
        TPLT(10) = 0
        TPLT(12) = 0
285  C.....
C
C X-AXIS LABEL
C.....
        LABEL1(9) = JLI(1)
        LABEL1(10) = JLI(2)
        LABEL1(11) = JLI(3)
        LABEL1(12) = JLI(4)
290  C.....
C
C Y-AXIS LABEL
C.....
        LABEL1(17) = JLI(5)
        LABEL1(18) = JLI(6)
300  C.....
C
C GRAPH LABEL
C.....
        WRITE (6, 120) CND
        120  FORMAT (32H NUMBER OF POINTS PER FREQUENCY,10.3)
        DT1 = INFO(4) - JSVVR
        DT2 = INVMIN - JSVVR
        DT3 = INVSEC - JSVSEC
305  G 224
      G 225
      G 226
      G 227
      G 228
      G 229
      G 230
      G 231
      G 232
      G 233
      G 234
      G 235
      G 236
      G 237
      G 238
      G 239
      G 240
      G 241
      G 242
      G 243
      G 244
      G 245
      G 246
      G 247
      G 248
      G 249
      G 250
      G 251
      G 252
      G 253
      G 254
      G 255
      G 256
      G 257
      G 258
      G 259
      G 260
      G 261
      G 262
      G 263
      G 264
      G 265
      G 266
      G 267
      G 268
      G 269
      G 270
      G 271
      G 272
      G 273
      G 274
      G 275
      G 276
      G 277
      G 278
      G 279
      G 280
      G 281
      G 282
      G 283
      G 284
      G 285
      G 286
      G 287
      G 288
      G 289
      G 290
      G 291
      G 292
      G 293
      G 294
      G 295
      G 296
      G 297
      G 298
      G 299
      G 300
      G 301
      G 302
      G 303
      G 304
      G 305
      G 306
      G 307
      G 308
      G 309
      G 310
      G 311

```

```

310      IF (DIF3 .GE. 0.0) GO TO 130
      DIF2 = DIF2 + 60.
      DIF2 = DIF2 - 1.
315      IF (DIF2 .GE. 0.0) GO TO 140
      DIF2 = DIF2 + 60.
      DIF2 = DIF2 - 1.
320      IF (DIF1 .GE. 0.0) GO TO 150
      DIF1 = 24. + DIF1
325      SECS = DIF1 * 360. + DIF2 * 60. + DIF3 * 1.
      THIS IS A MODIFICATION TO ALLOW US TO GET THE DURATION FROM THE
      NUMBER OF POINTS.
      SECS = SNP/200.0
      IF (SECS .GT. 40.) GO TO 170
      ENCODE (10, 140, LABEL1(5)) SECS
330      140 FORMAT (4H SECS=, F4.1)
      GO TO 210
335      170 IF (SECS .GT. 3600.) GO TO 190
      SECS = SECS / 60.
      ENCODE (10, 180, LABEL1(5)) SECS
340      180 FORMAT (4H MIN=, F4.1)
      GO TO 210
345      190 SECS = SECS / 3600.
      ENCODE (10, 200, LABEL1(5)) SECS
350      200 FORMAT (4H HRS=, F4.1)
355      210 CONTINUE
      ENCODE (10, 50, LABEL1(2)) ISAVNR, ISUMIN
      60 FORMAT (5H LMT=, 2I2, 1H )
      ISAVNR = INFO(4)
      ISUMIN = INFO(5)
      ISVSEC = INFO(6)
      TO = INFO(1)
      XMIN = 8.48588043705E - 02
      XMAX = 9.049916247342E + 1
      SNPM1 = SNP - 1.
      DO 220 J = 1, LOCVRB
360      YMIN = - 35.
      YMAX = 35.
      FD = FLOAT(INFCH, J) / 10000.
      ENCODE (10, 220, LABEL1(1)) J, FD
365      220 FORMAT (5H HREQ=, F5.2)
      ENCODE (10, 230, LABEL1(4)) ISAVST, J
370      230 FORMAT (2H0=, I2, 5H WCV=, I1)
      VPRMS(J) = SQRT(XPRMS(J) / SNPM1)
      IF (APRMS(J) .GT. 0.0) GO TO 240
      FA = 0.0
      GO TO 250
375      240 CONTINUE
      VRMSQ = APRMS(J) / SNPM1
      FA = 1. + .4LOG10(VRMSQ) - AVRMSQ(J)
      AHSXP(J) = AHSXP(J) / SNP
      VAVG = AHSXP(J)
380      VRMS = SQRT(VRMSQ)
      VD = 2. + .4LOG10(VRMS / VAVG)
      250 WRITE (6,255) J
      255 FORMAT (// * RECFIVER = I1)
      WRITE (6, 260) XPRMS(J), VRMS, AHSXP(J), VAVG, FA, VD
385      260 FORMAT (1H XPRMS=E10.3, 3H VRMS=E10.3, 3H AHSXP=E10.3, 3H V
      JAVG=E10.3, 4H FA=E10.3, 4H VD=E10.3)
      ENCODE (10, 265, LABEL1(6)) FA
390      265 FORMAT (5H RMS=, F5.2)
      ENCODE (10, 267, LABEL1(7)) VD
      267 FORMAT (4H VD=, F5.2, 1H )
      SUM = 0.0
      DO 270 I = 1, NNP
      SUM = SUM + PTSAPD(I, J)
      IF (SUM / SNP .GE. 0.0) GO TO 280
      PTRAPD(I, J) = 0.0
395      270 CONTINUE
      280 CONTINUE
      CALL COMPRC (PTRAPD(1, J), NNP, NNP, HSCAPD, SCAPL)
      SUM = 0.0
      DO 290 I = 1, NNP
      K = NNP - I + 1
      SUM = SUM + PTSAPD(K, J)
      VAL = SUM / SNP
      IF (VAL .GE. 1.) VAL = .999999
400      290 CONTINUE
      IF (INIL, EQ, 0) GO TO 390
      TPLOT(1) = 1
      TPLOT(3) = 1
      CALL GRAPHX (PTRAPD(1, J), SCAPL, NNP, J1, XMAX, XMIN, YMAX, Y1
405      11H, LABEL1, TPLOT)
      WRITE (6,330)
      330 FORMAT (1H0, 10X, SAWLEVEL (OR ABOVE RMS) PERCENT OF TIME LEVE
      IL IS EXCEEDED)

```

BEST AVAILABLE COPY

```

400      WRITE (A,340)
340  FORMAT (11X,20(1H-), 3X, 33(1H-)/)
      DO 345 I=1,NNP
      SAVAL(I) = SAVAL(I) * 100
      WRITE (A,350) SCAPL(I), SAVAL(I)
350  FORMAT (16X, F10.3, 19X, F10.3)
405      RECV(I) = RECVRY(I,J) - AVERMSG(J) - FA
360  CONTINUE
      IPRINT(I) = - 2
      IPRINT(I) = 1
      CALL GRAPH4 (RECNSE(I, J), RECV, NNP, JII, XMAX, XMIN, YMAX, YN
410      ITR, LABEL1, IPRAT)
      GO TO 300
300  K=NNP+1
      DO 305 I=NNP,50
305  PTSARD(I,J) = 0.0
415 300  CONTINUE
      IF (INIT, NE, 0) GO TO 120
      DO 310 I = 1, 50
      DO 310 J = 1, LRCVRS
310  RECNSE(I, J) = PTSARD(I, J)
420 320  SNO = 0.0
      DO 370 J = 1,4
      XPOWNS(J) = 0.0
      APOWNS(J) = 0.0
      AXCPO(J) = 0.0
425 370  CONTINUE
      DO 380 I = 1,50
      DO 380 J = 1,4
      PTSARD(I,J) = 0.0
380  CONTINUE
430  RETURN
      END
      G 391-

SUBROUTINE FINDPT (VAL, AP, N)
H 1
H 2
H 3
H 4
5  C .....
C  FINDPT      REVISED 05/07/74 KSH
H 5
C  THIS SUBROUTINE FINDS THE INDEX OF THE FIRST POINT GREATER
H 7
C  THAN OR EQUAL TO THE SPECIFIED VALUE.
H 8
C .....
H 9
10 C .....
C  DIMENSION AR(50)
H 10
H 11
H 12
15 C .....
C  FINDPT VARIABLES
H 13
H 14
H 15
H 16
C  AP      = SCALE
H 17
C  IADD    = INDEX INDICATES IN WHICH SECTION OF SCALE POINT LIES
H 18
C  N       = INDEX OF FIRST POINT GE VALUE
H 19
20 C  VAL    = VALUE
H 20
H 21
H 22
C .....
H 23
H 24
25 C  COMMON / PLOT / NOP, NTL, RECNSE(50, 4)
H 25
H 26
C .....
H 27
H 28
30 C  PLOT COMMON VARIABLES
H 28
H 29
H 30
C  NOP     = NUMBER OF RING IN SCALE
H 31
C  NTL     = NUMBER OF POINTS PER RECEIVER IN EACH RECORD ON DATA TAPE
H 32
C  RECNSE  = RECEIVER NOISE APP
H 33
H 34
35 C .....
H 35
H 36
C .....
H 37
H 38
      IF (VAL .LE. AR(NOP)) GO TO 10
      N = NOP
      RETURN
      H 39
      H 40
40 10 IF (VAL .GT. AR(1)) GO TO 20
      N = 1
      RETURN
      H 41
      H 42
20 20 I = NOP / 2
      IADD = I
      H 43
      H 44
45 30 IADD = IADD / 2
      IF (VAL = AR(I)) 50, 40, 120
      H 45
      H 46
      H 47
      H 48
      H 49
      H 50
50 40 IF (IADD) 90, 90, 60
      I = I - IADD
      H 51
      H 52
      H 53
70 CONTINUE
      H 54
      H 55
55 WRITE (6, 80) I
      H 55
      H 56
      H 57
      H 58
      H 59
      H 60
      H 61
      H 62
      H 63
      H 64
      H 65
      H 66
      H 67
      H 68
      H 69
      H 70
      H 71
      H 72
      H 73
      H 74
      H 75
      H 76
      H 77
      H 78
      H 79
      H 80
      H 81
      H 82
      H 83
      H 84
      H 85
      H 86
      H 87
      H 88
      H 89
      H 90
      H 91
      H 92
      H 93
      H 94
      H 95
      H 96
      H 97
      H 98
      H 99
      H 100
      H 101
      H 102
      H 103
      H 104
      H 105
      H 106
      H 107
      H 108
      H 109
      H 110
      H 111
      H 112
      H 113
      H 114
      H 115
      H 116
      H 117
      H 118
      H 119
      H 120
      H 121
      H 122
      H 123
      H 124
      H 125
      H 126
      H 127
      H 128
      H 129
      H 130
      H 131
      H 132
      H 133
      H 134
      H 135
      H 136
      H 137
      H 138
      H 139
      H 140
      H 141
      H 142
      H 143
      H 144
      H 145
      H 146
      H 147
      H 148
      H 149
      H 150
      H 151
      H 152
      H 153
      H 154
      H 155
      H 156
      H 157
      H 158
      H 159
      H 160
      H 161
      H 162
      H 163
      H 164
      H 165
      H 166
      H 167
      H 168
      H 169
      H 170
      H 171
      H 172
      H 173
      H 174
      H 175
      H 176
      H 177
      H 178
      H 179
      H 180
      H 181
      H 182
      H 183
      H 184
      H 185
      H 186
      H 187
      H 188
      H 189
      H 190
      H 191
      H 192
      H 193
      H 194
      H 195
      H 196
      H 197
      H 198
      H 199
      H 200
      H 201
      H 202
      H 203
      H 204
      H 205
      H 206
      H 207
      H 208
      H 209
      H 210
      H 211
      H 212
      H 213
      H 214
      H 215
      H 216
      H 217
      H 218
      H 219
      H 220
      H 221
      H 222
      H 223
      H 224
      H 225
      H 226
      H 227
      H 228
      H 229
      H 230
      H 231
      H 232
      H 233
      H 234
      H 235
      H 236
      H 237
      H 238
      H 239
      H 240
      H 241
      H 242
      H 243
      H 244
      H 245
      H 246
      H 247
      H 248
      H 249
      H 250
      H 251
      H 252
      H 253
      H 254
      H 255
      H 256
      H 257
      H 258
      H 259
      H 260
      H 261
      H 262
      H 263
      H 264
      H 265
      H 266
      H 267
      H 268
      H 269
      H 270
      H 271
      H 272
      H 273
      H 274
      H 275
      H 276
      H 277
      H 278
      H 279
      H 280
      H 281
      H 282
      H 283
      H 284
      H 285
      H 286
      H 287
      H 288
      H 289
      H 290
      H 291
      H 292
      H 293
      H 294
      H 295
      H 296
      H 297
      H 298
      H 299
      H 300
      H 301
      H 302
      H 303
      H 304
      H 305
      H 306
      H 307
      H 308
      H 309
      H 310
      H 311
      H 312
      H 313
      H 314
      H 315
      H 316
      H 317
      H 318
      H 319
      H 320
      H 321
      H 322
      H 323
      H 324
      H 325
      H 326
      H 327
      H 328
      H 329
      H 330
      H 331
      H 332
      H 333
      H 334
      H 335
      H 336
      H 337
      H 338
      H 339
      H 340
      H 341
      H 342
      H 343
      H 344
      H 345
      H 346
      H 347
      H 348
      H 349
      H 350
      H 351
      H 352
      H 353
      H 354
      H 355
      H 356
      H 357
      H 358
      H 359
      H 360
      H 361
      H 362
      H 363
      H 364
      H 365
      H 366
      H 367
      H 368
      H 369
      H 370
      H 371
      H 372
      H 373
      H 374
      H 375
      H 376
      H 377
      H 378
      H 379
      H 380
      H 381
      H 382
      H 383
      H 384
      H 385
      H 386
      H 387
      H 388
      H 389
      H 390
      H 391
      H 392
      H 393
      H 394
      H 395
      H 396
      H 397
      H 398
      H 399
      H 400
      H 401
      H 402
      H 403
      H 404
      H 405
      H 406
      H 407
      H 408
      H 409
      H 410
      H 411
      H 412
      H 413
      H 414
      H 415
      H 416
      H 417
      H 418
      H 419
      H 420
      H 421
      H 422
      H 423
      H 424
      H 425
      H 426
      H 427
      H 428
      H 429
      H 430
      H 431
      H 432
      H 433
      H 434
      H 435
      H 436
      H 437
      H 438
      H 439
      H 440
      H 441
      H 442
      H 443
      H 444
      H 445
      H 446
      H 447
      H 448
      H 449
      H 450
      H 451
      H 452
      H 453
      H 454
      H 455
      H 456
      H 457
      H 458
      H 459
      H 460
      H 461
      H 462
      H 463
      H 464
      H 465
      H 466
      H 467
      H 468
      H 469
      H 470
      H 471
      H 472
      H 473
      H 474
      H 475
      H 476
      H 477
      H 478
      H 479
      H 480
      H 481
      H 482
      H 483
      H 484
      H 485
      H 486
      H 487
      H 488
      H 489
      H 490
      H 491
      H 492
      H 493
      H 494
      H 495
      H 496
      H 497
      H 498
      H 499
      H 500
      H 501
      H 502
      H 503
      H 504
      H 505
      H 506
      H 507
      H 508
      H 509
      H 510
      H 511
      H 512
      H 513
      H 514
      H 515
      H 516
      H 517
      H 518
      H 519
      H 520
      H 521
      H 522
      H 523
      H 524
      H 525
      H 526
      H 527
      H 528
      H 529
      H 530
      H 531
      H 532
      H 533
      H 534
      H 535
      H 536
      H 537
      H 538
      H 539
      H 540
      H 541
      H 542
      H 543
      H 544
      H 545
      H 546
      H 547
      H 548
      H 549
      H 550
      H 551
      H 552
      H 553
      H 554
      H 555
      H 556
      H 557
      H 558
      H 559
      H 560
      H 561
      H 562
      H 563
      H 564
      H 565
      H 566
      H 567
      H 568
      H 569
      H 570
      H 571
      H 572
      H 573
      H 574
      H 575
      H 576
      H 577
      H 578
      H 579
      H 580
      H 581
      H 582
      H 583
      H 584
      H 585
      H 586
      H 587
      H 588
      H 589
      H 590
      H 591
      H 592
      H 593
      H 594
      H 595
      H 596
      H 597
      H 598
      H 599
      H 600
      H 601
      H 602
      H 603
      H 604
      H 605
      H 606
      H 607
      H 608
      H 609
      H 610
      H 611
      H 612
      H 613
      H 614
      H 615
      H 616
      H 617
      H 618
      H 619
      H 620
      H 621
      H 622
      H 623
      H 624
      H 625
      H 626
      H 627
      H 628
      H 629
      H 630
      H 631
      H 632
      H 633
      H 634
      H 635
      H 636
      H 637
      H 638
      H 639
      H 640
      H 641
      H 642
      H 643
      H 644
      H 645
      H 646
      H 647
      H 648
      H 649
      H 650
      H 651
      H 652
      H 653
      H 654
      H 655
      H 656
      H 657
      H 658
      H 659
      H 660
      H 661
      H 662
      H 663
      H 664
      H 665
      H 666
      H 667
      H 668
      H 669
      H 670
      H 671
      H 672
      H 673
      H 674
      H 675
      H 676
      H 677
      H 678
      H 679
      H 680
      H 681
      H 682
      H 683
      H 684
      H 685
      H 686
      H 687
      H 688
      H 689
      H 690
      H 691
      H 692
      H 693
      H 694
      H 695
      H 696
      H 697
      H 698
      H 699
      H 700
      H 701
      H 702
      H 703
      H 704
      H 705
      H 706
      H 707
      H 708
      H 709
      H 710
      H 711
      H 712
      H 713
      H 714
      H 715
      H 716
      H 717
      H 718
      H 719
      H 720
      H 721
      H 722
      H 723
      H 724
      H 725
      H 726
      H 727
      H 728
      H 729
      H 730
      H 731
      H 732
      H 733
      H 734
      H 735
      H 736
      H 737
      H 738
      H 739
      H 740
      H 741
      H 742
      H 743
      H 744
      H 745
      H 746
      H 747
      H 748
      H 749
      H 750
      H 751
      H 752
      H 753
      H 754
      H 755
      H 756
      H 757
      H 758
      H 759
      H 760
      H 761
      H 762
      H 763
      H 764
      H 765
      H 766
      H 767
      H 768
      H 769
      H 770
      H 771
      H 772
      H 773
      H 774
      H 775
      H 776
      H 777
      H 778
      H 779
      H 780
      H 781
      H 782
      H 783
      H 784
      H 785
      H 786
      H 787
      H 788
      H 789
      H 790
      H 791
      H 792
      H 793
      H 794
      H 795
      H 796
      H 797
      H 798
      H 799
      H 800
      H 801
      H 802
      H 803
      H 804
      H 805
      H 806
      H 807
      H 808
      H 809
      H 810
      H 811
      H 812
      H 813
      H 814
      H 815
      H 816
      H 817
      H 818
      H 819
      H 820
      H 821
      H 822
      H 823
      H 824
      H 825
      H 826
      H 827
      H 828
      H 829
      H 830
      H 831
      H 832
      H 833
      H 834
      H 835
      H 836
      H 837
      H 838
      H 839
      H 840
      H 841
      H 842
      H 843
      H 844
      H 845
      H 846
      H 847
      H 848
      H 849
      H 850
      H 851
      H 852
      H 853
      H 854
      H 855
      H 856
      H 857
      H 858
      H 859
      H 860
      H 861
      H 862
      H 863
      H 864
      H 865
      H 866
      H 867
      H 868
      H 869
      H 870
      H 871
      H 872
      H 873
      H 874
      H 875
      H 876
      H 877
      H 878
      H 879
      H 880
      H 881
      H 882
      H 883
      H 884
      H 885
      H 886
      H 887
      H 888
      H 889
      H 890
      H 891
      H 892
      H 893
      H 894
      H 895
      H 896
      H 897
      H 898
      H 899
      H 900
      H 901
      H 902
      H 903
      H 904
      H 905
      H 906
      H 907
      H 908
      H 909
      H 910
      H 911
      H 912
      H 913
      H 914
      H 915
      H 916
      H 917
      H 918
      H 919
      H 920
      H 921
      H 922
      H 923
      H 924
      H 925
      H 926
      H 927
      H 928
      H 929
      H 930
      H 931
      H 932
      H 933
      H 934
      H 935
      H 936
      H 937
      H 938
      H 939
      H 940
      H 941
      H 942
      H 943
      H 944
      H 945
      H 946
      H 947
      H 948
      H 949
      H 950
      H 951
      H 952
      H 953
      H 954
      H 955
      H 956
      H 957
      H 958
      H 959
      H 960
      H 961
      H 962
      H 963
      H 964
      H 965
      H 966
      H 967
      H 968
      H 969
      H 970
      H 971
      H 972
      H 973
      H 974
      H 975
      H 976
      H 977
      H 978
      H 979
      H 980
      H 981
      H 982
      H 983
      H 984
      H 985
      H 986
      H 987
      H 988
      H 989
      H 990
      H 991
      H 992
      H 993
      H 994
      H 995
      H 996
      H 997
      H 998
      H 999
      H 1000

```


BEST AVAILABLE COPY

```

      RETURN
      IF (VAL = AR(1) = 1) 110, 100, 40
      T = 1 - 1
      GO TO 40
      110 T = 1 - 1
      IF (1) 70, 70, 90
      120 IF (IADD) 140, 140, 130
      130 T = 1 + IADD
      IF (T = NRC) 30, 30, 70
      140 T = 1 + 1
      IF (T = NRC) 150, 150, 70
      150 IF (VAL = AR(1)) 40, 40, 140
      END
      SUBROUTINE FINDATA
      .....
      5  C  FINDATA      REVISED FEB. 1974      JHW
      C
      C      THIS SUBROUTINE LOCATES N COMPLEX DATA POINTS FROM THE
      C      SPECIFIED TIME.
      .....
      10 .....
      C
      C      FINDATA VARIABLES
      .....
      15 C
      C      INIT = RECEIVER NUMBER
      C      ITDA = TAPE ACTION FLAG (1 = READ RECORD AND UNPACK PREAMBLE,
      C              2 = UNPACK DATA)
      C      LDAY = DAY
      C      LHOUP = HOUR
      C      LMIN = MINUTES
      C      LMONTH = MONTH
      C      LNI = RECEIVER NUMBER MINUS ONE
      C      LNREC = LENGTH OF RECORD
      25 C      LDATE = SAMPLING RATE
      C      LRCVRS = NUMBER OF RECEIVERS SAMPLED
      C      LSEC = SECONDS
      C      LSITE = SITE IDENTIFICATION CODE
      C      NTL = TOTAL NUMBER OF COMPLEX DATA POINTS IN INPUT ARRAY
      30 .....
      C
      C      COMMON /RECORD/ INFO(9), INRC(8,R), ISAVST, LREAL(2048),
      C      1 LREC, NDATA
      .....
      35 .....
      C
      C      RECORD COMMON VARIABLES
      .....
      40 C      INRC = ARRAY CONTAINING PREAMBLE VALUES PERTAINING TO EACH RECEIVER
      C      IMAG = UNPACKED IMAGINARY DATA
      C      INFO = ARRAY CONTAINING PREAMBLE VALUES PERTAINING TO SITE, EXACT
      C              TIME, DATE AND NUMBER OF RECEIVERS
      C      ISAVST = SAVE PREVIOUS SITE
      C      LREAL = UNPACKED REAL DATA
      45 C      LREC = LENGTH OF RECORD
      C      NDATA = NUMBER OF SAMPLES
      .....
      50 .....
      C
      C      COMMON /SAMPLE/ ARE(512, R), AMPSQ(512, R), N, NRC, NCALL, MON
      C      1TH, IDAY, IHOUP, MINIT, ISEC, RATE, MPTS, ARSQ(512, R)
      .....
      55 .....
      C
      C      SAMPLE COMMON VARIABLES
      .....
      60 C      AMPSQ = SQUARE OF AMPLITUDE
      C      ARE = ARRAY CONTAINING REAL DATA VALUES
      C      ARSQ = SUM OF SQUARES OF CORRECTED REAL VALUES
      C      IDAY = -1
      C      IHOUP = -1
      C      ISEC = -1
      C      MINIT = -1
      C      MONTH = -1
      65 C      NCALL = COUNTER INDICATES NUMBER OF TIMES SUBROUTINE FINDATA HAS
      C              BEEN CALLED
      C      NRC = RECEIVER NUMBER
      C      RATE = 50
      .....
      70 .....
      C
      C      EQUIVALENCE (INFO(1), LSITE), (INFO(2), LMONTH), (INFO(3), LDAY)
      C      1, (INFO(4), LHOUP), (INFO(5), LMIN), (INFO(6), LSEC), (INFO(7)
      C      2, LDATE), (INFO(8), LRCVRS), (INFO(9), LCONT)
      C      EQUIVALENCE (LREC, LNREC)
      .....

```

BEST AVAILABLE COPY

```

      IF (NCALL .EQ. 1) GO TO 10
      .....
      C NOT INITIAL CALL
      .....
      IF (ITDA .NE. 2) GO TO 120
      GO TO 20
      .....
      C INITIAL CALL
      .....
      10 REWIND 40
      20 ITDA = 1
      CALL RETAPE (ITDA)
      .....
      C CHECK VALIDITY OF RECORD
      .....
      IF (LNREC .EQ. 0) GO TO 180
      IF (LNREC .LT. 5) GO TO 20
      IF (LNREC .EQ. 415) GO TO 40
      IF (LRCVRS .EQ. 6 .AND. LNREC .EQ. 312) 50, 20
      40 IF (LRCVRS .EQ. 2 .OR. LRCVRS .EQ. 4) 50, 20
      50 IF (NCALL .NE. 1) GO TO 110
      IF (MONTH .LT. 0 .OR. MONTH .EQ. (MONTH) 60, 20
      60 IF (IDAY .LT. 0 .OR. IDAY .EQ. (IDAY) 70, 20
      70 IF (IMHUR .LT. 0 .OR. IMHUR .EQ. (IMHUR) 80, 20
      80 IF (IMINUT .LT. 0 .OR. IMINUT .EQ. (IMINUT) 90, 20
      90 IF (ISEC .LT. 0 .OR. ISEC .EQ. (ISEC) 100, 20
      100 NTLL = 0
      GO TO 120
      110 IF (ISVST .NE. LSITE) GO TO 180
      120 ITDA = 2
      .....
      C UNPACK DATA WORDS IN TAPE RECORD
      .....
      CALL RETAPE (ITDA)
      INIT = APC
      130 CONTINUE
      NL = 1
      DO 140 L = INIT, NDATA, 8
      NTLL = NTLL + 1
      DO 150 LL = 1, LRCVRS
      ARE (NTLL, LL) = LREAL (NL)
      AMPRO (NTLL, LL) = LREAL (NL) * 2
      ARSQ (NTLL, LL) = LREAL (NL) * 2
      145 NL = NL + 2
      150 CONTINUE
      160 CONTINUE
      NTLL = 0
      180 RETURN
      END
      .....
      SUBROUTINE RETAPE (ITDA)
      .....
      PETAPE      REVISED FEB., 1975   JRW
      .....
      THIS SUBROUTINE READS AND/OR UNPACKS ONE RECORD FROM THE
      DATA TAPE.
      .....
      DIMENSION NUPAK(2050)
      .....
      RETAPE VARIABLES
      .....
      ITN      = LENGTH OF RECORD
      ITDA     = FLAG INDICATES WHETHER OR NOT TO
      1) BUFFER IN NEXT DATA RECORD
      2) UNPACK WORDS IN PREAMBLE
      3) UNPACK COMPLEX DATA VALUES
      1 = DO 1) AND 2) ONLY,
      2 = DO 3) ONLY
      .....
      JI      = IMAGINARY INDEX
      JP      = REAL INDEX
      LNREC   = LENGTH OF RECORD
      MP      = PARITY ERROR FLAG (1 = NO ERROR, -1 = ERROR)
      NPAK    = NUMBER OF PACKED DATA WORDS TO BE UNPACKED
      NUPAK   = UNPACKED ARRAY
      .....

```

BEST AVAILABLE COPY

```

125  IN = 1
      LAST = 15
      LOC = 1
      CALL RYTHMK (TR, LOC, LAST, IN)
      TRVST = INFO(1)
      INFO(1) = 10 * IN(1) + IN(2)
      INFO(2) = 10 * IN(3) + IN(4)
      INFO(3) = 10 * IN(5) + IN(6)
      INFO(4) = 10 * IN(7) + IN(8)
      INFO(5) = 10 * IN(9) + IN(10)
      INFO(6) = 10 * IN(11) + IN(12)
      INFO(7) = IN(13)
      INFO(8) = IN(14)
      INFO(9) = IN(15)
135  IF (IPRIN, EQ, 0) GO TO 90
      WRITE (6, 70)
70  FORMAT (1H0,62H SITE MONTH DAY HOUR MIN SEC RATE NO,RE
      ICV CONTINUE
      WRITE (6, 80) INFO
80  FORMAT (2X,61A,215,17,19)
      GO CONTINUE
C .....
145  C RECEIVER INFORMATION IN PREAMBLE
      C .....
      LAST = 12
      LOC = 10
      DO 110 J = 1, NRCVR
      CALL RYTHMK (TR, LOC, LAST, IN)
      IF (IPRIN, EQ, 0) GO TO 100
      INTR = IN(1)
      TORC(1, J) = (INTR, AND, 8) / 8
      TORC(2, J) = (INTR, AND, 4) / 4
      TORC(3, J) = (INTR, AND, 2) / 2
      TORC(4, J) = INTR, AND, 1
      TORC(5, J) = IN(2)
      TORC(6, J) = IN(3)
      TORC(7, J) = 20 * IN(4) - 50 * IN(5) - 5 * IN(6) + 55
160  CONTINUE
      TORC(8, J) = 10000 * IN(7) + 10000 * IN(8) + 1000 * IN(9) + 10
      * IN(10) + 10 * IN(11) + IN(12)
170  CONTINUE
      IF (IPRIN, EQ, 0) GO TO 140
      WRITE (6, 120)
120  FORMAT (1H0,72H PW GAIN L/R CALR L/R C ON/OFF C SPEC C L
      LEVEL GAIN FREQUENCY)
      WRITE (6, 130) TORC
130  FORMAT (21X,519,110)
140  CONTINUE
      IF (ITDA, NE, 0) GO TO 200
C .....
175  C UNPACK AND STORE DATA VALUES
      C .....
      150 N = 0
      IF (ILN, LT, 415) GO TO 160
      NPAK = 410
      NDATA = 2048
      GO TO 170
160  IF (ILN, LE, 5) GO TO 200
      NPAK = 307
      NDATA = 1536
170  NOCHAR = 16 * (NRCVR + 8)
      AMOD = MOD(NOCHAR, 10)
      NWORD = NOCHAR/10 + 1
      IF (NMOD, EQ, 0) GO TO 175
      N = (10 - AMOD)/2
      DO 173 J=1,N
      N = N - J + 1
      INTR = MX1FXTA(THUF(NWORD), -2)
      NUPAK(K) = INTR, AND, MASK
195  173 THUF(NWORD) = MX1FXTA(THUF(NWORD), -10)
C .....
      C SUBROUTINE UNPACK SEPARATES EACH PACKED WORD INTO FIVE 12-BIT
      C SAMPLES AND THEN SHIFTS EACH SAMPLE 2 BITS TO THE RIGHT
      C DATA IS IN TWO'S COMPLEMENT. NEW TAPE (JANUARY, 1975) HAS DATA
      C WITH A SCALE FROM 0 TO 10. PREVIOUS TAPE HAD SCALE FROM -5 TO +5 AND NUMBERS
      C ABOVE 511 HAD TO HAVE 1024 SUBTRACTED FROM THEM FOR NEGATIVE NUMBERS.
      C THIS TEST IS NOW BY-PASSED.
      C .....
205  175 N = N + 1
      IREGIN = NOCHAR/10 + 2
      IF (NMOD, EQ, 0) IREGIN = NWORD
      CALL UNPACK (THUF(IREGIN), NUPAK(N), NPAK)
210  DO 180 J = 1, NDATA

```

30

40

2

50

50

5

6

7

74

9

21

9

9

100

105

11

11

12

L	33
L	34
L	35
L	36
L	37
L	38
L	39
L	40
L	41
L	42
L	43
L	44
L	45
L	46
L	47
L	48
L	49
L	50
L	51
L	52
L	53
L	54
L	55
L	56
L	57
L	58
L	59
L	60
L	61
L	62
L	63
L	64
L	65
L	66
L	67
L	68
L	69
L	70
L	71
L	72
L	73
L	74
L	75
L	76
L	77
L	78
L	79
L	80
L	81
L	82
L	83
L	84
L	85
L	86
L	87
L	88
L	89
L	90
L	91
92	92
L	93
L	94
L	95
L	96
L	97
L	98
L	99
L	100
L	101
L	102
L	103
L	104
L	105
L	106
L	107
L	108
L	109
L	110
L	111
L	112
L	113
L	114
L	115
L	116
L	117
L	118
L	119

BEST AVAILABLE COPY

```

      INTR = NUPAK(J)
      GO TO 190
      IF (INTR .EQ. 511) GO TO 160
      NUPAK(J) = INTR = 1024
      190 CONTINUE
      DO 195 J = 1, NDATA
      195 LREAL(J) = NUPAK(J)
      200 RETURN
      END

```

L 193
L 194
L 195
L 196
L 197
L 198
L 199
L 200

```

      SUBROUTINE RNOISE (ICRG)
      C
      C .....
      C
      5   C   RNOISE          DEVICES 05/07/74 RSH
      C
      C   THIS SUBROUTINE CALCULATES THE SQUARE OF THE AVERAGE NOISE
      C   VOLTAGE.
      C
      10  C .....
      C
      C   DIMENSION AVRSQ(4), SUMR(4), SUMT(4)
      C
      C .....
      C
      15  C
      C   NOISE VARIABLES
      C
      C   AVRSQ = AVERAGE NOISE VOLTAGE SQUARED
      C   ICRG = SITE CHANGE FLAG (0 = SAME SITE, 1 = CHANGE IN SITE)
      20  C   IENTRY = NUMBER OF RECORDS PROCESSED
      C   LECVRS = NUMBER OF RECEIVERS BEING SAMPLED
      C   SCAL = NUMBER OF POINTS PER RECEIVER IN EACH RECORD
      C   SUMR = SUM OF SQUARES OF AMPLITUDE FOR ONE RECEIVER
      C   SUMT = SUM OF SQUARES OF AMPLITUDE FOR ALL RECEIVERS
      25  C   SUMV = CUMULATIVE SUM OF REAL VALUES
      C   SUMR = SUM OF REAL VALUES
      C
      C .....
      C
      30  C   COMMON / CONST / P104
      C
      C .....
      C
      35  C   CONST COMMON VARIABLES
      C
      C   P104 = ONE-FOURTH PI
      C
      C .....
      C
      40  C   COMMON / CONTR / IPPIN
      C
      C .....
      C
      45  C   CONTRL COMMON VARIABLES
      C
      C   IPPIN = PRINT FLAG (0 = NO HEADINGS PRINTED, 1 = PRINT HEADINGS)
      C
      C .....
      C
      50  C   COMMON / PLOT / NOP, NTL, RECNS(50, 4)
      C
      C .....
      C
      55  C   PLOT COMMON VARIABLES
      C
      C   NOP = NUMBER OF HITS IN SCALE
      C   NTL = NUMBER OF POINTS PER RECEIVER IN EACH RECORD ON DATA TAPE
      60  C   RECNS = RECEIVER NOISE APP
      C
      C .....
      C
      65  C   COMMON /RECORD/ INFO(4), IORC(4,4), ISAVS, LREAL(2048),
      C   I LREC, NDATA
      C
      C .....
      C
      70  C   RECORD COMMON VARIABLES
      C
      C   IORC = ARRAY CONTAINING PREAMBLE VALUES PERTAINING TO EACH RECEIVER
      C   INFO = ARRAY CONTAINING PREAMBLE VALUES PERTAINING TO SITE, EXACT
      75  C   TIME, DATE AND NUMBER OF RECEIVERS
      C   ISAVS = SAVED PREVIOUS SITE
      C   LREAL = UNPACKED REAL DATA
      C   LREC = LENGTH OF RECORD
      C   NDATA = NUMBER OF SAMPLES
      C
      C .....

```

M 1
M 2
M 3
M 4
M 5
M 6
M 7
M 8
M 9
M 10
M 11
M 12
M 13
M 14
M 15
M 16
M 17
M 18
M 19
M 20
M 21
M 22
M 23
M 24
M 25
M 26
M 27
M 28
M 29
M 30
M 31
M 32
M 33
M 34
M 35
M 36
M 37
M 38
M 39
M 40
M 41
M 42
M 43
M 44
M 45
M 46
M 47
M 48
M 49
M 50
M 51
M 52
M 53
M 54
M 55
M 56
M 57
M 58
M 59
M 60
M 61
M 62
M 63
M 64
M 65
M 66
M 67
M 68
M 69
M 70
M 71
M 72
M 73
M 74
M 75
M 76
M 77
M 78
M 79
M 80
M 81
M 82
M 83
M 84
M 85

BEST AVAILABLE COPY

```

C      COMMON / SAMPLE / AFF(512, R), AMPSQ(512, R), N, NRC, NCALL, MON
C      1TH, IDAY, IHOOR, MINIT, ISEC, RATE, MPTS, ARGO(512, R)
C
C      .....
C      SAMPLES COMMON VARIABLES
C
C      AMPSQ = SQUARE OF AMPLITUDE
C      AFF = ARRAY CONTAINING REAL DATA VALUES
C      ARSQ = SUM OF SQUARES OF CORRECTED REAL VALUES
C      IDAY = -1
C      IHOOR = -1
C      ISEC = -1
C      MINIT = -1
C      MONTH = -1
C      MPTS = 12H
C      N = NUMBER OF COMPLEX DATA POINTS DESIGNED IN FOURIER PROCESSING
C      NCALL = COUNTER INDICATES NUMBER OF TIMES SUBROUTINE FINDATA HAS
C      BEEN CALLED
C      NRC = RECEIVER NUMBER
C      RATE = 50
C      TDWASF = PHASE
C
C      .....
C      DATA IENTRY/0/
C
C      IF (IENTRY .GT. 0) GO TO 20
C      DO 10 J = 1, P
C      SUMR(J) = 0.0
C
C      10 SUMRL(J) = 0.0
C      SNAL = 0.0
C      20 CONTINUE
C      IENTRY = IENTRY + 1
C      IF (ICMG .EQ. 1) GO TO 50
C      IRCVRS = INFO(R)
C      DO 40 J = 1, IRCVRS
C      SUMR = 0.0
C      TSUMR = 0.0
C      DO 30 I = 1, NTL
C      TSUMR = TSUMR + ARE(I, J)
C      SUMR = SUMR + AMPSQ(I, J)
C      30 CONTINUE
C      SUMRL(J) = SUMRL(J) + SUMR
C      SUMR(J) = SUMR(J) + TSUMR
C      40 CONTINUE
C      SNAL = SNAL + 256.
C      RETURN
C      50 CONTINUE
C      DO 70 J = 1, IRCVRS
C      AVRMSQ(J) = SUMRL(J) / SNAL
C      70 CONTINUE
C      WRITE (6, R0) (AVRMSQ(J), J = 1, IRCVRS)
C      80 FORMAT (20H AVERAGE NOISE VOLTAGE SQUARED, RE10, 3)
C      WRITE (6, R0) IENTRY
C      90 FORMAT (23H NUMBER OF RECORDS USED, I5)
C      IENTRY = 0
C      RETURN
C      END

```

```

0 25162001031300000003
1 00000000000000000000

```

```

IDENT UNPACK
ENTRY UNPACK
VFD 54/6LUNPACK, A/3
DATA 0
* ARG 1 FWA OF PACKED ARRAY
* ARG 2 FWA OF UNPACKED ARRAY
* ARG 3 N == ADDRESS OF THE NUMBER OF WORDS TO BE UNPACKED
* UNPACKS EACH WORD INTO FIVE 12-BIT SAMPLES
* ALSO SHIFTS EACH SAMPLE 2 BITS TO THE RIGHT
* EXAMPLE
* DIMENSION P(10), U(50)
* CALL UNPACK (P, U, 10)

```

```

2 63117
   501100000
   73010
3 501100000
   53110
   63310
4 66400
   66500
   616000005
5 5120000014
6 56116
7 20116
   11612
   21602
   53600

```

NEXT
CYCLE

```

SH1 X1 ,ARG1 = R1(A)
SA1 A1+1
SX0 X1 ,ARG2 = X0(A)
SA1 A1+1
SA1 X1
SR3 X1 ,ARG3 = H3
SH4 R0 ,R4 = SAMPLE INDEX (J - 5)
SR5 R0 ,R5 = PACKED ARRAY INDEX (I - N)
SH6 5
SA2 MASK ,X2 = MASK FOR LOW ORDER SAMPLE
SA1 R1+R5 ,X1 = NEXT PACKED WORD
LX1 12
RX6 X1+X2 ,X6 = SAMPLE MASKED FROM PACKED WORD
AX6 2 ,SHIFT SAMPLE RIGHT 2 BITS
SAB X0 ,STORE SAMPLE

```

10	7200000001		SX0	X0+1	.INCREMENT UNPACKED ARRAY ADDRESS
		6144000001	SP4	H4+1	.INCREMENT SAMPLE INDEX
11	0544000007 *		NF	H4,H0,CYCLE	.JUMP IF SAMPLE INDEX NOT 5
		66400	SP4	H0	.SET SAMPLE INDEX BACK TO 0
12	6155000001		SP5	RS+1	.INCREMENT PACKED ARRAY INDEX
		0635000006 *	NF	H3,H5,NEXT	.JUMP IF PACKED ARRAY INDEX NOT 6
13	0400000001 *		ZP	H0,UNPACK	
14	00000000000000007777		DATA	4005	
15			END		

42100R CM STORAGE USED
MODEL 71 ASSEMBLY

37 STATEMENTS
0.189 SECONDS

4 SYMBOLS
9 REFERENCES

BEST AVAILABLE COPY

REFERENCES

1. K. E. Gillilland, "The NAVELEX Man-Made Radio Noise Program," Final Report ESD-TR-75-007, Electromagnetic Compatibility Analysis Center, Annapolis, Maryland, 21402 (April 1975).
2. D. J. Cohen, "A Statistical Ignition Noise Model," ECAC-PR-72-041, Electromagnetic Compatibility Analysis Center, Annapolis, Maryland (October 1972).
3. R. A. Shepherd, J. C. Gaddie, V. E. Hatfield, and G. H. Hagn, "Measurements of Automobile Ignition Noise at HF," Final Report, SRI Project 2051, Contract N00039-71-A-0223, Delivery Order 0003, Stanford Research Institute, Menlo Park, California (February 1973).
4. K. E. Gillilland and T. A. Brewer, "Experimental Verification of Ignition Noise APD Model and Digital-Receiver Bit-Error Probability Model," Final Report ESD-TR-73-036, Electromagnetic Compatibility Analysis Center, Annapolis, Maryland, 21402 (January 1974).
5. K. E. Gillilland, "Initial Verification of Intersymbol Interference-Filter Distortion Model and Digital Receiver Bit Error Probability Model," Final Report ESD-TR-74-087, Electromagnetic Compatibility Analysis Center, Annapolis, Maryland, 21402 (December 1974).
6. R. B. Churchill, "Modeling the Relative Amplitude Probability Distribution of Power Line Noise," Final Report ESD-TR-75-019, Electromagnetic Compatibility Analysis Center, Annapolis, Maryland, 21402 (October 1975).
7. H. N. Shaver, "Propagation Measurement Systems," Final Report Contract DAAB07-68-C-0343, Research and Development Technical Report ECOM-00343-F, for U.S. Army Electronics Command, Fort Monmouth, New Jersey 07703, Stanford Research Institute, Menlo Park, California (October 1970).
8. G. W. Juette, "Evaluation of Television Interference from High Voltage Transmission Lines," IEEE Trans. Power Apparatus and Systems, Vol. PAS-91, No. 3 (1972).

9. W. E. Pakala et al., "Radio Noise Measurements on High Voltage Lines from 2.4 to 345 kV," 1968 IEEE Electromagnetic Compatibility Symposium Record, IEEE 68C12-EMC (1968).
10. W. I. Thompson, III, "Bibliography on Ground Vehicle Communications and Control: A KWIC INDEX," Report No. DOT-TSC-UMTA-71-3, Urban Mass Transportation Administration, U.S. Dept. of Transportation, Cambridge, Mass., Vol. II (July 1971).
11. R. T. Disney, A. D. Spaulding, and A. G. Hubbard, "Man-Made Radio Noise; Part II: Bibliography of Measurement Data, Applications, and Measurement Methods," OT Report 74-38, Office of Telecommunications, U.S. Dept. of Commerce (1974).
12. G. H. Hagn and R. A. Shepherd, "Man-Made Electromagnetic Noise from Unintentional Radiators: A Summary," Paper No. 3 presented at NATO/AGARD Meeting on Electromagnetic Noise, Interference and Compatibility, Paris, France, 21-25 October 1974, AGARD Conference Proceedings No. 159, 7 Rue Ancelle, 92200 Neuilly Sur Seine, France.
13. R. T. Disney and A. G. Longley, "Preliminary Telemetry Link Performance Estimate for Department of Transportation High-Speed Test Track," OTM 73-130, Institute for Telecommunications Sciences, Boulder, Colorado (1973).
14. A. D. Spaulding and R. T. Disney, "Man-Made Radio Noise, Part I: Estimates for Business, Residential, and Rural Areas," OT Report 74-38, Office of Telecommunications, U.S. Dept. of Commerce, Boulder, Colorado (1974).
15. W. R. Lauber, "Amplitude Probability Distributions at the Apple Grove 775 kV Project," paper presented at IEEE Power Engineering Society Winter Meeting and Tesla Symposium, New York, New York (January 25-30 1976).
16. F. W. Warburton et al., "Power Line Radiations and Interference above 15 MHz," IEEE Trans. Power Apparatus and Systems, Vol. PAS-88, No. 10 (October 1969).
17. J. J. LaForest, "Seasonal Variation of Fair-Weather Radio Noise," IEEE Trans. Power Apparatus and Systems, Vol. PAS-87, No. 4 (1968).
18. W. E. Pakala and V. L. Chartier, "Radio Noise Measurements on Overhead Power Lines from 2.4 to 800 kV," IEEE Trans. Power Apparatus and Systems, Vol. PAS-90, No. 3 (May/June 1971).

19. IEEE Radio Noise Subcommittee of the IEEE Transmission and Distribution Committee, "Transmission System Radio Influence," IEEE Trans. Power Apparatus and Systems, Vol. PAS-84, No. 8 (August 1965).
20. IEEE Radio Noise Subcommittee-Working Group No. 3, "Radio Noise Design Guide for High-Voltage Transmission Lines," IEEE Trans. Power Apparatus and Systems, Vol. PAS-90, No. 2 (March/April 1971).
21. B. M. Bailey and M. W. Belsher, discussion on paper by H. H. Newell et al., IEEE Trans. Power Apparatus and Systems, Vol. PAS-87, No. 4 (1968).
22. J. S. Forrest, discussion of paper by F. W. Warburton et al., IEEE Trans. Power Apparatus and Systems, Vol. PAS-88, No. 10, p. 1498 (October 1969).
23. G. H. Hagn, "MF and HF Man-Made Radio Noise and Interference Survey - Bremerhaven, Germany," Technical Memorandum 2, Contract N00039-71-A-0223, SRI Project 1022-1, Stanford Research Institute, Menlo Park, California (February 1972).
24. G. H. Hagn, "MF and HF Man-Made Radio Noise and Interference Survey - Keflavik, Iceland," Technical Memorandum 1, SRI Project 1022-1, Contract N00039-71-A-0223, Stanford Research Institute, Menlo Park, California (February 1972).
25. J. W. Engles and R. S. Hicks, Jr., "MF and HF Man-Made Radio-Noise and Interference Survey--Rota, Spain," Technical Report TR-5/74-032, Naval Electronic Systems Security Engineering Center, Washington, D.C., 20390 (March 1974).
26. R. A. Shepherd, J. B. Lomax, V. D. Cone, D. L. Nielson, G. C. Edwards, "MF and HF Man-Made Radio Noise and Interference Survey - Guam," Final Report SRI Project 3328, Contract N00039-74-C-0292, Stanford Research Institute, Menlo Park, California (June 1974).
27. W. R. Lauber, "Mill Cove High Frequency Radio Noise Survey," CRC Report 1263, Communications Research Centre, Department of Communications, Ottawa, Canada (November 1974).
28. "Naval Shore Electronics Criteria," NAVALEX 0101,108, Naval Electronic Systems Command, Washington, D.C., 20360 (May 1973).

29. L. C. Crippen, "EMI Site Surveys on Okinawa at Naval Security Group Activity, Hanza, and Army Security Agency Field Station, Sobe," Final Report, Project No. 75-15-24, Naval Electronic Systems Test and Evaluation Detachment, Patuxent River, Maryland, 20670 (November 1975).
30. "IEEE Standard for the Measurement of Impulse Strength and Impulse Bandwidth," IEEE Std. 376-1975, Institute of Electrical and Electronic Engineers, Inc., 345 East 47 Street, New York, New York, 10017 (November 1975).
31. R. J. Matheson and K. R. Beasley, "Field Intensity Meter Modified to Measure RMS and Average Noise Envelope Voltage," ITS Technical Memorandum OT TM-119, Institute for Telecommunications Sciences, Boulder, Colorado (November 1972).
32. M. R. Moreau and C. H. Gary, "Predetermination of the Radio-Interference Level of High Voltage Transmission Lines, I--Predetermination of the Excitation Function," IEEE Trans. Power Apparatus and Systems, Vol. PAS-91, No. 1 (January/February 1972).
33. "World Distribution and Characteristics of Atmospheric Radio Noise," Report 322, International Radio Consultative Committee (CCIR), International Telecommunication Union, Geneva, Switzerland (1964).